1985

Determination of inorganic sulfur species in alkaline solutions using high performance liquid chromatography with polarographic detection

Zamir Uddin
Iowa State University

INFORMATION TO USERS

This reproduction was made from a copy of a manuscript sent to us for publication and microfilming. While the most advanced technology has been used to photograph and reproduce this manuscript, the quality of the reproduction is heavily dependent upon the quality of the material submitted. Pages in any manuscript may have indistinct print. In all cases the best available copy has been filmed.

The following explanation of techniques is provided to help clarify notations which may appear on this reproduction.

1. Manuscripts may not always be complete. When it is not possible to obtain missing pages, a note appears to indicate this.

2. When copyrighted materials are removed from the manuscript, a note appears to indicate this.

3. Oversize materials (maps, drawings, and charts) are photographed by sectioning the original, beginning at the upper left hand corner and continuing from left to right in equal sections with small overlaps. Each oversize page is also filmed as one exposure and is available, for an additional charge, as a standard 35mm slide or in black and white paper format.*

4. Most photographs reproduce acceptably on positive microfilm or microfiche but lack clarity on xerographic copies made from the microfilm. For an additional charge, all photographs are available in black and white standard 35mm slide format.*

***For more information about black and white slides or enlarged paper reproductions, please contact the Dissertations Customer Services Department.**

Uddin, Zamir

DETERMINATION OF INORGANIC SULFUR SPECIES IN ALKALINE SOLUTIONS USING HIGH PERFORMANCE LIQUID CHROMATOGRAPHY WITH POLAROGRAPHIC DETECTION

Iowa State University PH.D. 1985

PLEASE NOTE:

In all cases this material has been filmed in the best possible way from the available copy. Problems encountered with this document have been identified here with a check mark ✓.

1. Glossy photographs or pages _____
2. Colored illustrations, paper or print _____
3. Photographs with dark background _____
4. Illustrations are poor copy _____
5. Pages with black marks, not original copy _____
6. Print shows through as there is text on both sides of page _____
7. Indistinct, broken or small print on several pages ✓
8. Print exceeds margin requirements _____
9. Tightly bound copy with print lost in spine _____
10. Computer printout pages with indistinct print _____
11. Page(s) _____ lacking when material received, and not available from school or author.
12. Page(s) _____ seem to be missing in numbering only as text follows.
13. Two pages numbered _____. Text follows.
14. Curling and wri ıkled pages _____
15. Dissertation contains pages with print at a slant, filmed as received _____
16. Other _____

_____

_____

University
Microfilms
International

Determination of inorganic sulfur species in alkaline solutions using high performance liquid chromatography with polarographic detection

by

Zamir Uddin

A Dissertation Submitted to the
Graduate Faculty in Partial Fulfillment of the
Requirements for the Degree of
DOCTOR OF PHILOSOPHY

Department: Chemistry
Major: Analytical Chemistry

Approved:

Signature was redacted for privacy.

In Charge of Major Work

Signature was redacted for privacy.

For the Major Department

Signature was redacted for privacy.

For the Graduate College

Members of the Committee:

Signature was redacted for privacy.

Iowa State University
Ames, Iowa

1985

TABLE OF CONTENTS

LIST OF TABLES

LIST OF FIGURES

LIST OF ACRONYMS

AOB	Antioxidant buffer
CV	Cyclic voltammetry
DC	Direct current
DME	Dropping mercury electrode
FIA	Flow injection analysis
FI/EC	Flow injection with electrochemical detection
HMDE	Hanging mercury drop electrode
LCEC	Liquid chromatography with electrochemical detection
nm	Nanometer
NPP	Normal pulse polarography
PAR	Princeton Applied Research
RDE	Rotating disk electrode
SCE	Saturated calomel electrode
SDCP	Sampled DC polarography

LIST OF NOTATIONS

C^b	Bulk concentration; same as $C(x=\infty)$
C^s	(Electrode) surface concentration; same as $C(x=0)$
D	Diffusion coefficient
E	Electrode potential
E^o	Standard electrode potential
$E^{o'}$	Formal electrode potential
E_p	Peak potential
$E_{p,a}$	Anodic peak potential
$E_{p,c}$	Cathodic peak potential
ΔE_p	$\lvert E_{p,a} - E_{p,c} \rvert$ in cyclic voltammetry
$E_{1/2}$	Half-wave potential
e	Electron
F	The Faraday constant (96,487 coul equiv^{-1})
ΔG	Gibbs free energy change
i	Faradic current
i_ℓ	Limiting current
i_p	Peak current
i_{ss}	steady-state current
k_{mt}	Mass-transfer rate constant
N	Number of moles of electroactive species
s	Seconds
T	Absolute temperature
t	Time

t_p	Pulse duration in pulse polarography
V_f	Flowrate
x	Number of sulfur atoms in polysulfide, e.g., S_x^{2-}
$\bar{x}$	Average x for polysulfide species
α	A constant, characteristic of the electrode geometry and fluid dynamics, used in flow injection analysis
δ	Diffusion layer thickness in voltammetry

CHAPTER I. INTRODUCTION

The conventional methods available for the determination of various sulfur compounds, in general, are long and tedious. Direct determination of sulfide, for example, can be done by adding cadmium chloride solution to the sample (1). The cadmium sulfide precipitate is filtered, washed, dissolved in hydrochloric acid, and titrated with standard iodine or potassium iodate solution. Simultaneous determination of sulfide and thiosulfate is done by putting the sample in an acidic solution containing a known excess of iodine. The mixture is back-titrated with standard thiosulfate, using starch indicator. The sulfides in a second portion of sample are precipitated by the addition of lead carbonate. The precipitate is filtered off, and the thiosulfate alone is determined by an iodometric titration. The sulfides are calculated from the difference between the two titrations. Sulfide, sulfite and thiosulfate have been determined using iodometric methods (2), whereas polysulfides have been determined potentiometrically (3).

The simultaneous determination of these compounds has always been a problem because of their reactivity towards molecular oxygen present in aqueous solutions. Most of the inorganic sulfur compounds are thermodynamically unstable in the presence of oxygen. Although the rates of reactions of these sulfur compounds with oxygen are relatively slow, the spontaneity of the reactions poses a formidable challenge for the analytical chemist. The fact that it is virtually impossible to elimi-

nate dissolved oxygen adds further to the complexity of the analytical problem; hence, it is highly desirable to have an analytical method for the rapid and simultaneous determination of as many sulfur compounds as possible under the ambient conditions of temperature, solution composition, pH and dissolved oxygen. By far the most efficient method for the simultaneous determination of various anionic sulfur species appears to be that of Story (4). However, the detection method described is complicated and requires prior chemical treatment for the conversion of all sulfur species to sulfate which is eventually determined spectrophotometrically after chelation with Fe(III).

The analytical method investigated in the present research is based on the limiting polarographic currents for the sulfur compounds. The compounds present in a mixture are separated by liquid chromatography and are detected in a flow-through amperometric detector based on reactions at a dropping mercury electrode. The electrochemical detection of analytes after separation by liquid chromatography is commonly termed Liquid Chromatography with Electrochemical Detection (LCEC). No pre-treatment of alkaline sample solutions is required except dilution. The separated sulfur species are detected directly by the polarographic electrode without prior chemical conversion, as compared to Story's method. The instrumentation is simple and inexpensive. The method was tested successfully for the determination of sulfide, sulfite, and thiosulfate in samples derived from the caustic desulfurization of coal. The quantitative determination is based on the method

of standard additions which alleviates problems of interference by matrix effects usually encountered with samples of such complex composition.

The nature of the polysulfide anion was investigated with particular emphasis on the determination of the number of sulfur atoms, x, in the polysulfide anion, S_x^{2-}. This maximum value of x was determined to be 5 using the polarographic method, and this number was verified by spectrophotometric and gravimetric methods. The conclusion is in agreement with that of Pringle (5). The polarographic current-potential curve of the polysulfide anion is observed to have characteristic anodic and cathodic waves. The mathematical treatment of the limiting anodic and cathodic currents provides a means for estimating the number x.

A mercury electrode was selected for electrochemical detection for the following reasons:

1. A large activation overpotential exists for evolution of hydrogen by the reduction of H^+ ions in aqueous solution, thus permitting the use of a large negative range of applied electrode potentials.

2. The interference related to surface adsorption of reactants and reaction products is usually minimized because of the periodic renewal of the electrode surface.

3. The instrumentation related to the use of a mercury electrode is relatively simple and inexpensive and can be easily adapted for detection in liquid chromatography.

The LCEC method is potentially applicable to the determination of numerous other inorganic and organic sulfur-containing compounds. LCEC can be automated and adapted to the on-line monitoring of sulfur compounds in flowing streams for continuous industrial processes.

CHAPTER II. LITERATURE REVIEW

Sulfide

The polarographic response of sulfide was observed as early as 1934 by Ravenda (6), who reported the effect of adding a few drops of an aqueous solution of H_2S to a solution containing 0.1 M KNO_3 and 0.1 M KCN. According to Ravenda:

> The starting potential of mercury has become so negative that the exponential part at which mercury readily passes into solution through the anodic dissolution, occurs at an applied emf of 1.0 V.

The value of applied potential for onset of anodic mercury dissolution for a solution containing only the supporting electrolyte is ca. +0.4 V (SCE). Kolthoff and Miller (7) verified the existence of anodic sulfide waves at a potential of about -0.6 V (SCE) in the millimolar concentration range using NaOH as the supporting electrolyte. They observed that the waves have fairly steep slopes but flattened out at currents greater than about 2 mA. Trifinov (8) observed the presence of two waves: the first he described as an adsorption pre-wave controlled by the diffusion of sulfide to the electrode surface resulting in the formation of a monomulecular layer of HgS; followed by a second wave, limited by the diffusion of sulfide, corresponding to the formation of nonadsorbed HgS on the electrode surface.

The existence of three anodic waves for sulfide was reported by Zhadanov and Kiselev (9). As had been proposed by Trifinov (8), Zhadanov and Kiselev identified the first wave as an adsorption pre-

wave and the other two waves as diffusion controlled. Formation of three waves for sulfide in 0.01 M NaOH was reported also by Julien and Bernard (10). According to them, the waves resulted from the deposition of successive layers of HgS film on the surface of the electrode. Because of the inconsistent observations and interpretations, Canterford and Buchanan (11) undertook a detailed investigation of the polarographic behavior of sulfide ion in several supporting electrolytes using AC and DC polarographic methods. They identified up to four distinct DC waves in 1 M $NaClO_4$ at high sulfide concentrations (i.e., $\geq$1 mM) and explained them on the basis of the formation of successive layers of insoluble HgS on the electrode surface. Canterford used rapid scan polarographic methods (12-14) for the determination of sulfide in aqueous solutions. Canterford (15) also demonstrated that sulfide can be determined in the presence of cyanide which, previously, was observed to interfere with the sulfide determination using conventional polarographic methods. Yousseffi and Brike (16) reported the determination of sulfide in a mixture using normal pulse polarography (NPP) and differential pulse polarography (DPP). Trace amounts of sulfide have been determined by Miwa et al. (17) based on the anodic oxidation of mercury in the presence of sulfide, after a suggestion by Burge and Jeroscewski (18). Noel (19) determined sulfide in Kraft white and black liquors using NPP and DPP.

Polysulfide

Although a significant quantity of literature pertaining to polysulfides is devoted to the synthesis of polysulfide, little is known definitively of the chemistry of polysulfides of alkali metals. One of the earliest attempts at these syntheses was that of Boettger (20), in the later part of the nineteenth century, who claimed the preparation of sodium disulfide pentahydrate ($Na_2S_2 \cdot 5H_2O$), sodium trisulfide trihydrate ($Na_2S_3 \cdot 3H_2O$), sodium tetrasulfide octahydrate ($Na_2S_4 \cdot 8H_2O$) and sodium pentasulfide octahydrate ($Na_2S_5 \cdot 8H_2O$), by dissolving calculated amounts of sulfur in alcoholic aqueous solutions of Na_2S with evaporation to dryness. His work was criticized by Bloxam (21), and by Rule and Thomas (22), who were unable to repeat Boettger's work. Rule and Thomas synthesized anhydrous sodium disulfide and tetrasulfide using absolute alcohol as the solvent. However, they failed to prepare the tri- and pentasulfides using this method. Pearson and Robinson (23) reviewed the methods of synthesis of sodium polysulfide and reinvestigated most of the work already done. They characterized the polysulfides by performing the elemental analyses for sulfur, and the alkali metals, and confirmed Boettger's work. The polarographic behavior of polysulfide was studied by Werner and Konopik (24-26). The i-E curves of freshly prepared Na_2S_2 in 2 N NaOH were obtained (24). Two anodic waves with $E_{\frac{1}{2}}$ values of -0.58 V and -0.80 V were reported (25). At negative potentials, an ill-defined cathodic wave was reported. The polarographic behavior of Na_2S_4 was found to be

very similar to that of Na_2S_2 (26). Konopik and Werner attributed the wave at -0.58 V to the oxidation of Hg to Hg^{2+} which combined with S^{2-} present in the diffusion layer from dissociation of the polysulfide species; the reaction of Hg^{2+} with S^{2-} produces insoluble HgS on the mercury electrode surface. The cathodic wave was explained on the basis of reduction of free sulfur to S^{2-}. The cathodic maximum was explained as the result of the reduction of free S^{o} and the nonuniform adsorption of the resulting S^{2-} on the electrode surface. They speculated that the dissociation of S_x^{2-} to $S_{x-1}^{2-} + S^{o}$ is slower than the diffusion of S^{o} to the electrode surface; the cathodic wave was, consequently, irreversible. The S^{2-}, produced as a result of the cathodic reaction, was concluded to react with S^{o} to give S_x^{2-}; thus, explaining the similarity in the polarographic behavior of Na_2S_2 and Na_2S_4.

One of the main problems encountered in the polarographic study of S_x^{2-} was the characterization of the polysulfide species present in solution, i.e., the evaluation of x, the number of sulfur atoms present in the polysulfide species. The pentasulfide ion (S_5^{2-} was considered by Schwarzenbach and Fischer (27) to be the only stable polysulfide species in solution. However, studies by Arnston, Dickson and Tunnel (28), based on solubility measurements of aqueous solutions saturated with elemental sulfur, showed that the average number of sulfur atoms in S_x^{2-} is 4.8, which appears consistent with the coexistence of tetra- and pentasulfide ions. Giggenbach (29) studied the absorption spectra of the individual S_x^{2-} species and established the equilibrium distribu-

tion of various species present in an aqueous solution at room temperature. Giggenbach found no indication of the presence of any S_x^{2-} ion with x greater than 5, implying that the value of 4.8 is the average number of sulfur atoms for a polysulfide solution. According to Giggenbach, any aqueous polysulfide solution saturated with elemental sulfur at 20°C contains, approximately, equal amounts of tetra- and pentasulfide ions, with an average value of x being 4.6 ± 0.1. The results of studies reported in this dissertation are consistent with Pringle's conclusions (5) that a single polysulfide species is present in a solution of sulfide saturated with S^o corresponding to the pentasulfide ion, S_5^{2-}.

Flow Injection Analysis

Flow injection analysis (FIA) is a type of continuous analysis that utilizes a carrier stream into which reproducible aliquots of analyte are injected. The analyte is either carried directly to a detector, or it may be detected after being mixed with an appropriate reagent stream that facilitates detection. Nagy, Feher and Pungor, in 1970, were the first to describe the injection of a sample into a flowing stream of electrolyte (30). The stream passed through a magnetically stirred mixing chamber and over the surface of a silicone rubber-based graphite electrode. Later, in 1974, Ruzicka and Hansen (31) in Denmark, and Stewart, Beecher and Hare (32) in the U.S. simultaneously modified the technique by achieving controlled mixing within

the stream by flow-induced dispersion as the carrier stream passed through tubing of narrow diameter as opposed to the gross mixing affected by the bulk stirring of the sample in a larger chamber. Earlier, it had been assumed by Skeggs (33) that the presence of air bubbles in the carrier stream was necessary to limit the sample dispersion and effect mixing of sample with the reagent stream. Numerous publications have now appeared demonstrating that all these functions are accomplished without the use of air segmentation and that the use of continuous flow technique offers many more advantages. The extent of dispersion can be altered through variable flowrates, baseline stability is greater because of no interruption of detector response, and sample throughput can be very high. FIA is in widespread use for performing chemical analyses in flowing streams because of high sample throughput, reproducibility and reliability using inexpensive instrumentation. In many ways, FIA resembles closely liquid chromatography (LC). For example, both involve use of a sample-injection device, small (<100 μL) sample volumes, flow streams are unsegmented, flowrates can be varied, and peak height or peak area can be used for analytical quantification. As a result of the similarity of the detector functions in FIA and LC, the former is frequently utilized to test the reliability of detectors which ultimately are to be applied for LC.

Flow injection analysis was performed by injecting a small volume of unknown sample into a continuously flowing stream of solvent which eventually flows through an electrochemical detector.

Liquid Chromatography with Electrochemical Detection

Among the many approaches to detection in high performance liquid chromatography (HPLC), the three types emerging as most popular are: multiwavelength UV-VIS absorption, fluorescence, and electrochemical detection. Recently (34), liquid chromatography with electrochemical detection (LCEC) has been used with considerable success in solving a variety of analytical problems. The method offers mainly the distinct advantages of selectivity, sensitivity and economy. The chief consideration in determining the suitability of electrochemical detection is to find the voltammetric behavior of the species of interest in an appropriate mobile phase that can either be used directly as the supporting electrolyte or can be conveniently modified in order to serve this purpose.

Blaedel and Todd (35) used LCEC even before the advent of HPLC. They applied a flow-through polarographic detector for the continuous amperometric determination of Cd(II), Cu(II) and Pb(II), separated by a cation-exchange column; and for fumaric and maleic acid separated by an anion-exchange column at concentrations down to 10^{-6} M. Robertus, Cappell and Bond (36) used a similar method for the analysis of mixtures of Co(II), Cu(II), Ni(II) and Mn(II) in the concentration range of ca. 2-20 ppm. They used post-column mixing to provide an appropriate supporting electrolyte for the polarographic detection. Blaedel and Todd further utilized their flow-through polarographic detector

for the continuous determination of α-amino acids (37) in ion-exchange effluents. Buchanan and Bacon (38) used a flow-through cell with square-wave polarography for the continuous monitoring of Cu(II), Pb(II), Cd(II) and Zn(II) in ion-exchange effluents. Veradi, Feher and Pungor (39) used what they called chromato-voltammetry for the determination of purine bases at concentrations as low as 10^{-10} M.

The polarographic method was used by Drake (40) in 1950 for the continuous monitoring of proteins in column effluents with amperometric detection in the potential range of -1.8 to -2.0 V. Polarographic detection was developed further by Kemula (41) who made a significant contribution in cell design. Kemula demonstrated his detector in the complete separation and quantitative determination of Cu(II) and Co(II). Many more developments and improvements have been made since then in cell design and applications (36,42-47). Wasa and Musha (48) constructed a polarographic microdetector for liquid chromatography and described characteristics of the flow cell with a horizontal DME (HDME) and a mercury-plated platinum (Hg-Pt) electrode. The detector was utilized for the chromatographic analysis of a mixture of nitropyridine derivatives using an ion-exchange column.

Johnson and co-workers have developed a general methodology for the trace-level determination of ionic species in complex aqueous solutions using liquid chromatographic separation with in-stream electrochemical detection (49-53). Lown, Koil and Johnson (54) developed a Pt wire flow-through electrode for the detection of I^- and As(III).

Maitoza and Johnson (55) applied a polarographic detector using reverse pulse amperomery (RPA) for detection of metal ions in the column effluents without the requirement of deoxygenation. The RPA is based on the application of a square wave with a large negative initial potential for the deposition of the metal ion followed by a positive potential pulse for the anodic stripping of the deposited metal. The signal is measured during the anodic stripping process at a potential where oxygen is not electroactive. Hsi (56) applied this detection method recently for the determination of a mixture of heavy transition metal ions in limestone, ground water and power-plant water. Hughes and Johnson developed the pioneering method of detecting carbohydrates (57-58) on a miniature Pt electrode using a triple-step potential waveform in caustic HPLC effluents. The waveform automatically processes the electrode potential through the sequence of values for detection at -0.4 V, oxidative cleaning at +0.8 V followed by reduction with adsorption at -1.0 V. The purpose of using a triple-step potential waveform is to maintain a high and uniform electroactivity that ensures reproducible anodic detection. Conversely, the electrode response at a constant potential decays virtually to zero in a few seconds because the products of electrode reaction remain adsorbed on the electrode surface inhibiting the adsorption and detection of unreacted analyte molecules. The time of the execution of the waveform is sufficiently short (ca. 0.5-1 s) to allow continuous monitoring of the column effluent. The detection limits achieved were significant-

ly lower than reported for conventional refractive index detection. Polta and Johnson (59) applied the method of Hughes and Johnson for the determination of primary and secondary amino acids using Pt electrodes in alkaline anion-exchange chromatography effluents, achieving ng-levels of detection. The amperometric detection based on complex potential-step waveforms is becoming widely known as Pulsed Amperometric Detection (PAD) and has been commercialized by Dionex Corporation, Sunnyvale, CA.

Two recent and extensive reviews are worth mentioning. Fundamental aspects and numerous analytical applications of electrochemical detectors have been reviewed by Ryan (60), and Kissinger reviewed the applications of electrochemistry in LCEC (61).

Many organic sulfur-containing compounds are electroactive and can be determined by LCEC. Typical applications are the determinations of thiols (62), thioureas, thioamides (63) and isocyanates in urine (64), thiourea herbicides (65), pesticides such as parathion and methylparathion (46,66-67), cysteine in plasma and urine (68), homocysteine in plasma (68), cysteine and related compounds (69), penicillamine in blood and urine (70) and in plasma and albumin (71), and glutathione and cysteine in fruit (72). The electrodes used include the DME (64,66-67), Hg pool (69-73), and carbon paste (63). It has been found that amperometric detection is more sensitive than UV detection for many of these compounds. Thiols are electroactive on mercury electrode (63). Bard and Lund (74) have compiled extensive

polarographic characteristics about the anodic oxidation of thiols and other organic compounds. Pollard, McOmie and Jones (75) separated thionic acids by paper chromatography using the solvent system isopropylacetone-aqueous potassium acetate. Qualitative separation of polythionates (tri, tetra, penta- and hexathionate) was achieved also by Bighi, Trabanelli and Pancaldi (76), and Scoffone and Carini (77); but none of these authors applied their separations to the quantitative determination of these compounds for unknown samples. The separations were done on anion-exchange column using gravity flow and fraction collection. Wolkoff and Larose (78,79) separated the polythionates using fluorescence detection. Chapman and Beard (80) used an activated carbon column with UV detection; none of the procedures yielded satisfactory results (81). Story (4) developed a method for the determination of individual inorganic sulfur species in mixtures containing sulfide, sulfite, thiosulfate, sulfate, tri-, tetra, penta- and hexathionate employing high speed ion exchange chromatography for separation. He utilized the complex-formation reaction of Fe(III) with sulfate (81) as the basis for the spectrophotometric detection. The separated sulfur species in the column effluent undergo continuous in-stream oxidation with bromine to form sulfate followed by the addition of Fe(III) perchlorate to the effluent stream. The detection method was claimed to be specific for all inorganic sulfur species and capable of detecting up to 1 µg of sulfur. Detection was free also of interferences from UV-absorbing organic materials.

Based on research work presented in this dissertation, it is concluded that sulfide, sulfite, thiosulfate and polysulfide are easily detected polarographically in flow-through cells of small effective dead volume useful for flow injection analysis and liquid chromatography. Sulfide, sulfite and thiosulfate are separated by high performance liquid chromatography (HPLC) and the detection of sulfide, sulfite, thiosulfate and polysulfide is demonstrated by using the dropping mercury electrode (DME) as the HPLC-detector in the analysis of process-stream samples derived from the caustic desulfurization of coal samples.

CHAPTER III. CURRENT-POTENTIAL CURVES

Principles

Polarography is the general classification for all voltammetric techniques of electroanalysis applied to dropping mercury electrode (DME). A DME can be constructed from a glass capillary with an internal diameter of ca. 5×10^{-3} cm which is fed by a mercury reservoir of 20 to 100 cm height. Mercury issues through the capillary to form a nearly spherical drop which grows with time until it becomes too heavy to be supported by the surface tension. Typically, a mature drop has a diameter of ca. 0.1 cm and a drop life of 1-5 s. For reaction of an electroactive species, the electrode current is recorded as a function of potential applied to the DME according to the convention presented in Figure 1. The potential axis is defined, traditionally, with respect to a saturated calomel electrode (SCE). However, any electrode providing a stable and reproducible potential can be used to provide a reference potential. The mechanics of obtaining polarograms (i-E curves) are described in most textbooks of experimental electrochemistry (82).

There are several important subclassifications of polarography, including so called "constant-current" polarography (DCP), a misnomer since it is the potential and not current which is controlled in DCP; sampled dc polarography (SDCP); and normal pulse polarography (NPP). These subclassifications differ on the basis of the nature of the po-

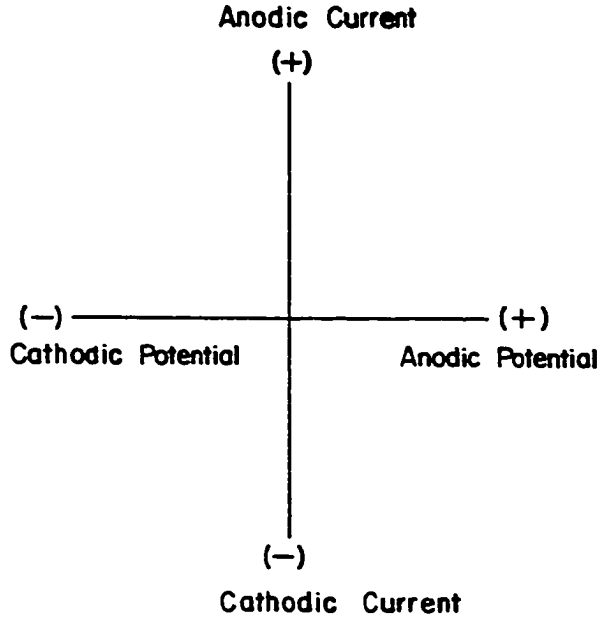

Figure 1. Format for polarographic current-potential (i-E) curves

Current, amps
Potential, volts vs. SCE

tential-time (E-t) waveforms applied and the manner of current measurement. They are described here briefly. In DCP, the electrode potential is varied slowly as a linear function of time as shown in Figure 2 (curve a). The electrode current is recorded as a continuous function of time (i.e., potential); and the i-E curve, called a polarogram, consists of a series of oscillations representing the current recorded as the drop grows and falls, periodically.

In SDCP, the potential is changed linearly with time as in DCP; however, the current, instead of being recorded continuously throughout the drop-life, is sampled electronically just before the drop falls. That value of sampled current is stored in the memory of the potentiostat and presented continuously to the recorder until being updated by the value sampled from the next drop. The i-E curve for SDCP, thus recorded, is a relatively smooth trace of the sampled current versus the applied potential without the record of wild oscillations observed in DCP. In NPP, the electrode is held at an initial potential, E_i, where almost no faradaic current flows, over the majority of the lifetime of a single drop. After a fixed waiting period of Δt, shown in Figure 2 (part b), the potential is changed abruptly by an increment, ΔE, applied for the pulse period, t_p, and the current is measured shortly before the drop falls. The value of ΔE is advanced for each successive drop in a manner simulating the linear scan in curve a of Figure 2. The detail of the waveform in curve b (Figure 2) for a single drop is shown by the enlargement in curve c.

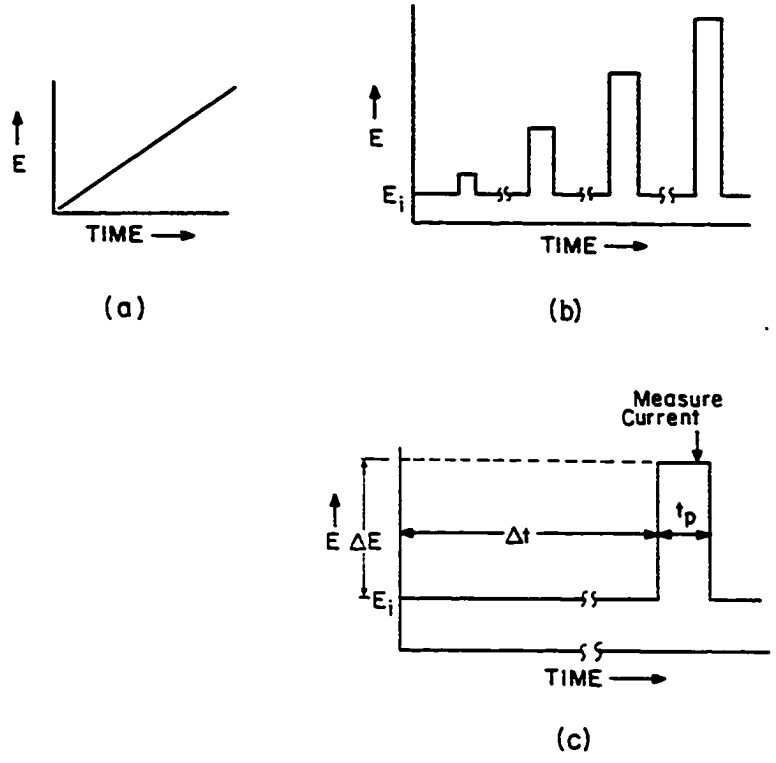

Figure 2. The potential waveforms

a. The applied potential as a function of time in DC polarography (DCP) and sampled DC polarography (SDCP)
b. The applied potential for NPP
c. Detail shown for waveform in curve b for a single drop

The three polarographic techniques, DCP, SDCP and NPP, were used in this work. Drop lifetimes for the DME were controlled mechanically in a fashion synchronized automatically with the waveform chosen. Values of drop lifetime could be chosen to be 0.5, 1.0, 2.0 and 5.0 s. The mass-transport limited current (i_{lim}), of a polarographic wave is related to the bulk concentration of the electroactive species in solution according to equation 1

$$i_{lim} = nFADC^b/\delta \tag{1}$$

where

i = electrode current (coul/s)

n = the number of electrons involved in the electrode process (equiv/mol),

F = the Faraday constant (96,486 coul/equiv),

A = the area of the electrode (cm^2),

D = the diffusion coefficient of electroactive species (cm^2/s)

C^b = the bulk concentration of electroactive species (mol/cm^3)

δ = the thickness of the Nernst diffusion layer (cm).

The empirical relationship given by equation 1 may be derived <u>ab initio</u> from the identity (82)

$$i = dQ/dt \tag{2}$$

where

Q = electrical charge (coul)

t = time (s).

The number of moles electrolyzed (N) is given by

$$N = Q/nF \tag{3}$$

Thus,

$$dN/dt = d/dt(Q/nF)$$
$$= (1/nF)(dQ/dt) \tag{4}$$

or

$$dN/dt = i/nF \tag{5}$$

Because the electrode reactions are heterogeneous, i.e., they occur only at the electrode-electrolyte interface, the reaction rates are expressed in units of mol/s per unit area of electrode surface. Therefore,

$$dN/dt = i/nFA = \text{mol/s cm}^2 \tag{6}$$

The quantity on the left-hand side of equation 6 is recognized as the flux (J) of the electroactive species.

$$J = dN/dt = D(dC/dx)_{x=0} \tag{7}$$

and, hence,

$$i = nFAD(dC/dx)_{x=0} \tag{8}$$

where x is the distance from surface of electrode and dC/dx is the con-

centration gradient measured normal to the electrode surface.

A concentration profile for the incomplete conversion of electroactive species reaching the electrode surface, i.e., $i < i_{lim}$, is shown in Figure 3. The concentration gradient in equation 8 is given approximately by

$$(dC/dx)_{x=0} = (C^b - C^s)/\delta \tag{9}$$

where C^s is the concentration at the electrode surface and δ, illustrated in Figure 3, is the thickness of the diffusion layer. When the applied electrode potential is large enough, i.e., $E >> E^o$, such that all of the electroactive species reaching the electrode surface undergoes immediate reaction, then $C^s = 0$ and the limiting current is given by

$$\underset{C^s \to 0}{\text{limit } i} = i_{lim} = nFADC^b/\delta \tag{10}$$

The current under this situation is limited only by the rate of mass transfer of the electroactive analyte to the surface of the electrode.

The equation of convective-diffusional mass transport has been solved exactly (82) for the three polarographic cases represented here. For DCP,

$$\delta = \left(\frac{D\pi t}{7/6}\right)^{1/2} \tag{11}$$

and

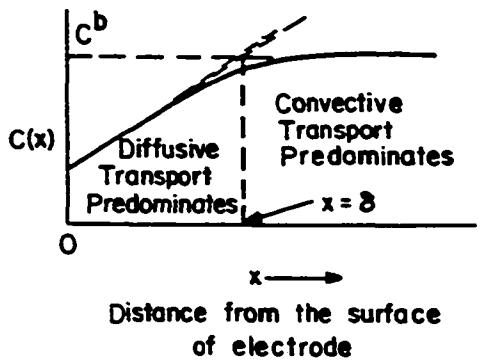

Figure 3. Concentration of electroactive species as a function of distance from the electrode surface

δ = the Nernst diffusion layer thickness

$$i_{lim} = (7/6)^{1/2}\, nFA(D/\pi t)^{1/2}\, C^{b} \qquad (12)$$

The area of a DME is a function of time, t(s), and the mass flowrate, m (mg/s), of Hg flowing through the glass capillary as given by

$$A = 4\pi\left(\frac{3mt}{4\pi d_{Hg}\ 1000}\right)^{2/3} \qquad (13)$$

where d_{Hg} is the density of Hg (13.6 g/cm^3). Substitution of A from equation 13 into equation 12, with evaluation of constants, gives the familiar Ilkovic equation for DCP at a DME:

$$i_{lim,DCP} = 706nm^{2/3}\, D^{1/2}\, t^{1/6}\, C^{b} \qquad (14)$$

In SDCP, i_{lim} is sampled at the end of the drop life, $t = \tau$,

$$i_{lim,SDCP} = 706nm^{2/3}\, D^{1/2}\, \tau^{1/6}\, C^{b} \qquad (15)$$

For NPP,

$$\hat{\delta} = (D/\pi t)^{1/2} \qquad (16)$$

and

$$i_{lim,NPP} = nFA(D/\pi t_p)^{1/2}\, C^{b}$$

$$= \frac{460nm^{2/3}\, \tau^{2/3}\, D^{1/2}\, C^{b}}{t_p^{1/2}} \qquad (17)$$

where τ is the drop lifetime at which the current is measured and t_p is the pulse time for the waveform.

The residual anodic wave obtained at a DME in the absence of an analyte that can react with Hg(I,II) corresponds to the half-reaction (83)

$$2Hg \rightarrow Hg_2^{2+} + 2e; \quad E^o = 1.03 \text{ V} \tag{18}$$

The concentration of Hg^{2+} formed is about one-hundredth that of Hg_2^{2+} (7). The i-E curve may, therefore, be described on the basis of the Nernst equation for the Hg_2^{2+}/Hg couple.

$$E = E^o_{Hg_2^{2+},Hg} + (RT/2F)\ln [Hg_2^{2+}]_{x=0} \tag{19}$$

The surface concentration of Hg_2^{2+}, i.e., $[Hg_2^{2+}]_{x=0}$ is described by

$$[Hg_2^{2+}]_{x=0} = (i_{l,c} - i)/2FA(D/\delta)_{Hg_2^{2+}} \tag{20}$$

where $i_{l,c}$ is the limiting cathodic current, which is zero in this case. Hence, equation 19 becomes

$$E = E^{o'}_{Hg_2^{2+},Hg} - (2.303RT/2F)\log[\frac{i}{2FA(D/\delta)_{Hg_2^{2+}}}] \tag{21}$$

Since the DME is a limitless source of mercury, there is no anodic limiting current plateau. Alternatively, equation 21 can be written as

$$i = 2FA(D/\delta)_{Hg_2^{2+}} \exp\left(\frac{E - E^o_{Hg_2^{2+},Hg}}{2.30RT/nF}\right) \tag{22}$$

Polarographic studies of sulfide and polysulfide were performed in alkaline solutions to prevent volatilization of toxic H_2S. An anodic wave is obtained for hydroxide ions at the DME in an alkaline solution (83) at approximately +0.08 V according to the reaction

$$Hg + 2OH^- \rightarrow Hg(OH)_2 \rightarrow HgO \cdot H_2O + 2e, \; E^o = +0.08 \text{ V} \qquad (23)$$

When 0.1 M NaOH is used as a supporting electrolyte, no practical value for the limiting current plateau can be obtained for OH^- within the current limits of the stripchart recorder. This is shown by the curve marked "The Residual Current" in Figure 4.

Experimental

Analytical grade chemicals were used throughout without further purification. A stock solution of sodium sulfide (Na_2S) was prepared using deoxygenated, triply distilled water, and the solution was stored under nitrogen. To minimize air oxidation of sulfide, small aliquots of the concentrated stock solution were transferred by microsyringe to a known volume of aqueous supporting electrolyte solution, previously deoxygenated with high-purity nitrogen.

Stock solutions of Na_2S_x with a maximum value of x were prepared by mixing an excess of elemental sulfur in aqueous Na_2S under nitrogen and stirring the solution continuously for 3-4 days until the solution turned an orange-red color of constant intensity. To minimize air oxidation, the stock solutions were stored under nitrogen. Small aliquots

of the concentrated stock solution were transferred directly to the polarographic cell containing deoxygenated electrolyte solution. It is noted here that the results described in a later section verified Pringle's (5) conclusion that the maximum number of x is 5. Hence, the soluble species in this stock solution will be referred to as Na_2S_5 (or S_5^{2-}).

Solutions of R_4NOH, where R stands for methyl, ethyl and tertiary butyl groups, were prepared fresh by passing the corresponding aqueous R_4NBr solutions through an anion exchange column in the hydroxide form. The solutions of R_4NOH thus obtained were standardized by titrating with primary standard potassium hydrogen phthalate.

The anti-oxidant buffer (AOB) solution was prepared by dissolving 250 g of sodium acetate, 65 g of ascorbic acid and 85 g of NaOH in 600 mL of distilled water and diluting to 1 L. This solution was diluted 1:1 with distilled water for using as the supporting electrolyte.

Sulfide solutions were standardized by oxidation to sulfate by KIO_3 in alkaline solution according to a method by Vogel (84). A 10-mL aliquot of the sulfide solution (ca. 0.01 M) was mixed with 15 mL of 0.1 N KIO_3 (3.5666 g/L KIO_3) and 10 mL of 10 M NaOH. The solution was boiled gently for 10 min, cooled, and 5 mL of 5%-KI solution and 20 mL of 4 M sulfuric acid solution were added. The liberated iodine was titrated with 0.1 N sodium thiosulfate solution. The normality of sulfide solutions is 8 times the molarity because the electron change from sulfide to sulfate is 8. The iodine formed in the determination represents the unused iodate, which must be subtracted from the initial

iodate to obtain the equivalents of periodate consumed which, in turn, represents the equivalents of sulfide. Thus,

$$N_{sulfide} = (15N_{KIO_3} - N_{th}V_{th})/10 \quad (24)$$

$$M_{sulfide} = (15N_{KIO_3} - N_{th}V_{th})/(8)(10) \quad (25)$$

where the subscript "th" designates thiosulfates

The polysulfide solution was standardized also using the iodometric method outlined above. In this case, only the ionic sulfur, not S^o, is determined (85).

Polarograms were recorded using a Princeton Applied Research (PAR) Model 174-A Polarographic Analyzer and a PAR Model K23 DME kit, with a Model 1747 drop knocker and a three-electrode polarographic cell. A Houston Instruments Model RE 0074 X-Y recorder was employed. A 22-gauge platinum wire was used as auxiliary electrode. All potentials reported are relative to the saturated calomel electrode (SCE). The applied potential was monitored using a Dynascan Model 2P3 Digital Multimeter. The supporting electrolyte solutions were transferred to the polarographic cell and deoxygenated by dispersing nitrogen for 5 min. An aliquot of concentrated stock solutions of Na_2S was transferred to the polarographic cell using a micrometer buret and the mixture purged for an additional 1 min. A blanket of nitrogen was maintained over all solutions while the polarographic measurements were made to minimize air oxidation of sulfide.

Cyclic voltammograms were obtained using the Pine Instruments Model RDE2 potentiostat and Houston Instruments Model RE 0074 X-Y recorder.

The potential scan was monitored by a Hewlett Packard Model 3466A Digital Multimeter. A three-electrode cell employing a hanging mercury drop electrode (HMDE), a 22-gauge platinum auxiliary electrode, and a saturated calomel electrode were used.

Results and Discussion

Sulfide

Sulfide is detected at a dropping mercury electrode on the basis of the anodic current from the reaction:

$$Hg + S^{2-} \rightarrow HgS + 2e \qquad (26)$$

The i-E curve of a 0.1 mM sulfide solution in 0.1 M NaOH is shown in Figure 4. The half-wave potential is observed to be -0.76 V, which agrees well with the value reported in the literature (83). As the sulfide ion concentration is increased beyond 0.2 mM, a distortion, marked "d" in Figure 5, is observed in the rising portion of the wave. HgS, the product of the anodic electrode reaction, is insoluble and stays at the surface of the electrode forming a protective film around the mercury drop. The film restricts the electron-transfer reaction and is responsible for the discontinuity, d, observed in the rising portion of current in the i-E curve shown in Figure 5. As the potential is scanned further in the positive direction, the inhibited electron transfer reaction is again able to proceed at a transport-limited rate because of the additional energy applied at the higher anodic potentials. The current keeps rising past the distortion until it levels off corresponding to the diffusion-limited region of the wave. A com-

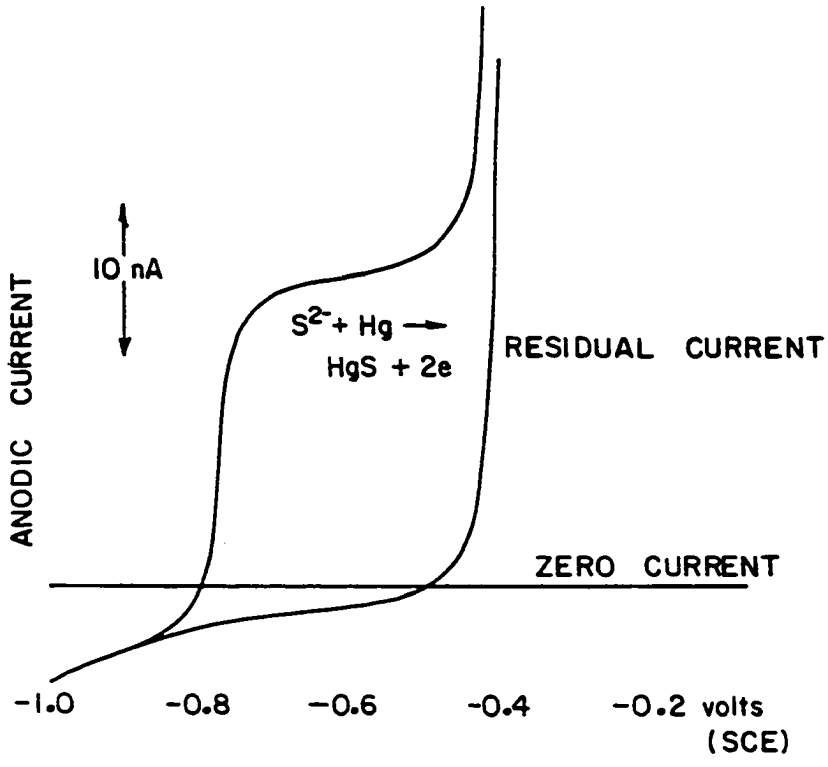

Figure 4. Polarographic behavior of Na_2S

SDCP
0.1 M Na_2S
1:1 anti-oxidant buffer solution
DME, 1 s
5 mV/s
Anodic current: $Hg + S^{2-} \rightarrow HgS + 2e$

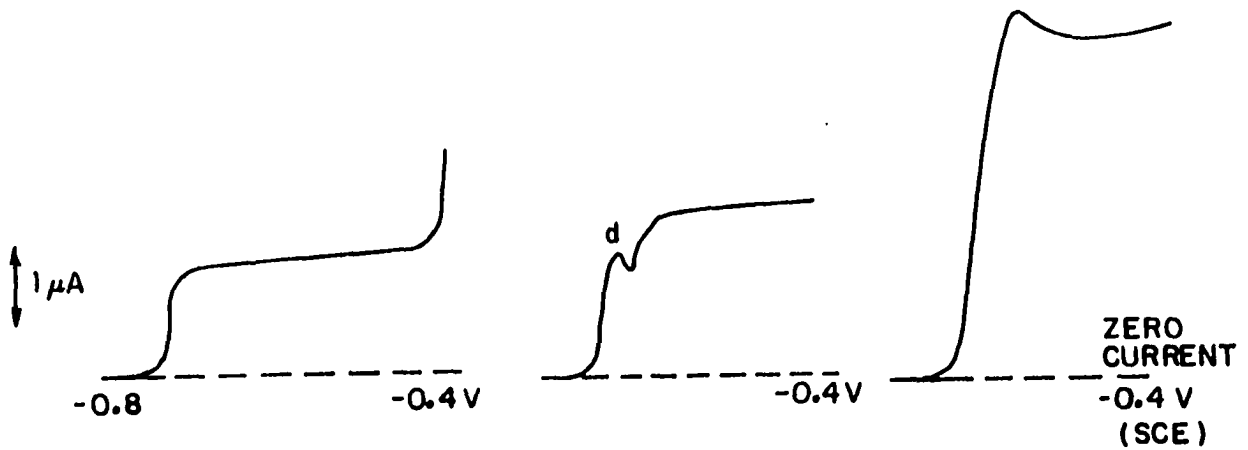

Figure 5. Formation of the insoluble HgS film at the electrode surface

a. SDCP, 0.2 mM S^{2-}

b. SDCP, 0.3 mM S^{2-}

c. NPP, 0.3 mM S^{2-}

d. The distortion because of HgS film

parison of the polarogram from SDCP for 0.3 mM Na_2S with that from NPP at the same concentration shows that no distortion appears for NPP. In the NP mode, as described earlier, the drop is held at the "initial potential" at which no reaction occurs for the majority of drop life except during the pulse when the potential is stepped to the limiting current region of potential. The pulse duration is only ca. 50 ms, as opposed to 1000 ms for the drop lifetime. During the shorter pulse time, not enough HgS is produced to cover completely the surface of the electrode; consequently, a smooth polarographic wave is obtained. At very high concentrations, enough HgS is formed and the distortion will appear even for the NPP mode.

A similar decrease in current in the rising portion of the i-E curve of S^{2-} is observed at longer drop time. For a 0.2 mM S^{2-} solution, a well-behaved polarographic wave is obtained as long as the drop time is 1 sec or less, but the distortion appears when the drop time is increased to 2 secs or more. Obviously, at a longer drop time the electrode reaction continues for a longer period of time producing a larger quantity of HgS that covers the surface of electrode to a greater extent, thereby hindering further reaction at the electrode surface.

Polysulfide

The polarographic response for a 0.14 mM solution of Na_2S_5 in 0.1 M NaOH is shown in Figure 6. Anodic and cathodic waves are obtained. The reactions responsible for the two processes are

$$S_x^{2-} + Hg \rightarrow HgS_x + 2e \quad \text{(anodic process)} \qquad (27)$$

$$S_x^{2-} + 2(x-1)e \rightarrow xS^{2-} \quad \text{(cathodic process)} \qquad (28)$$

The anodic reaction takes place in the potential range of -0.77 V to -0.2 V, whereas the cathodic reaction occurs in the range of -1.8 V to -0.77 V.

It is readily apparent in Figure 6, that instead of a limiting cathodic current plateau, a minimum is observed in the region of -1.8 V to ca. -0.95 V. This is explained as follows: The cathodic current shown by the segment abc in Figure 6 is obtained by the reduction of S_x^{2-}. Sulfide, the product of the cathodic reaction, is a surface-active anion (83) and adsorbs strongly on the surface of mercury electrode. The adsorbed anionic sulfide on the already negatively charged Hg surface repels electrostatically the anionic polysulfide, thereby restricting the approach of the latter to the reaction plane in the double-layer region. As a result, the electron-transfer reaction for S_x^{2-} is impeded and the current follows the segment abc instead of the expected plateau marked ac and indicated by the dashed line in Figure 6. At a very low polysulfide concentration, not enough S^{2-} ions are produced to saturate the surface of the electrode. Hence, the electron transfer reaction is expected to proceed at a moderate rate. This was confirmed for a very small S_x^{2-} concentration as seen in Figure 7.

Zhadanov and Kiselev (86) obtained polarographic curves for the reduction of sulfur in alcoholic solution containing $LiClO_4$ similar to those in Figure 7 and proposed the following reaction sequence for

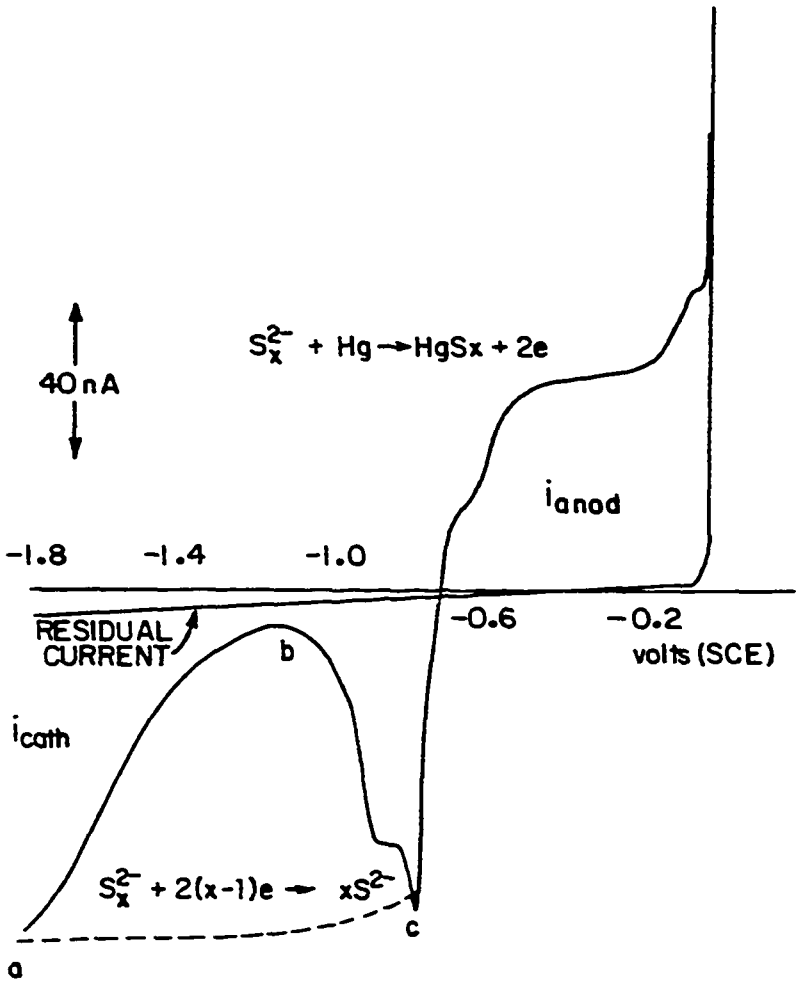

Figure 6. The polarographic behavior of Na_2S_5
0.14 mM Na_2S_5
0.1 M NaOH
SDCP
DME, 1 s
10 mV/s

Figure 7. The limiting cathodic current plateau at very low polysulfide concentration

Na_2S_5
SDCP
DME, 1 s
0.1 M carbonate buffer, pH 9

No.	S_5^{2-}, µM
0	0
1	20
2	40
3	60
4	100
5	140
6	180
7	220
8	260
9	320
10	380

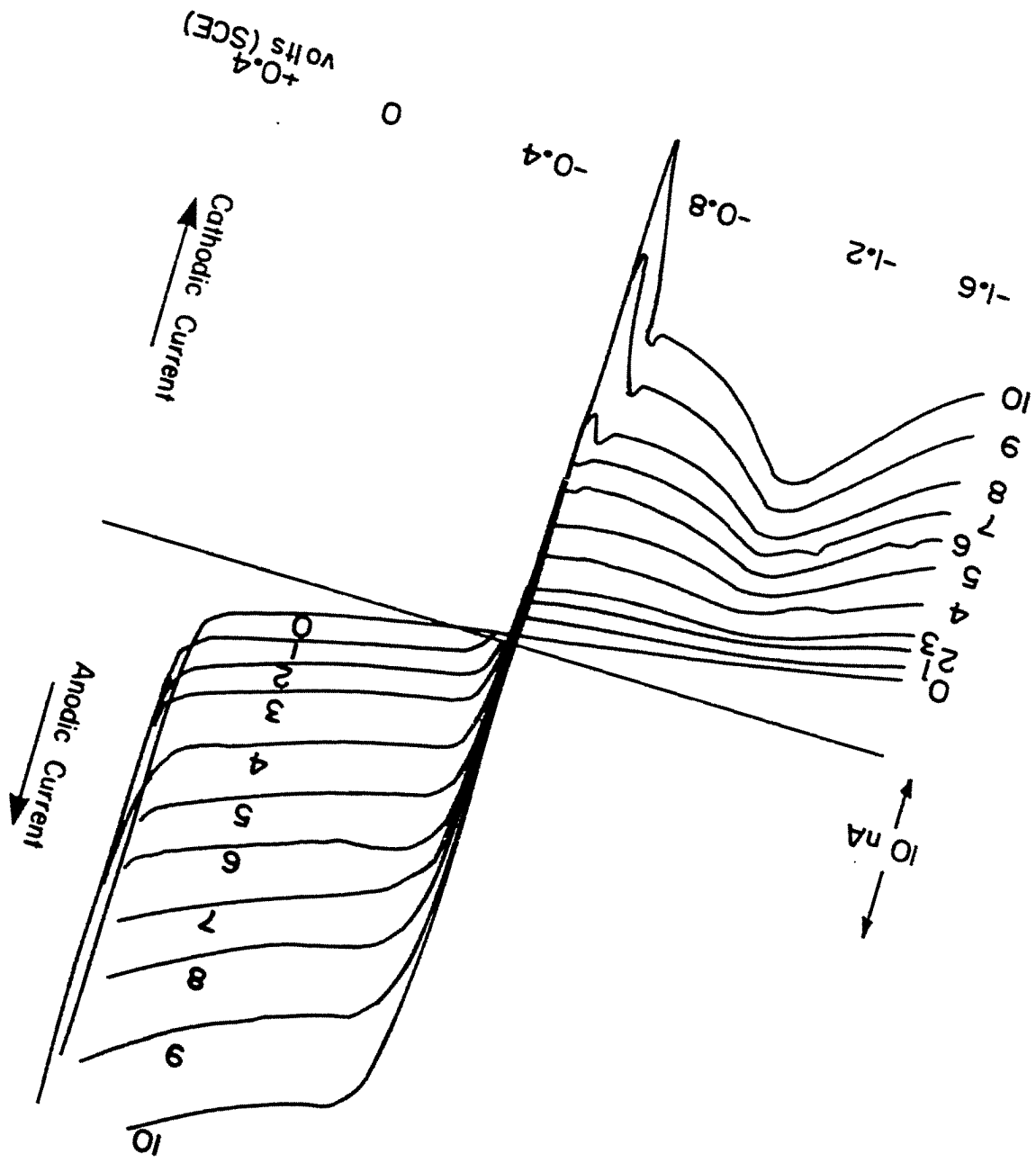
+0.4
Volts (SCE)
0
-0.4
-0.8
-1.2
-1.6
Cathodic Current
10
9
8
7
6
5
4
3
2
1
0
10 nA
0
1
2
3
4
5
6
7
8
9
10
Anodic Current

the reduction of sulfur at the DME:

$$Hg + S^{o} \rightarrow HgS \quad (29)$$

$$HgS + 2e \rightarrow Hg + S^{2-} \quad (30)$$

$$S^{o} + S^{2-} \rightarrow S_2^{2-} \quad (31)$$

$$S_2^{2-} + 2e \rightarrow 2S^{2-} \quad (32)$$

net: $$S^{o} + 2e \rightarrow S^{2-} \quad (33)$$

They attributed the minimum in the cathodic wave to inhibition of the reduction of S_2^{2-} by the negative charge of the electrode and observed that the minimum deepened after addition of Na_2S, which they concluded to correspond to the shift of the equilibrium in equation 31 to the right. A suppression of the cathodic current by addition of S^{2-} to a solution of S_5^{2-} was not observed in research reported here, as is demonstrated in Figures 8 and 9 and Table 1. Therefore, the results given by Zhadanov and Kiselev are concluded to be questionable. Zhadanov and Kiselev (86) reported that elemental sulfur not only enters into reaction with S^{2-} ions to yield S_x^{2-} ions, but also forms addition compounds with the supporting electrolyte, e.g., $S_8ClO_4^-$, S_8K^+ and $S_8Bu_4N^+$. They deduced the formation of these addition compounds on the basis of electrophoretic measurements and on the observation that the minimum disappeared after the addition of Bu_4NBr.

A series of i-E curves for solutions with successively increasing concentrations of Na_2S_5 are shown in Figure 10. The current changes sign from negative to positive value at ca. -0.72 V. A second anodic wave with a half-wave potential at ca. -0.50 V appears at concentrations

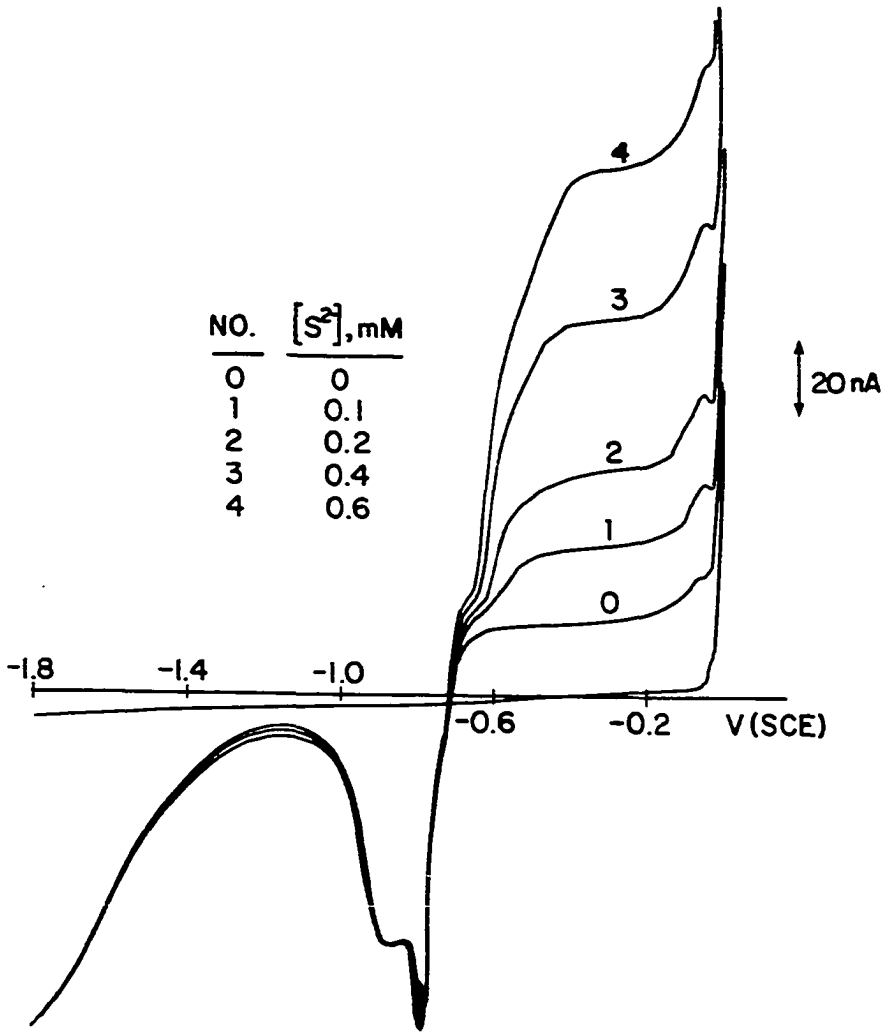

Figure 8. Standard additions of sulfide to a solution of Na_2S_5

SDCP
DME, 1 s
0.1 M NaOH
anodic current measured at -0.3 V

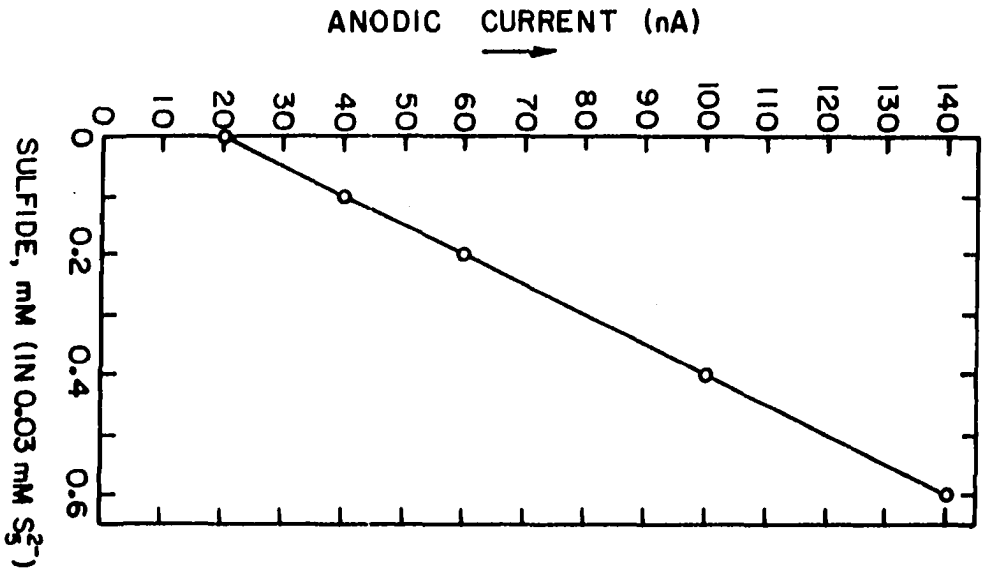

Figure 9. Standard additions of Na_2S to a 0.14 mM solution of Na_2S_5

SDCP
DME, 1 s
0.1 M NaOH
anodic current measured at -0.3 V

Table 1. Standard additions of S^{2-} to a 0.14 mM S_5^{2-} solution

No.	$[S^{2-}]$, mM	i_{anodic} nA (-0.2 V)	$i_{cathodic}$ nA (-1.8 V)
0	0	20	80
1	0.1	40	80
2	0.2	60	80
3	0.4	100	80
4	0.6	140	80

$\geq$ 0.3 mM. The wave at -0.50 V may be attributed to the formation of subsequent layers of insoluble HgS at the electrode surface, after the completion of a monolayer corresponding to the wave having $E_{\frac{1}{2}}$ value of -0.72 V. This behavior is consistent with the i-E curves in Figure 11 showing the effect of increasing concentration of Na_2S. The additional waves at potentials positive of -0.60 V were established by Canterford and Buchanan (11) to occur because of the reaction of the same anion, sulfide and reported the formation of up to three waves corresponding to the formation of successive layers of HgS at the electrode surface. Such multiple waves were reported earlier by Werner and Konopik (24). They attributed the first wave ($E_{\frac{1}{2}}$ = -0.58 V) to the reaction of S_x^{2-} and the second wave ($E_{\frac{1}{2}}$ = -0.80 V) to that of S^{2-}. However, based on my observations, it seems more probable that the multiple waves appear because of the reaction of S^{2-} only, each additional wave corresponding to the deposition of a new monolayer of HgS at the

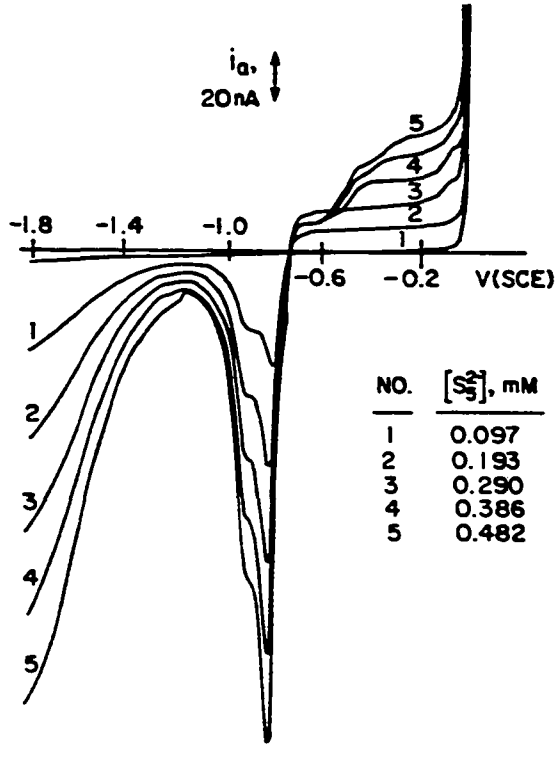

Figure 10. The i-E curve of Na_2S_5

SDCP
DME, 1 s
0.1 M NaOH

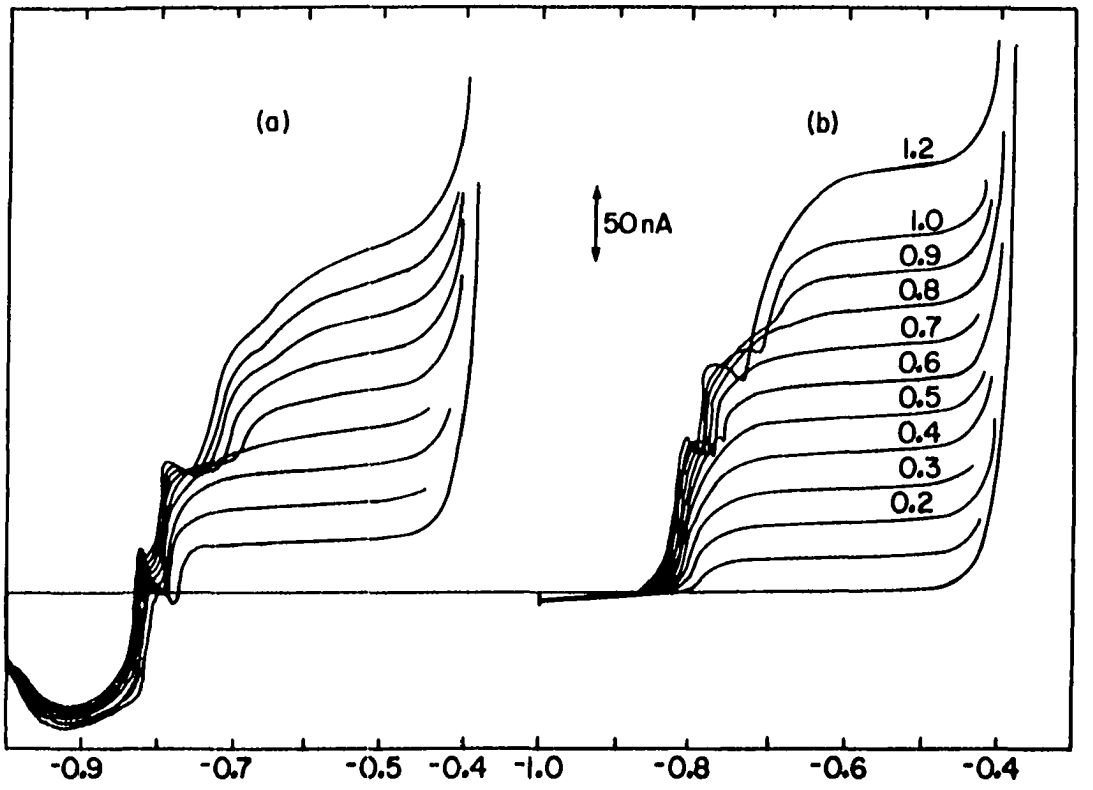

Figure 11. Concentration dependence of the i-E curves

SDCP

DME, 1 s

a. S_x^{2-} b. S^{2-}

surface of electrode.

It is noted from Figures 8 and 9 and Table 1 that when standard additions of S^{2-} are made to a solution of S_x^{2-} the total anodic current is the sum of the constituent anodic currents for S^{2-} and S_x^{2-}. It is concluded, therefore, that S^{2-} and S_x^{2-} exist as noninteracting species in solution. It is evident from the variability of explanations offered in the literature that the case of possible reequilibration which might occur when S^{2-} is added to a solution of S_x^{2-}, to produce a polysulfide of smaller x value, has not yet been resolved. Calculations based on free energy data (87) given in Table 2 show that reactions between S^{2-} and S_5^{2-} are spontaneous (i.e., $\Delta G^\circ < 0$) as shown in Table 3.

Experimental results are presented in the next section which confirm the conclusion that, whereas the reaction, $S^{2-} + S_{x=5}^{2-} \rightarrow S_{x<5}^{2-}$ is thermodynamically allowed, the reaction is not appreciable on the time scale of polarographic analysis.

Determination of maximum x in S_x^{2-} Polysulfide is reduced to sulfide through reaction 28 in the potential range -1.8 to -0.8 V. The number of electrons involved in the cathodic process is a direct function of the number of sulfur atoms present in the S_x^{2-} ion, $n = 2(x-1)$. In principle, therefore, it should be possible to vary the cathodic current by varying the number of sulfur atoms, x, in S_x^{2-} for the same S_x^{2-} concentration.

Increasing amounts of elemental sulfur were added to Na_2S solu-

Table 2. ΔG_f^o (86) for the reactions involving S^{2-} and S_x^{2-}

Reaction	$\Delta G^o_{f,298}$ K cal/mol
Na_2S (aq) + S → Na_2S_2 (aq)	-1.5
Na_2S (aq) + S → Na_2S_3 (aq)	-1.4
Na_2S_3 (aq) + S → Na_2S_4 (aq)	-1.1
Na_2S_4 (aq) + S → Na_2S_5 (aq)	-0.9
Na_2S (aq) + 4S → Na_2S_5 (aq)	-4.9

Table 3. ΔG_f^o values for formation of various S_x^{2-} species by reaction of S^{2-} and S_5^{2-} calculated from values in Table 2

Reaction	$G^o_{f,298}$ K cal/mol
$Na_2S_5 + 3Na_2S \rightarrow 4Na_2S_2$	-1.5
$Na_2S_5 + Na_2S \rightarrow 2Na_2S_3$	-0.9
$Na_2S_5 + Na_2S \rightarrow Na_2S_4 + Na_2S_2$	-0.6

tion in eight volumetric flasks such that the mole ratio of Na_2S:S^o was 1:1, 1:2, 1:3, 1:4, 1:5, 1:6 and 1:7. Mixing was done under nitrogen with magnetic stirrers. After ca. 48 hours, it was observed that the elemental sulfur had completely dissolved in the flasks with S^{2-}:S^o up to 1:4, whereas some sulfur remained undissolved in the flasks marked onwards. Aliquots of each solution were withdrawn and i-E curves were

obtained. The results are presented in Table 4 and Figure 12. The cathodic current is expected to level off at the maximum value of x for S_x^{2-}.

The solutions prepared were orange-yellow in color which made it apparent that the value of x could be investigated spectrophotometrically. Based on the absorption spectrum obtained by using a Perkin Elmer Model 552 spectrophotometer, the absorbance of all eight solutions of

Table 4. Polarographic determination of x in S_x^{2-}

S_x^{2-} solution	$i_{cathodic}$, nA (-1.75 V)	$i_{cathodic}$, nA (-0.9 V)
1:0	0	0
1:1	28	28
1:2	60	63
1:3	102	92
1:4	128	114
1:5	128	114
1:6	122	118
1:7	126	119

S_x^{2-} was measured at 365 nm. The data are given in Table 5 and plotted in Figure 13 which confirm that the maximum value of x is 5.

Polysulfide is precipitated quantitatively by adding excess Zn^{++} ions. The ZnS_x precipitate so obtained can be acidified to liberate H_2S and elemental sulfur. The precipitated sulfur is separated by fil-

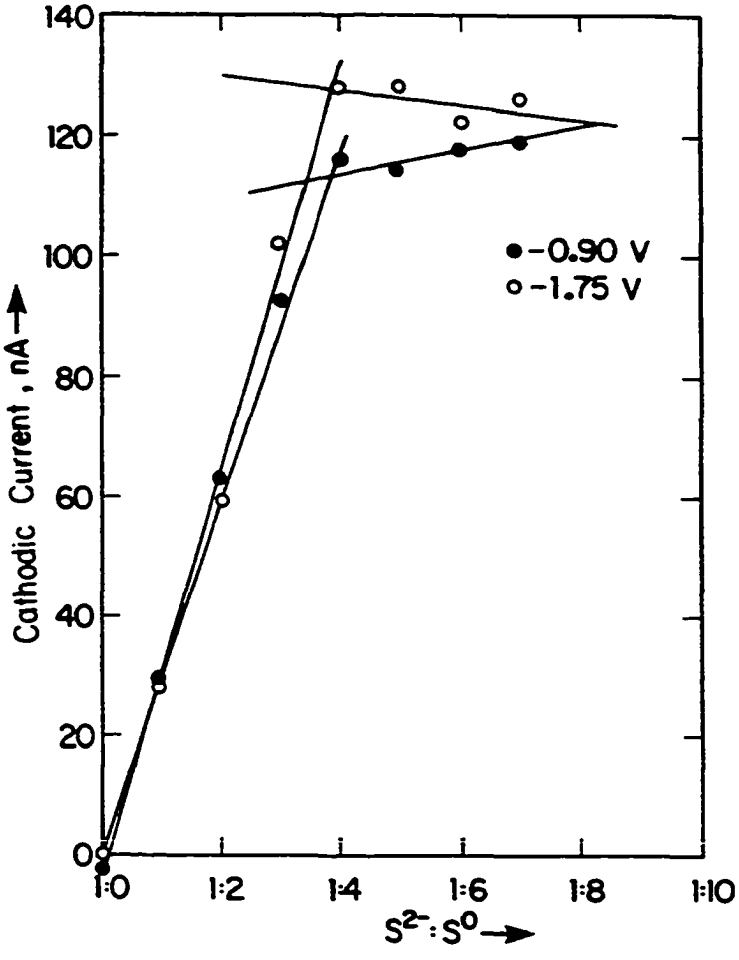

Figure 12. The limiting cathodic currents of S_x^{2-} solutions containing increasing amounts of S^o in AOB

SDCP
DME, 1 s
Cathodic current measured at -0.90 V and -1.75 V

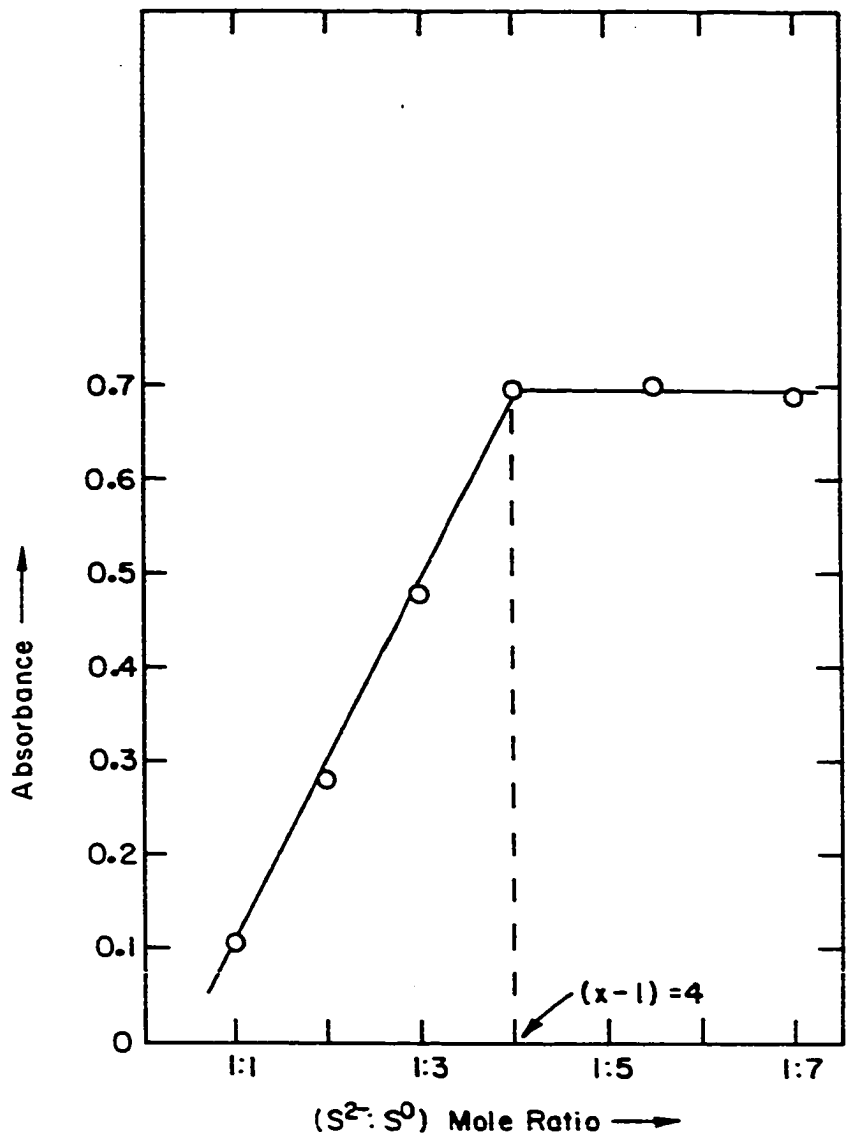

Figure 13. The spectrophotometric measurement of x in S_x^{2-}
0.5 mM Na_2S
λ_{max} = 365 nm

Table 5. Spectrophotometric determination of x in S_x^{2-}

$S^{2-}:S^{o}$ ratio in S_x^{2-} solution	Absorbance
1:1	0.105
1:2	0.276
1:3	0.481
1:4	0.698
1:5	0.700
1:6	0.698
1:7	0.688

tration, dried and weighed to determine x in S_x^{2-}. A plot of the weight of sulfur precipitate versus the mole ratio of $S^{2-}:S^{o}$ is shown in Figure 14 and Table 6.

Table 6. Gravimetric determination of x in S_x^{2-}

$S^{2-}:S^{o}$ ratio in S_x^{2-} solution	Weight of sulfur, g
1:1	50.63
1:2	107.19
1:3	146.70
1:4	193.30
1:5	204.00
1:6	187.50
1:7	203.10

Figure 14. The gravimetric determination of x in S_x^{2-}

$$S_x^{2-} + Zn^{++} \rightarrow AnS \cdot S_{x-1}$$

$$ZnS \cdot S_{x-1} + 2H^{+} \rightarrow Zn^{++} + H_2S + (x-1)S^{o}$$

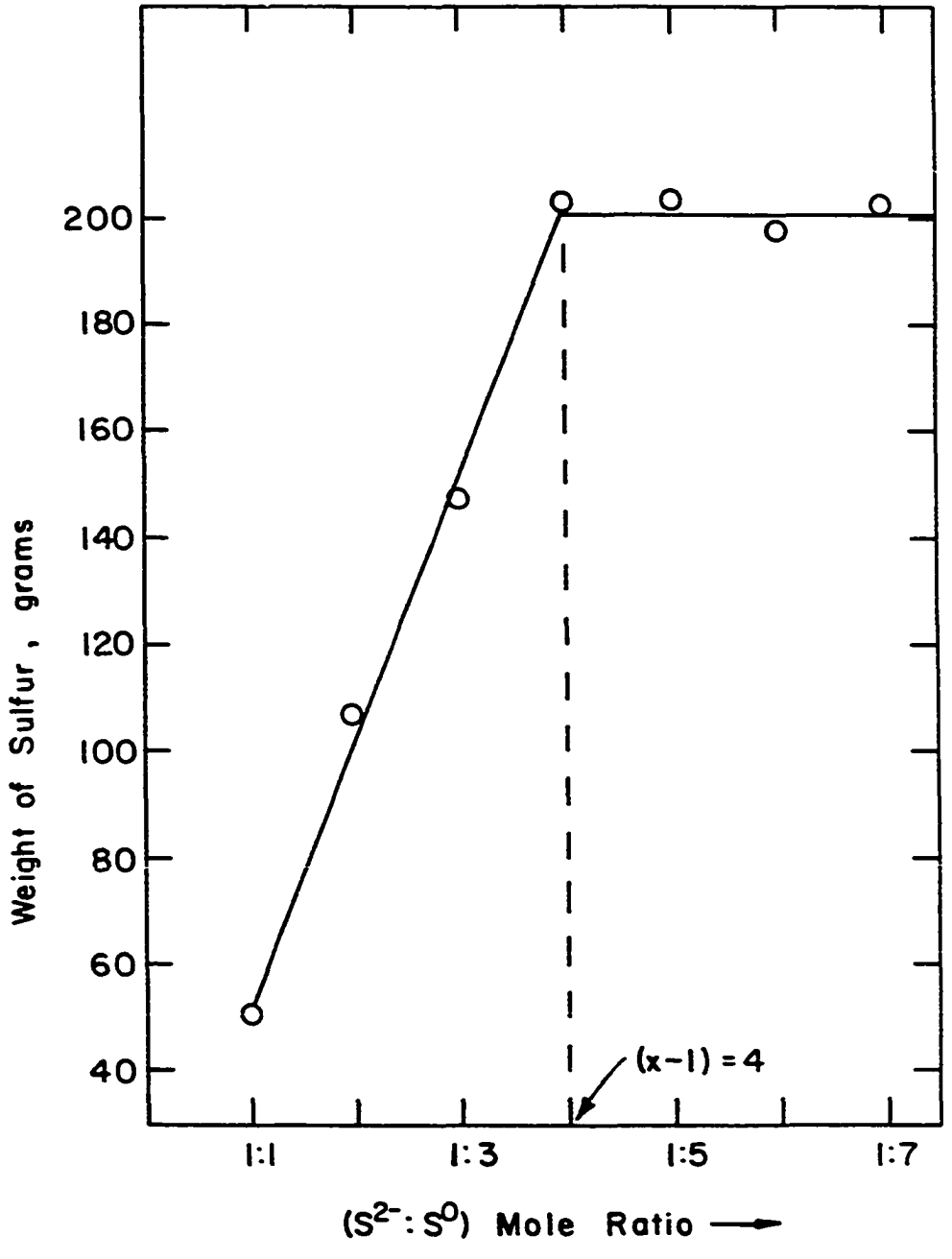
200
180
160
140
120
100
80
60
40
Weight of Sulfur, grams
(x-1) = 4
1:1
1:3
1:5
1:7
(S2-: S0) Mole Ratio

Based on the data obtained using the polarographic, spectrophotometric and gravimetric methods, it is therefore concluded that the maximum value of x in S_x^{2-} is 5. This conclusion is in full agreement with that of Pringle (5).

The diffusion coefficients of S_x^{2-} species The limiting anodic and cathodic currents plotted as a function of total sulfur (mM S^o), instead of mM S_x^{2-} are shown in Figures 15 and 16, respectively. It is very apparent from these plots that as x increases in S_x^{2-}, the diffusion coefficient decreases dramatically. Furthermore, the variation of diffusion coefficient with x is not a linear function of x. It was observed in Figure 6 that the i-E curve of S_x^{2-} solution consists of an anodic and a cathodic wave. The limiting currents for these waves can be represented by equation 10 already described. Here a and c signify anodic and

$$i_{l,a} = -n_a FAD\, C^b/\delta \tag{34}$$

$$i_{l,c} = n_c FAD\, C^b/\delta \tag{35}$$

cathodic values, respectively. The anodic reaction was given by equation 27 where the value of n_a is 2. Taking the ratio of limiting anodic and cathodic currents represented above and substituting $n_a = 2$, the number of electrons for the cathodic reaction, of any polysulfide anion, S_x^{2-}, can be calculated by

$$n_{x,c} = 2(i_{l,c}/i_{l,a}) \tag{36}$$

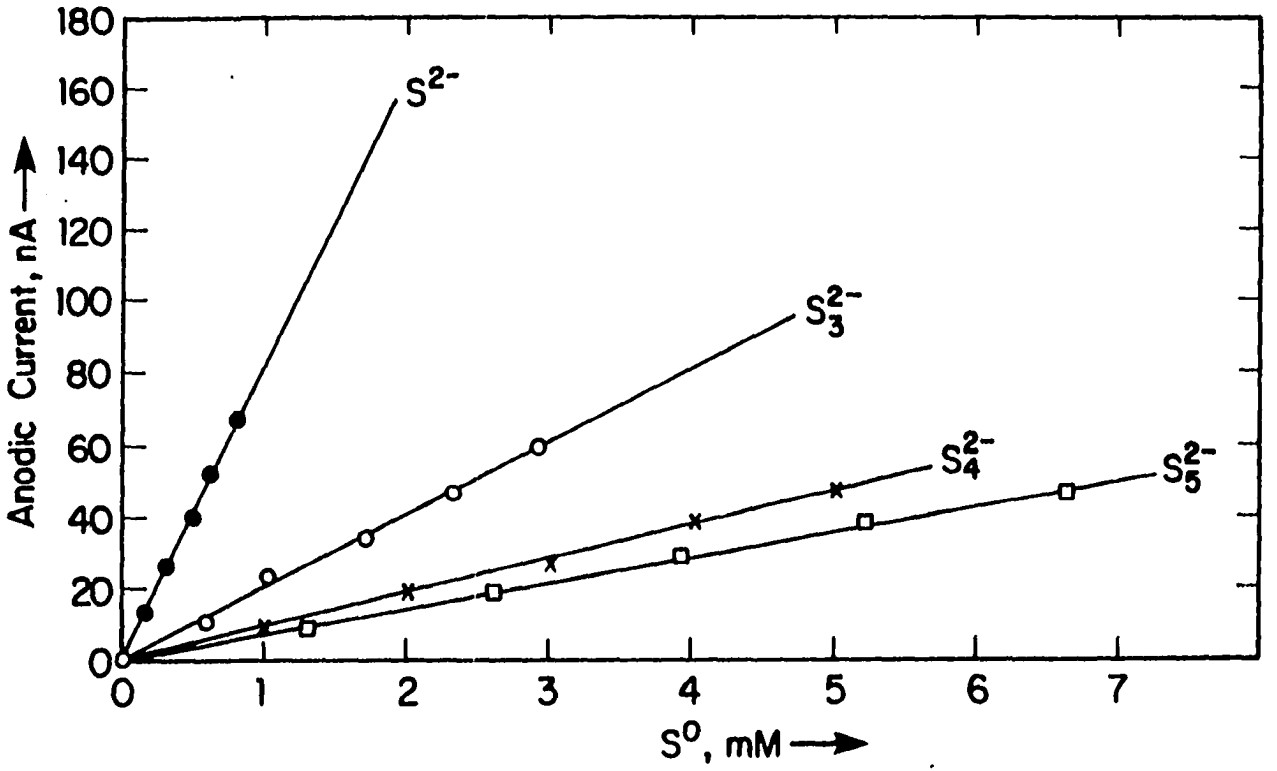

Figure 15. The anodic currents of S_x^{2-} solutions containing increasing amounts of S^o
SDCP
DME, 1 s
The anodic current measured at -0.3 V

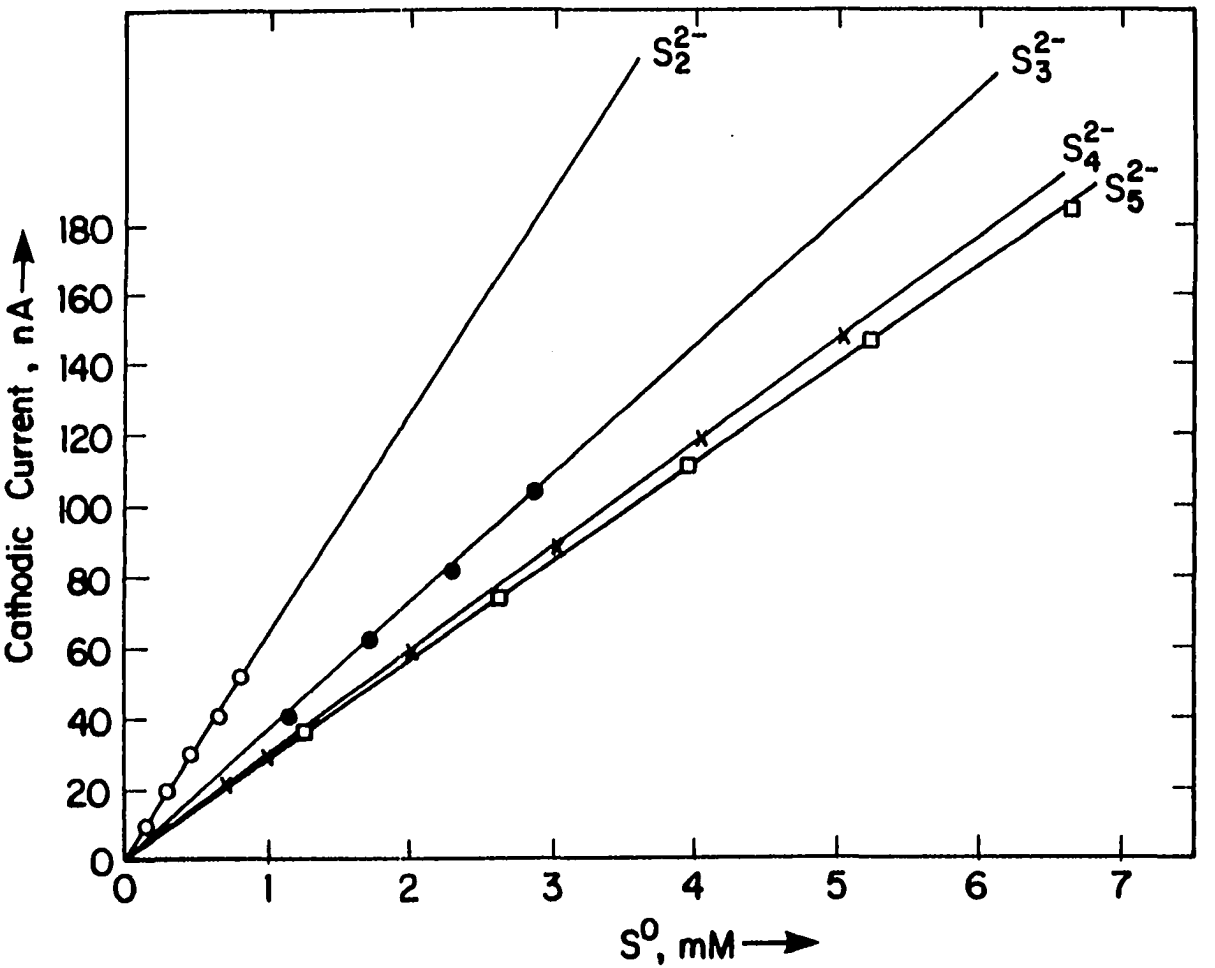

Figure 16. The cathodic currents of S_x^{2-} solutions containing increasing amounts of S^o
SDCP
DME, 1s
The cathodic current measured at -1.75 V

This relationship can be used to calculate the number of electrons apparently involved in the cathodic reaction, $n_{x,c,app}$ for any S_x^{2-} species. The results of these calculations are presented in Table 7 in comparison to theoretical values, $n_{x,c,theor}$, for solutions with integral values of x.

The relative diffusion coefficients can be calculated from the ratio of limiting anodic currents of S^{2-} and S_x^{2-} from their respective i-E curves.

$$\frac{i_{l,S^{2-},a}}{i_{l,S_x^{2-},a}} = \left(\frac{n_{a,S^{2-}}}{n_{a,S_x^{2-}}}\right)\left(\frac{D_{S^{2-}}}{D_{S_x^{2-}}}\right)^{1/2} \tag{37}$$

The number of electrons involved in the anodic reactions for S^{2-} and S_x^{2-} is 2. The ratio of the limiting anodic currents for S^{2-} and S_5^{2-} can be obtained by taking the ratio of slopes of the calibration curves for the corresponding solutions. The relative diffusion coefficients calculated accordingly are given in Table 7.

Alternatively, the ratio of diffusion coefficients for S^{2-} and S_x^{2-} can be calculated by equation

$$\frac{i_{l,a,S^{2-}}}{i_{l,c,S_x^{2-}}} = \left(\frac{n_{a,S^{2-}}}{n_{c,S_x^{2-}}}\right)\left(\frac{D_{S^{2-}}}{D_{S_x^{2-}}}\right)^{1/2} \tag{38}$$

Assuming n_c for S_5^{2-} to be 8, the ratios calculated are shown in Table 8. There is excellent agreement between the values for $D_{S^{2-}}/D_{S_x^{2-}}$ determined by the two methods.

Table 7. Calculation of the number of electrons involved in cathodic reaction of S_x^{2-} species

S_x^{2-}	i_c/mM	i_a/mM	i_c/i_a	$n_{x,c,app}$	$n_{x,c,theor}$
S^{2-}	-	155.56	-	-	0
S_2^{2-}	64.71	83.33	0.78	1.6	2
S_3^{2-}	75.00	40.91	1.83	3.7	4
S_4^{2-}	86.67	28.57	3.03	6.1	6
S_5^{2-}	105.26	26.92	3.91	7.8	8

Table 8. Relative diffusion coefficients of various S_x^{2-} species using the anodic and cathodic current data

Calculation based on	D_1/D_5 [a]	D_2/D_5	D_3/D_5	D_4/D_5
The anodic currents	33.1	9.5	2.5	1.2
The cathodic currents	NA	9.5	2.3	1.1

[a] D_i represents the diffusion coefficient of a S_x^{2-} species for i=x thus, D_2 is the diffusion coefficient of S_2^{2-} and so on.

The largest error is observed for S_x^{2-} species having the lower x values. The S_x^{2-} solutions, as already mentioned, were prepared by allowing to react the stoichiometric amounts of S^{2-} and S^o necessary to produce S_x^{2-} at equilibrium if the reaction is quantitative. It appears that the reaction is not quantitative, particularly for the formation

of S_2^{2-} and S_3^{2-}, which is reflected by a large negative error in n for these S_x^{2-} species. It is concluded from the results in Table 8 that the values of diffusion coefficients decrease drastically as x increases from 2 to 5.

The cathodic current plateau for S_x^{2-} For an electroactive species, it is customary to obtain a current plateau that corresponds to the diffusion-limited transport of electroactive species to the electrode surface. Since the cathodic current plateau could not be obtained for S_5^{2-} using NaOH as the supporting electrolyte, an attempt was made to find out why such a plateau is lacking and, whether such a plateau is obtainable. The analytical implications of obtaining a current plateau is that since the current is virtually independent of applied potential in the plateau region, small variations in applied potential will be inconsequential to analytical precision and accuracy.

The i-E curve of an S_5^{2-} solution, using Me_4NOH instead of NaOH as the supporting electrolyte, is shown in Figure 17. A well-defined cathodic current plateau is observed. Tetramethylammonium ions (Me_4N^+) are adsorbed and are expected to decrease the extent of S^{2-} adsorption. Hence, the adsorbed species is cationic which eliminates or substantially decreases the repulsive effect of adsorbed S^{2-} and the cathodic reaction proceeds unimpeded. A decrease in the plateau current is observed if the size of the alkyl group (R) increases in R_4NOH molecule. The i-E curves of 0.4 mM S_x^{2-} solutions in tetramethyl-, tetraethyl-

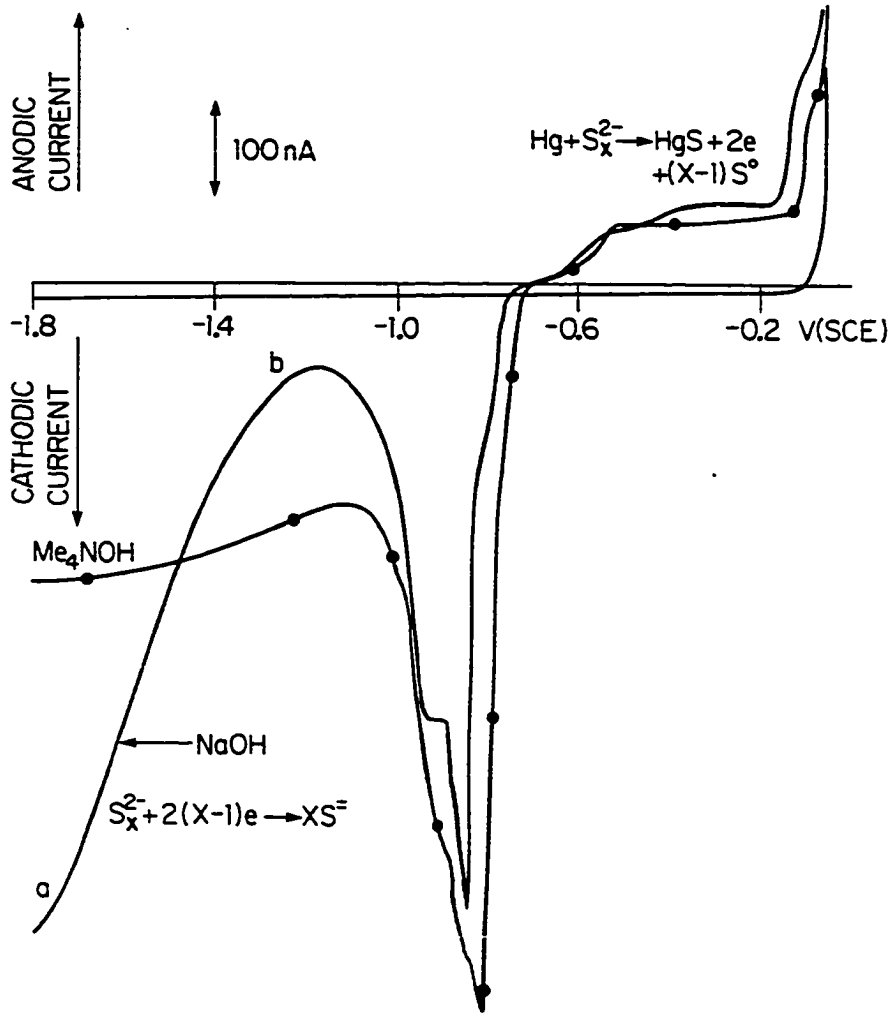

Figure 17. Polarographic behavior of Na_2S_5 using Me_4NOH as the supporting electrolyte

0.4 mM Na_2S_5
0.1 M Me_4NOH
SDCP
DME, 1 s

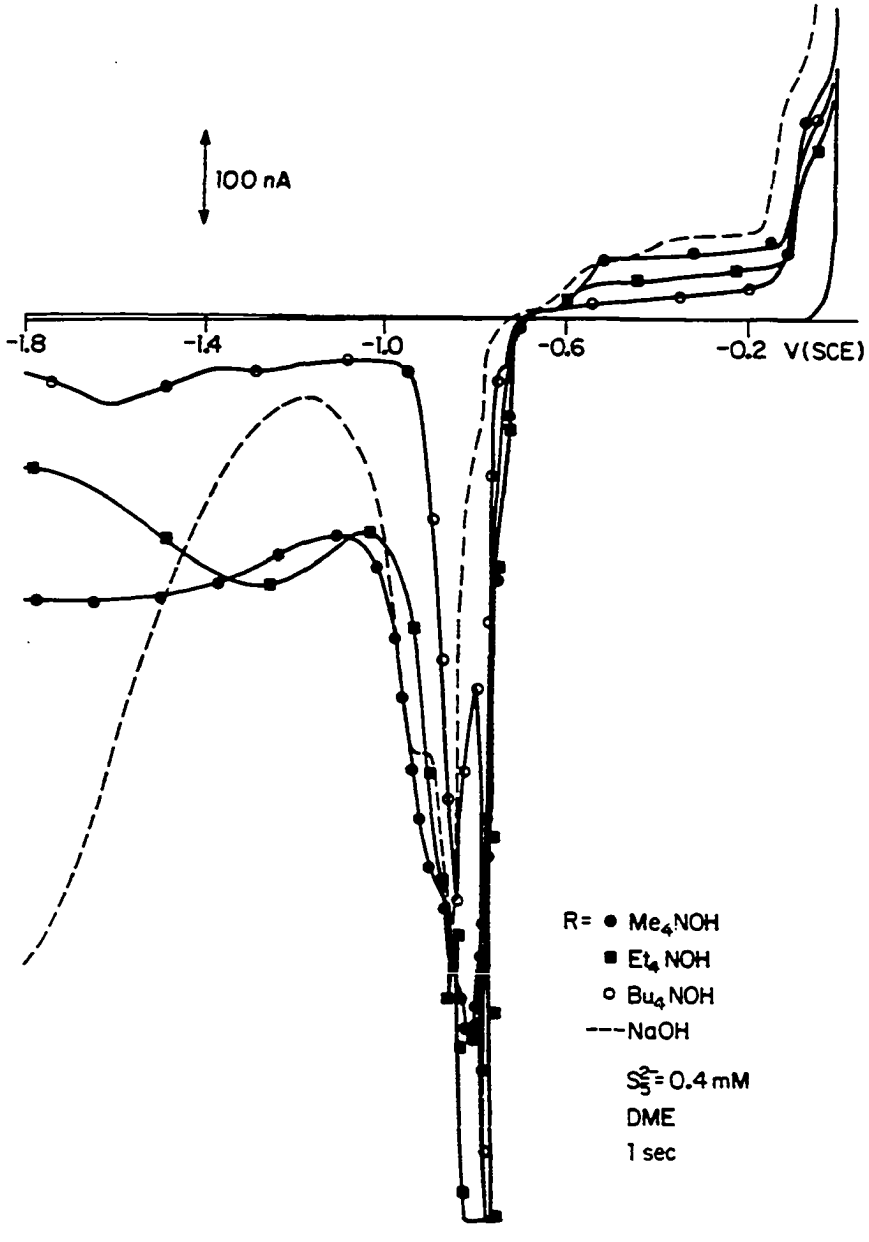

Figure 18. The i-E curves of Na_2S_5 using R_4NOH as the supporting electrolyte (R = alkyl group)

0.4 mM Na_2S_5

0.1 M R_4NOH
SDCP
DME, 1 s

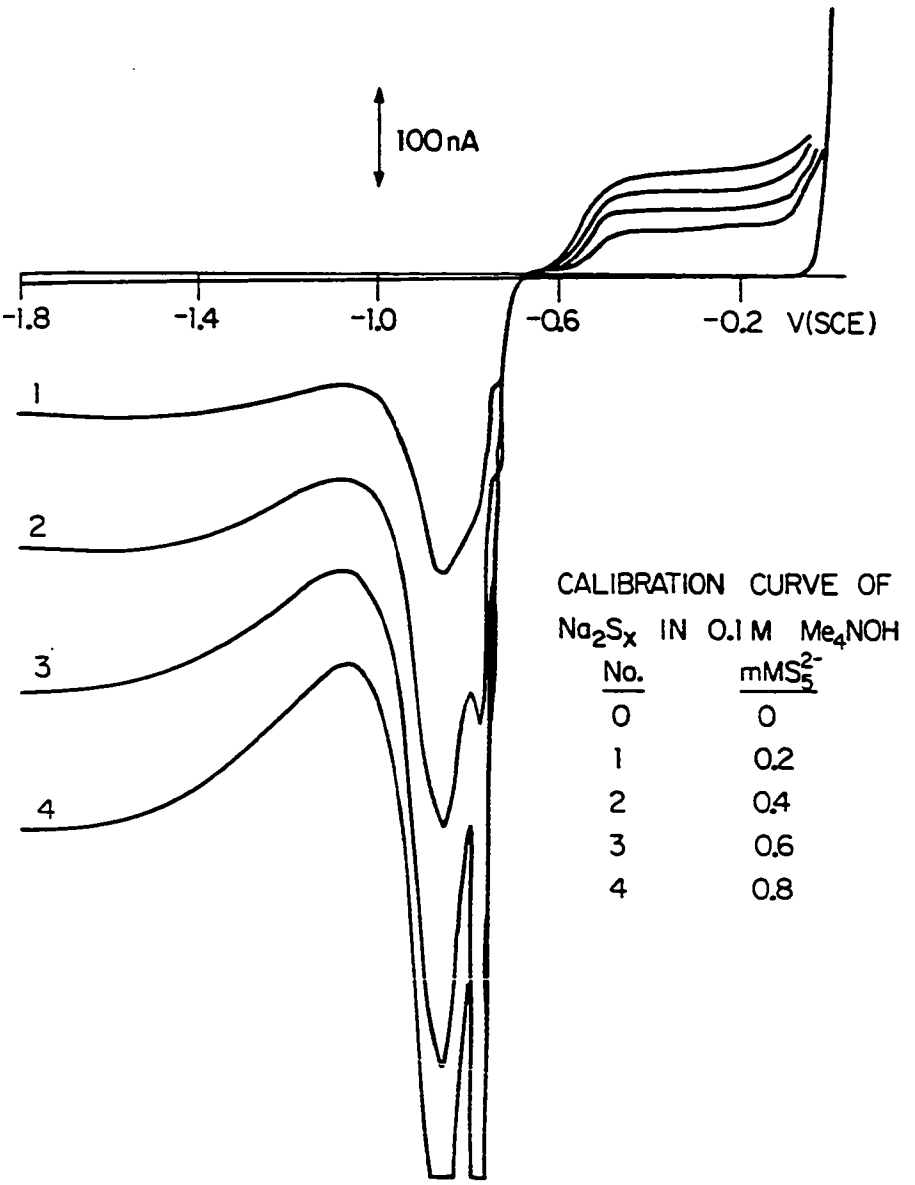

Figure 19. The i-E curves for Na_2S_5 in 0.1 M Me_4NOH
SDCP
DME, 1 s

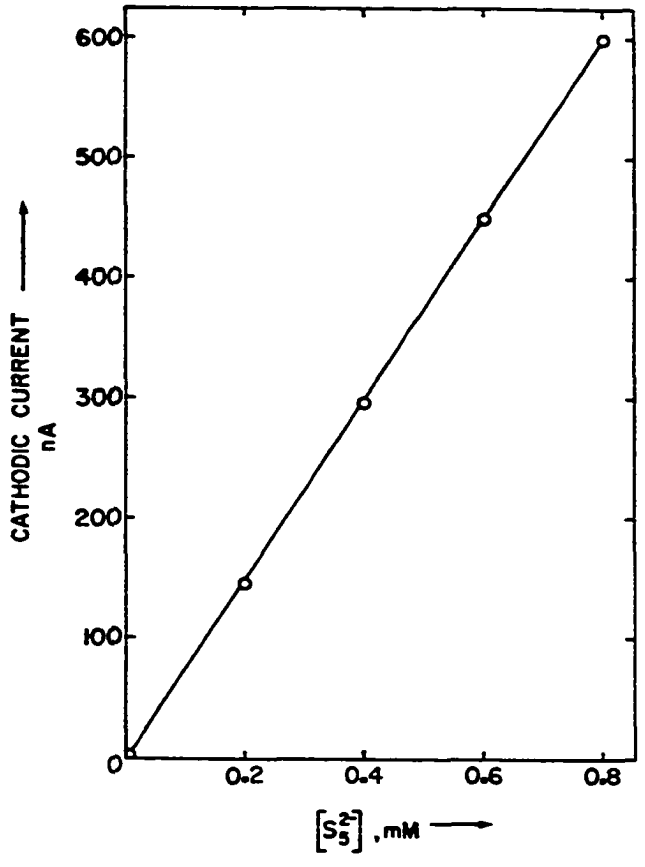

Figure 20. The calibration curve of Na_2S_5 in 0.1 M Me_4NOH

SDCP
DME, 1 s

and tetrabutylammonium hydroxide are shown in Figure 18. The current decreases with progressively increasing size of the alkyl group. This is expected because the extent of adsorption should increase with the increasing hydrophobic character of the more bulky R_4N^+ cations, leaving fewer reaction sites on the mercury drop electrode for S_x^{2-}.

The i-E curces for different concentrations of Na_2S_5 in 0.1 M Me_4NOH are shown in Figure 19. The limiting cathodic current data obtained from Figure 19 are given in Table 9 and plotted in Figure 20. The current-concentration plot is observed to be linear with a correlation coefficient, r, of 1.00.

Table 9. The cathodic currents of S_5^{2-} using Me_4NOH as the supporting electrolyte

No.	$[S_5^{2-}]$, mM	$i_{cathodic}$ (nA)
1	0	0
2	0.2	145
3	0.4	290
4	0.6	450
5	0.8	600

The use of an anti-oxidant buffer Sulfur anti-oxidant buffer (SAOB-II), an alkaline solution containing EDTA and ascorbic scid, was used by Noel (19) to keep the test solution relatively free of dissolved oxygen. Stephenson (88) used anti-oxidant buffer (AOB) solution, an alkaline solution containing salicylate and as-

sorbic acid, to achieve the same purpose. Both SAOB and AOB were tested and AOB was found to produce a wider potential range for performing polarographic work.

The i-E curve of S_5^{2-} in AOB as the supporting electrolyte is presented in Figure 21. A well-defined cathodic current plateau is obtained in comparison to the case of NaOH alone. AOB seems to produce a similar effect on the surface of electrode as the tetraalkylammonium hydroxide. In this case, the salicylate, being a bulky atomic species, is expected to adsorb preferentially at the electrode surface thereby minimizing the adsorption of S^{2-}. The ascorbate is responsible for reducing the dissolved oxygen.

A series of i-E curves for different concentrations of S_5^{2-}, using AOB as the supporting electrolyte is shown in Figure 22. The cathodic current data deduced from Figure 22 are shown in Table 10 and plotted in Figure 23. The calibration curve, thus, obtained is linear with a correlation coefficient, r, of 0.9997.

Table 10. The cathodic currents of S_5^{2-} using AOB as the supporting electrolyte

No.	$[S_5^{2-}]$, mM	$i_{c,\mu A}$
1	2	0.7
2	4	1.4
3	6	2.2
4	8	2.9
5	10	3.6

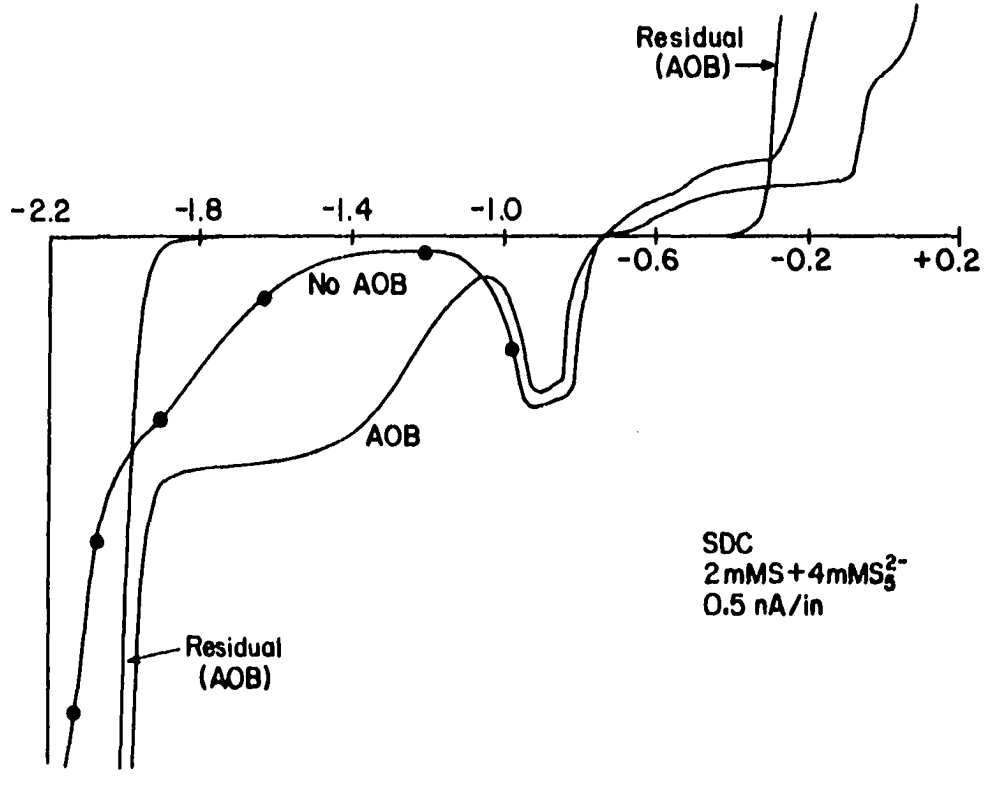

Figure 21. The cathodic current plateau in the presence of the anti-oxidant buffer (AOB)

5 mM Na_2S_5

SDCP

DME, 1 s

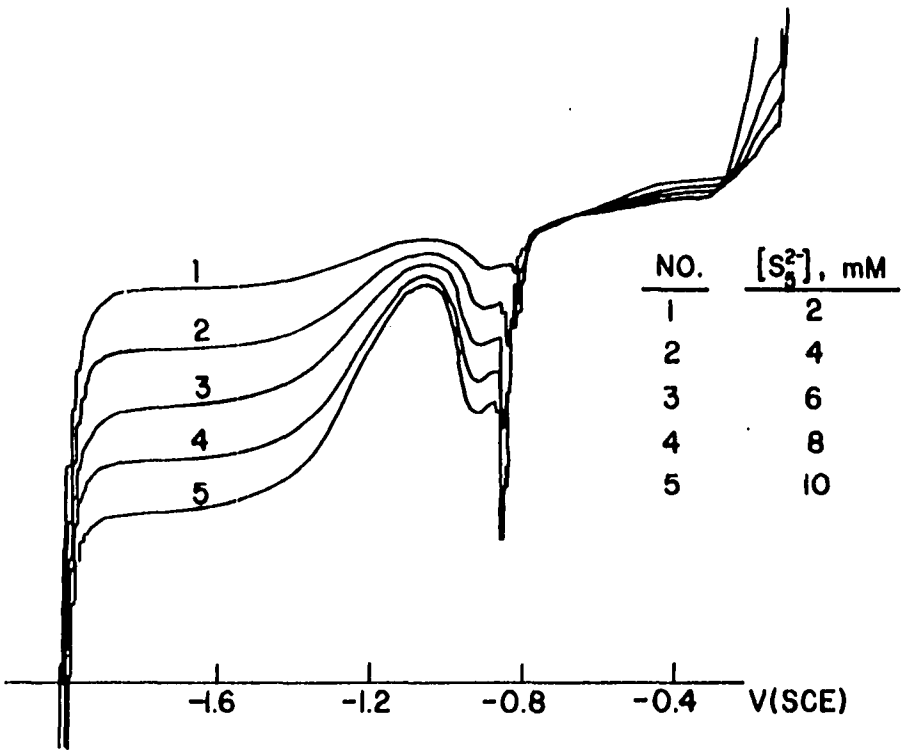

Figure 22. The i-E curves of Na_2S_5 solutions using AOB as the supporting electrolyte

SDCP
DME, 1 s

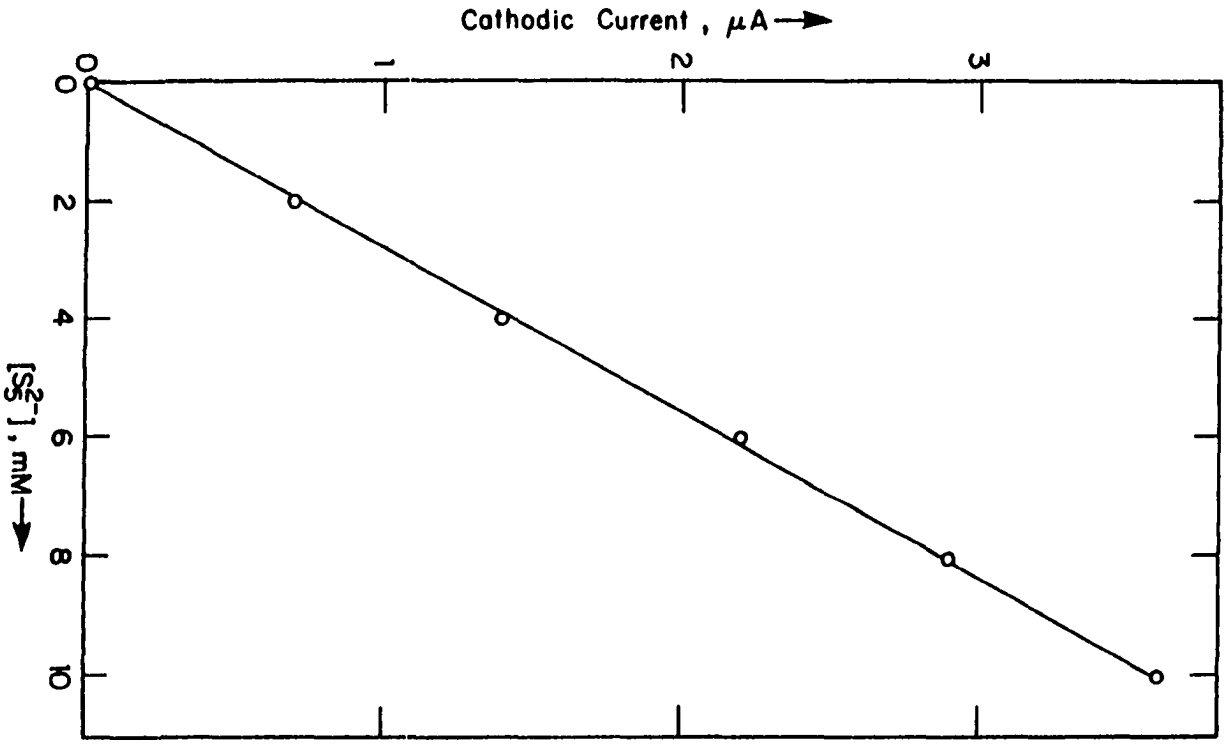

Figure 23. The calibration curve of Na_2S_5 in AOB

SDCP
DME, 1 s
The cathodic current measured at -1.75 V

It is observed that in the positive scan the cathodic wave in the presence of AOB passes through a peak at ca. -0.94 V before the current changes sign. The peak is found to decrease in height by addition of Triton X-100. This is evidence that the peak is a current maximum of the sort frequently observed in polarographic work. The peak is observed, not only in the i-E curves of inorganic polysulfide, but also in alcoholic solutions of elemental sulfur (71) and in many organic polysulfide solutions (88-90). According to Werner and Konopik (25), the cathodic peak is observed because of inhibition of the part of reaction which is caused by S_x^{2-} ions when the electrode-surface charge changes sign from positive to a negative value; this is termed the "anionic effect."

The value of the electrocapillary maximum (ECM) was determined in 0.1 M NaOH solution by counting the number of drops falling per minute as a function of electrode potential. The results are shown in Table 11 and Figure 24. The ECM is concluded to be at ca. -0.55 V and a relationship of the ECM to the peak maximum at -0.94 V is not obvious.

In conclusion, an anodic wave is obtained for S^{2-} corresponding to the oxidation of Hg with simultaneous deposition of insoluble HgS at the surface of electrode. At high S^{2-} concentrations, the anodic wave becomes distorted because of the insoluble film formation at the electrode surface. As reported earlier by Canter-

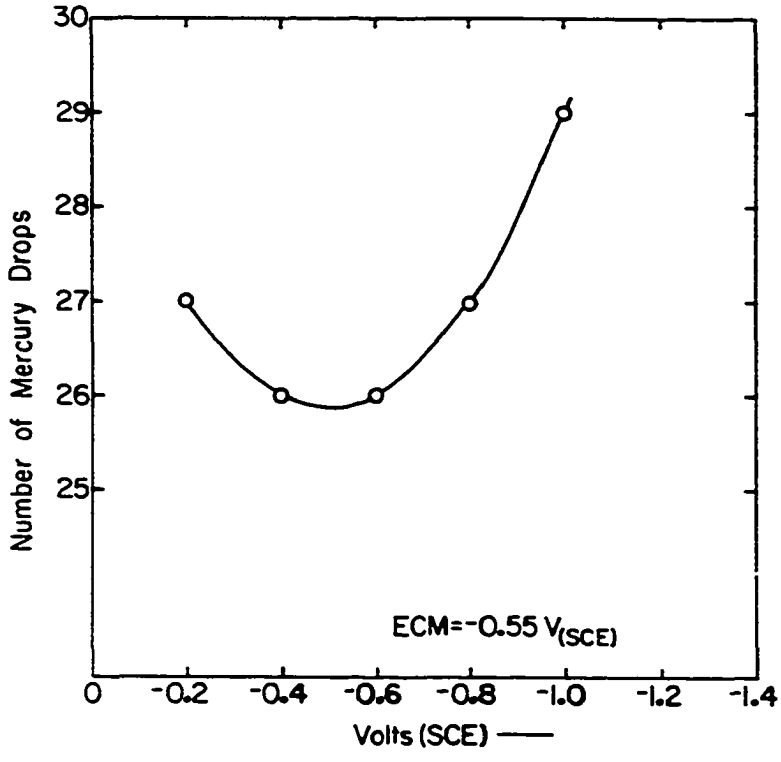

Figure 24. The electrocapillary maximum in 0.1 M NaOH

DME

Table 11. Determination of the electrocapillary maximum

E, V	Number of drops per minute
-0.2	27
-0.4	26
-0.6	26
-0.8	27
-1.0	29

ford and Buchanan (11), several anodic waves concluded to correspond to the formation of different layers of HgS are obtained at high S^{2-} concentrations.

The i-E curve of S_5^{2-} consists of an anodic wave and a cathodic wave. The anodic wave has a well-defined plateau which, at high S_5^{2-} concentrations, breaks into multiple anodic waves, each wave is concluded to correspond to the complete formation of a monolayer of the insoluble HgS film at the electrode surface. A limiting cathodic current plateau is not obtained because of the restricted approach of polysulfide to the electrode surface. The approach of polysulfide is restricted because of the adsorption of the product of cathodic reaction, S^{2-}, at the electrode surface and the anionic S^{2-} electrostatically repels the anionic S_x^{2-}, thereby hindering the electron-transfer reaction. The mutual electrostatic repulsion of S^{2-} and S_x^{2-} is not so severe at low

polysulfide concentration and a cathodic current plateau is observed. The plateau is observed also when the electrostatic repulsion by adsorbed S^{2-} is substantially decreased by allowing either the larger tetramethylammonium (Me_4N^+) ions or salicylate ions to adsorb preferentially at the electrode surface.

The cathodic peak ascribed by Werner and Konopik (25) to the anionic effect, i.e., at a potential where the electrode charge changes sign, is found not to correspond to the electrocapillary maximum (ECM). The ECM was determined to be at -0.55 V, whereas the cathodic peak is positioned at -0.94 V.

Determination of S^{2-} in the presence of S_x^{2-} It is observed that the total anodic current obtained for a solution containing S^{2-} and S_x^{2-} is the algebraic sum of the individual currents for solutions of S^{2-} and S_x^{2-}, as shown earlier in Figure 8. This fact might possibly be utilized for the determination of S^{2-} and S_x^{2-} in a mixture. However, let us first consider a simple case of a mixture of S^{2-} and S_5^{2-} only.

Assuming the equilibrium shown in 39, two possibilities seem to exist:

$$3S^{2-} + S_5^{2-} \rightleftarrows 4S_2^{2-} \qquad (39)$$

(i) Sulfide reacts with S_5^{2-}, thus converting S_5^{2-} to S_2^{2-}, and

(ii) although the reaction between S^{2-} and S_5^{2-} is thermodynamically spontaneous, as described in the literature (91) and Table 3, but the rate constant is so small that the components of reaction mixture essentially exist as nonreacting S^{2-} and S_5^{2-} ions.

If S^{2-} reacts with S_5^{2-} to form S_2^{2-}, as shown by (i) above, a significantly large increase in the limiting cathodic current is expected because of the large difference in the diffusion coefficients of S^{2-} and S_5^{2-} ($D_{S_2}{}^{2-}/D_{S_5}{}^{2-} = 9.5$). However, when the standard additions of S^{2-} in a solution of S_5^{2-} are made, no change in the cathodic current is obtained, as shown in Figure 8 and Table 1. The anodic current, on the other hand, increases linearly with the added S^{2-}, as shown in Figure 9.

Considering the spontaneous conversion of S_2^{2-} to S^{2-} and S_5^{2-}, it is expected that cathodic current of S_5^{2-}, characteristic of $D_{S_5}{}^{2-}$, be obtained. However, the calibration curve of S_2^{2-}, shown in Figure 26, is an evidence that no such conversion occurred. The evidence is supported by the fact that the value of relative diffusion coefficients evaluated by using the procedure shown on page 55, agree well with the value of $D_{S_2}{}^{2-}/D_{S_2}{}^{2-}$ stated in Table 8. The calibration curve of S_5^{2-} and S_2^{2-} solutions are shown in Figures 25 and 26 (Tables 13 and 14) and the calculation of $D_{S_2}{}^{2-}/D_{S_5}{}^{2-}$ is shown in Table 12.

It is, therefore, concluded that S^{2-} and S_5^{2-} in a mixture do not equilibrate to form new S_x^{2-} species, at least over the course of experimental measurements.

Table 12. The value of $(D_{S_2^{2-}}/D_{S_5^{2-}})^{1/2}$

Source of evidence	$(D_{S_2^{2-}}/D_{S_5^{2-}})^{1/2}$
Figures 25 and 26	3.5
Table 8	3.1

The fact that the anodic current for a solution containing S^{2-} and S_5^{2-} is observed to be the sum of the anodic currents of the individual S^{2-} and S_5^{2-} species, is presumably because the reaction between S^{2-} and S_x^{2-} to form other S_x^{2-} species is kinetically hindered and, during the course of the polarographic measurements, does not proceed to an appreciable extent.

The quantitative characterization of a solution of S^{2-} and S_x^{2-} requires determination of three parameters:

1. x, the number of S atoms in S_x^{2-};
2. $C_{S^{2-}}^{b}$, the bulk concentration of S^{2-}; and
3. $C_{S_x^{2-}}^{b}$, the bulk concentration of S_x^{2-}.

From the i-E curve, one can obtain only two useful parameters, the values of $i_{l,a}$ and $i_{l,c}$. However, three variables are needed for solving the three simultaneous equations describing this analytical problem.

One might hope, in an alternate approach, to determine the analytical concentration of sulfur defined by

$$A_s = \Sigma x C_x^b \tag{40}$$

Table 13. The calibration curve for S_5^{2-}

No.	$[S_5^{2-}]$, mM	i_a nA	i_c nA
1	0.21	20.0	5.4
2	0.42	40.0	10.8
3	0.63	61.6	16.0
4	0.98	96.0	25.4
5	1.26	124.0	32.8
6	1.61	159.6	41.5

Table 14. The calibration curve for S_2^{2-}

No.	$[S_2^{2-}]$, mM	i_a	i_c
1	0.30	27.6	8.6
2	0.60	55.6	17.2
3	0.90	84.2	25.6
4	1.20	111.8	33.2
5	1.52	137.8	41.2

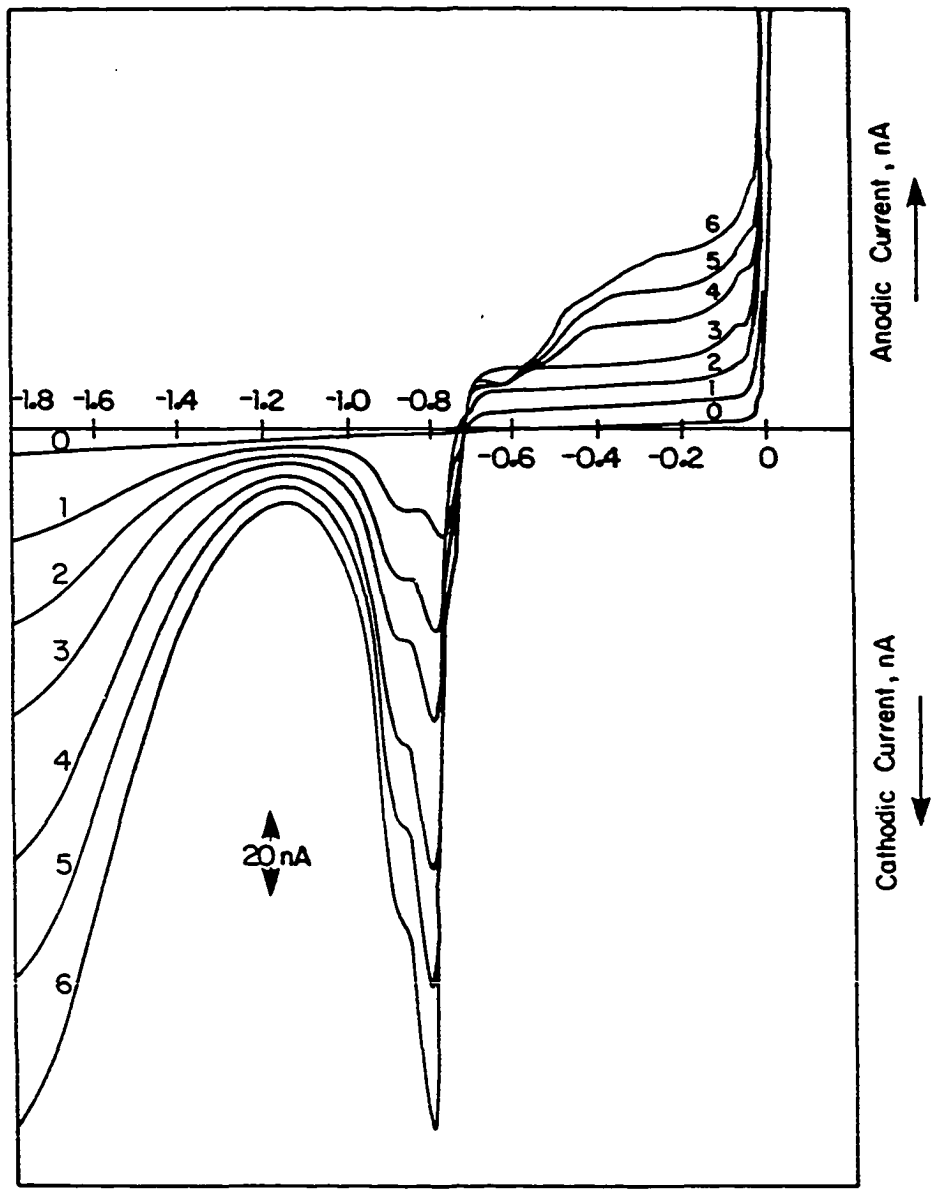

Figure 25. The calibration curve of Na_2S_5

SDCP
DME, 1 s
0.1 M NaOH
5 mV/s

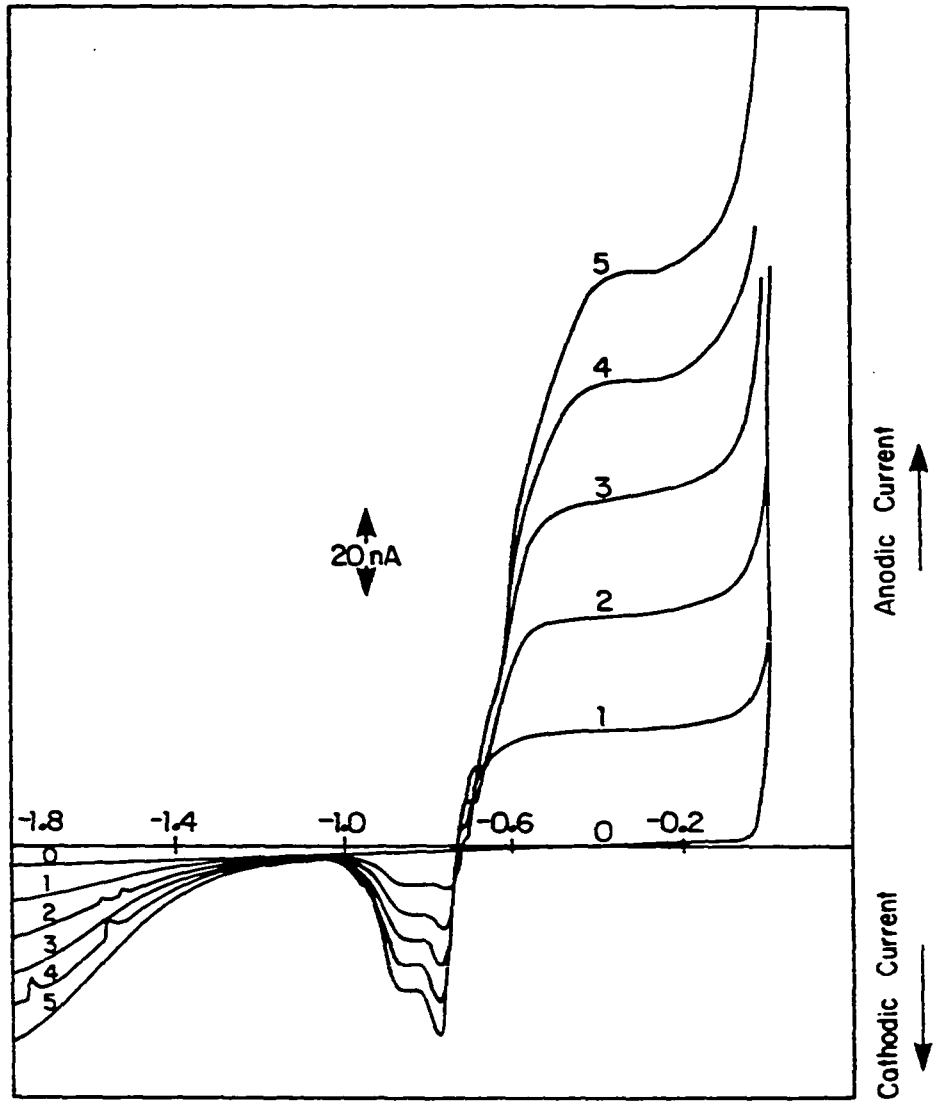

Figure 26. The calibration curve of Na_2S_2

SDCP
DME, 1 s
0.1 M NaOH
5 mV/s

This would be possible only if the diffusion coefficients for all sulfur species are identical. Of course, this equality does not exist.

Cyclic Voltammetry

Cyclic voltammetry at a hanging mercury drop electrode (HMDE) was performed to verify the various features of the i-E curves of S^{2-} and S_x^{2-} observed earlier by DCP and to confirm the conclusion based on the studies whose results presented earlier in this dissertation.

Sulfide

The i-E curve of 12 μM Na_2S in 0.1 M NaOH solution is shown in Figure 27. Anodic and cathodic peaks are obtained because of the reactions in equations 41 and 42.

$$\text{anodic:} \quad Hg + S^{2-} \rightarrow HgS + 2e \tag{41}$$

$$\text{cathodic:} \quad HgS + 2e \rightarrow Hg + S^{2-} \tag{42}$$

A peak current for the anodic process is observed at ca. -0.78 V which agrees with the polarographic half-wave potential, -0.76 V, shown in Figure 4. An anodic peak rather than an anodic wave is obtained as expected for a reversible transport-limited process at a stationary electrode in the absence of solution agitation. For the reverse scan from -0.20 V, a cathodic peak is observed because of the reduction of the insoluble HgS accumulated on the electrode as a result of reaction (39). A peak is expected because of the conversion of HgS to S^{2-} by this surface-controlled process. The ratio of anodic and cathodic

Figure 27. Cyclic voltammogram of Na_2S

Hanging mercury drop electrode (HMDE)
0.012 mM Na_2S
0.1 M NaOH
6 V/in

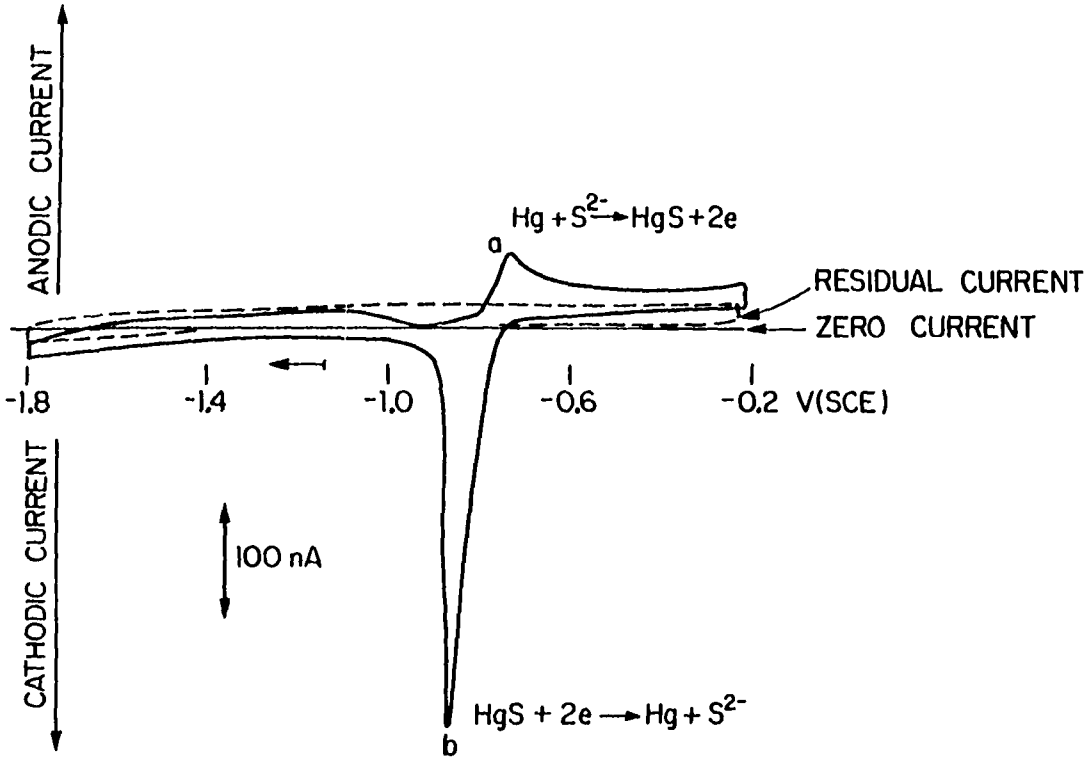
ANODIC CURRENT
Hg + S2- → HgS + 2e
a
RESIDUAL CURRENT
ZERO CURRENT
-1.8
-1.4
-1.0
-0.6
-0.2 V(SCE)
CATHODIC CURRENT
100 nA
HgS + 2e → Hg + S2-
b

peak currents, $i_{p,a}/i_{p,c}$, is 0.25. The ratio for a redox reaction, when both species are soluble, is 1. The observed ratio deviates significantly because HgS, the product of the anodic reaction, is insoluble and adsorbs on the electrode surface. Hence, the cathodic process of dissolution of HgS is no longer diffusion controlled. It is important to note that the peak separation, $\Delta E = E_{p,a} - E_{p,c}$ is 100 mV. For a reversible two-electron process involving soluble redox species, ΔE_p is expected to be 29 mV at 25°C (82). The observed peak displacement is concluded to indicate a kinetically hindered cathodic dissolution as well as the fact that HgS is not soluble. The effect of varying scan range is shown in Figure 28. The cathodic current increases as the potential is scanned further into the positive direction which is because of the formation of a greater quantity of HgS film at the electrode surface. However, since no reaction occurs for a soluble species in the cathodic region of potential more negative of -1.0 V, the choice of switching potential, i.e., the point where the cathodic scan direction is reversed, is inconsequential.

Polysulfide

The cyclic voltammogram of 0.04 mM polysulfide at a hanging mercury drop electrode is shown in Figure 29. It is readily recognized that the i-E curve has similar features as observed in the i-E curve obtained by using the DME, shown in Figure 6.

The current passes through a cathodic maximum before it changes sign as the potential is moved further in the positive direction. The

Figure 28. The effect of varying scan range on the i-E curve of Na_2S

a. Positive potentials
b. Negative potentials

HMDE
7.5 μM

0.1 M NaOH
6 V/in

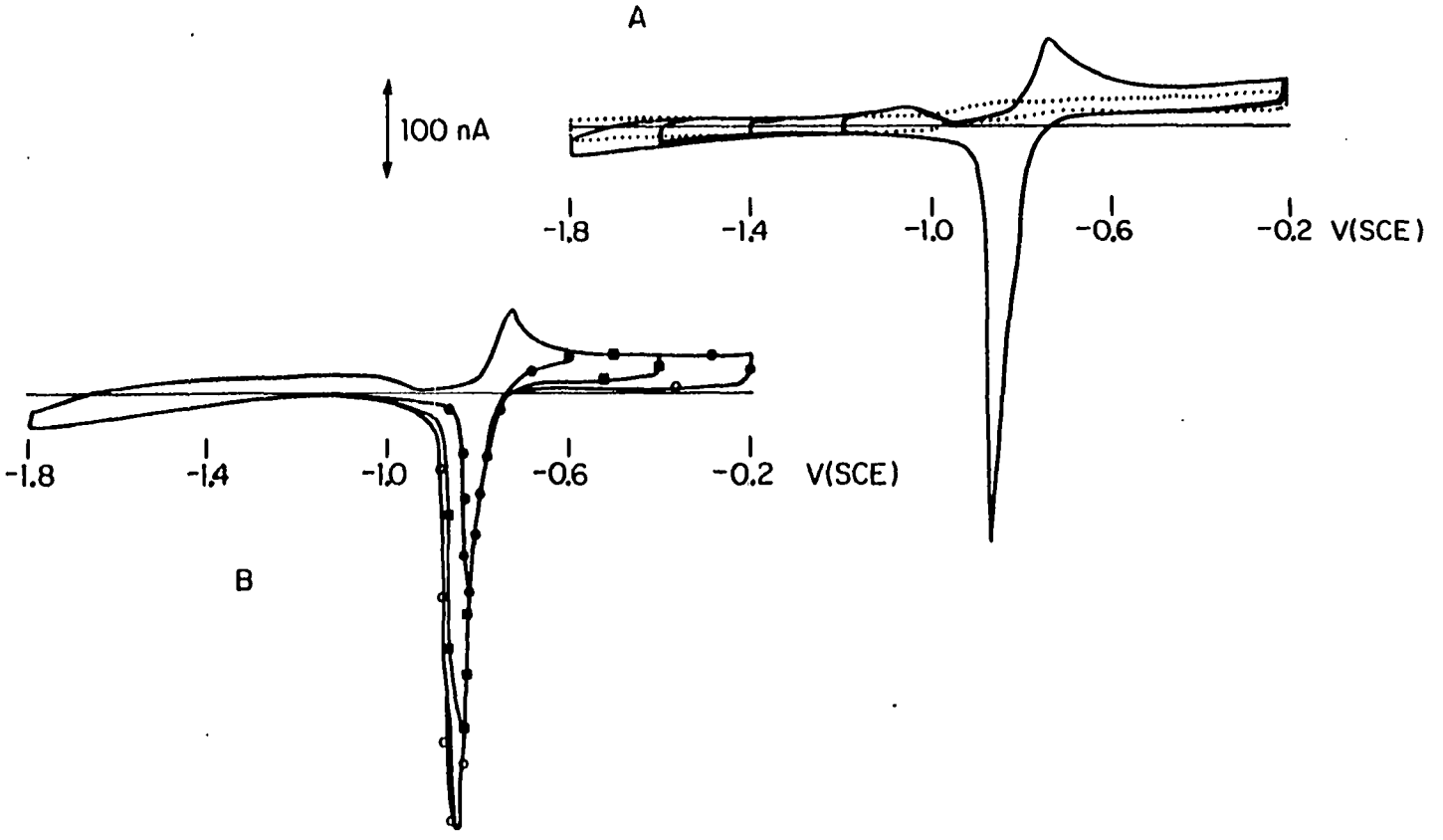
A
100 nA
-1.8
-1.4
-1.0
-0.6
-0.2 V(SCE)
-1.8
-1.4
-1.0
-0.6
-0.2 V(SCE)
B

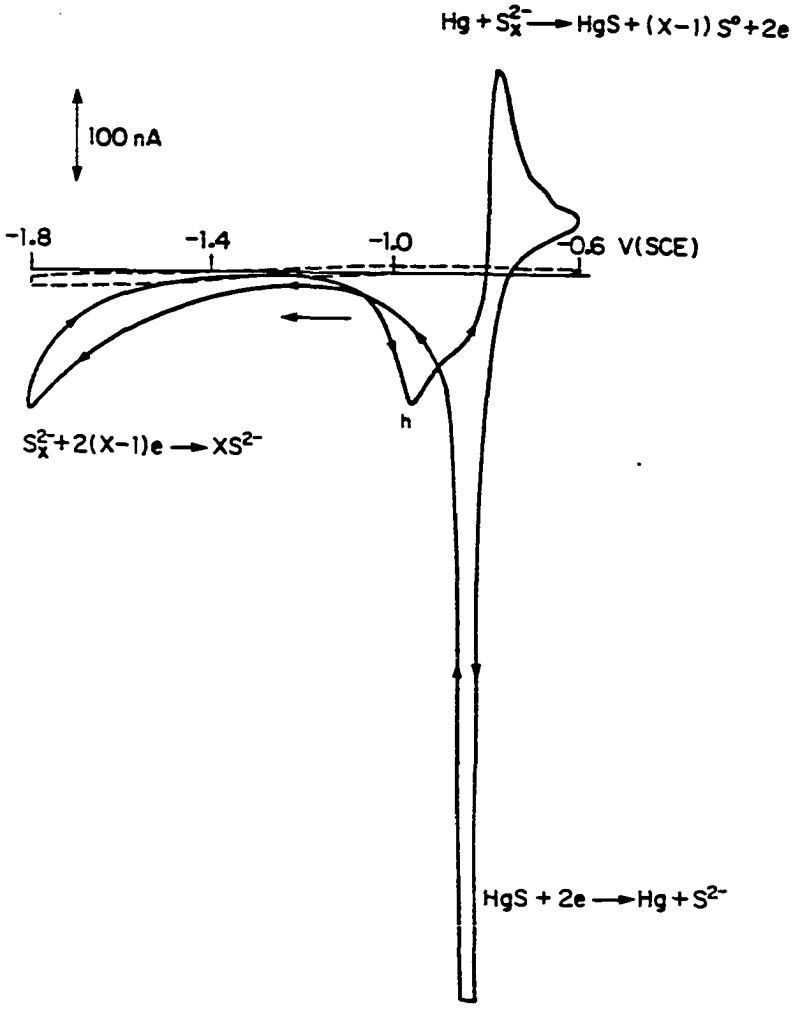

Figure 29. Cyclic voltammogram of Na_2S_5
0.04 mM Na_2S_5
0.1 M NaOH
HMDE
5 V/in

cathodic maximum is obtained because of the reduction of HgS. It is interesting to note that in the negative scan the current rises and then drops sharply to a near-zero value, whereas in the positive scan one observes a hump (h in Figure 29) at ca. -1.0 V. It is very likely that both the hump and the cathodic maximum are obtained because of the same electrode process, namely, the reduction of HgS. In the negative scan, a sharp and smooth peak is observed as a result of immediate depletion of insoluble HgS. In the positive scan, the residual HgS is reduced at ca. -1.0 V. This residual HgS is formed probably as a result of recombination (not the anodic reaction) of Hg and sulfur present in equilibrium with the S_x^{2-} ions. A similar hump was observed in the polarographic curve of S_x^{2-} shown in Figure 6. It is very likely that the elemental sulfur part, i.e., the "polysulfidic" portion of the S_x^{2-} ion forms some sort of addition compound with the supporting electrolyte to provide a polarographic curve which is very similar to that of elemental sulfur, as reported by Zhadanov and Kiselev (86).

In conclusion, an anodic current peak is observed at ca. -0.78 V in the cyclic voltammogram of a S^{2-} solution. This value agrees with the polarographic half-wave potential of -0.76 V reported in Figure 3. A cathodic peak rather than a cathodic wave is obtained as a result of the reverse scan from -0.2 V to -1.8 V indicating that the reduction of HgS is not a diffusion-controlled process as the dissolution of HgS formed as a result of anodic process, rather than the diffu-

sion, controls the rate of electron-transfer reaction. The separation between the anodic and cathodic peak, ΔE_p of 100 mV is a further evidence of the irreversibility of the cathodic process. The cyclic voltammogram of S_5^{2-} has the features expected on the basis of the polarographic i-E curves shown earlier for S_5^{2-}.

Summary

A well-behaved anodic wave is obtained for S^{2-}, based on the oxidation of Hg with the formation of insoluble HgS. The i-E curve of S_x^{2-}, on the other hand, is characterized by an anodic and a cathodic wave. The anodic portion of the i-E curve is based on the oxidation of Hg and has a well-defined anodic current plateau, but a corresponding plateau in the cathodic region of potential is not observed. The following explanation, based on the results of the polarographic and the cyclic voltammetric studies presented in this dissertation, is proposed for the reduction of S_x^{2-} on the DME.

The polysulfide ion is spontaneously reduced to produce S^{2-} ions in the potential range -1.8 V to -0.80 V. The strong surface activity, and the similarity of anionic charge, of S_x^{2-} and S^{2-} ions, results in a competition of sites at the electrode surface resulting in the decrease of cathodic current and the lack of cathodic plateau, as the potential is moved slightly in the positive direction. When R_4NOH is used as the supporting electrolyte, the positively charged R_4N^+ ions adsorb on the negatively charged electrode surface and, because of

their large size, offer steric hindrance to the S_x^{2-} ions, thus keeping them from coming in contact with the electrode surface. The R_4N^+ ions serve not only to keep the S_x^{2-} ions from reaching the electrode surface, but also tend to decrease the electrostatic repulsion between the S_x^{2-} and S^{2-} ions, resulting in a cathodic plateau. This explanation is consistent with the earlier observation that at very low S_x^{2-} concentration a cathodic plateau is observed showing no minimum. The minimum deepens as the S_x^{2-} concentration is progressively increased.

In conclusion, the polarographic method alone cannot provide the necessary data for the quantitative description of an unknown solution containing S^{2-} and S_x^{2-}. The polarographic method has been verified to produce a sensitive response useful for characterization of the simpler solutions of S^{2-} and S_x^{2-} in the absence of the other. In the next chapter, liquid chromatography with polarographic detection is tested for providing the necessary prior separation of complex mixtures.

CHAPTER IV. DETECTION IN A FLOW SYSTEM

Principles

Flow injection analysis (FIA) is a style of analytical methodology in which a small volume of sample, V_s, is injected into a continuously flowing carrier stream of solvent flowing at a rate of V_f (ml/min) through a detector, D, as illustrated in Figure 30. The retention volume, V_r, in Figure 30 represents the retention volume of the system and corresponds to the volume of tubing connecting the detector and the sample injection valve. The sample can be detected directly without prior chemical reaction, as shown in part A of Figure 30, in which case the value of V_r is kept as small as possible to minimize the dispersion of the sample into the carrier stream. Alternatively, the detection can be achieved after reaction of the analyte with an appropriate chemical reagent present in the carrier stream. In that case, V_r is intentionally increased to achieve uniform and thorough mixing to allow for significant reaction between the reagent and the analyte, as shown in part B of Figure 30.

The detection process may be based on any of the common instrumental methods including spectrophotometry, fluorometry, potentiometry, amperometry, etc. The detection cell should have a very small internal volume (dead volume), for example, much less than 100 µL, to achieve maximum sensitivity with a minimized loss of resolution between samples.

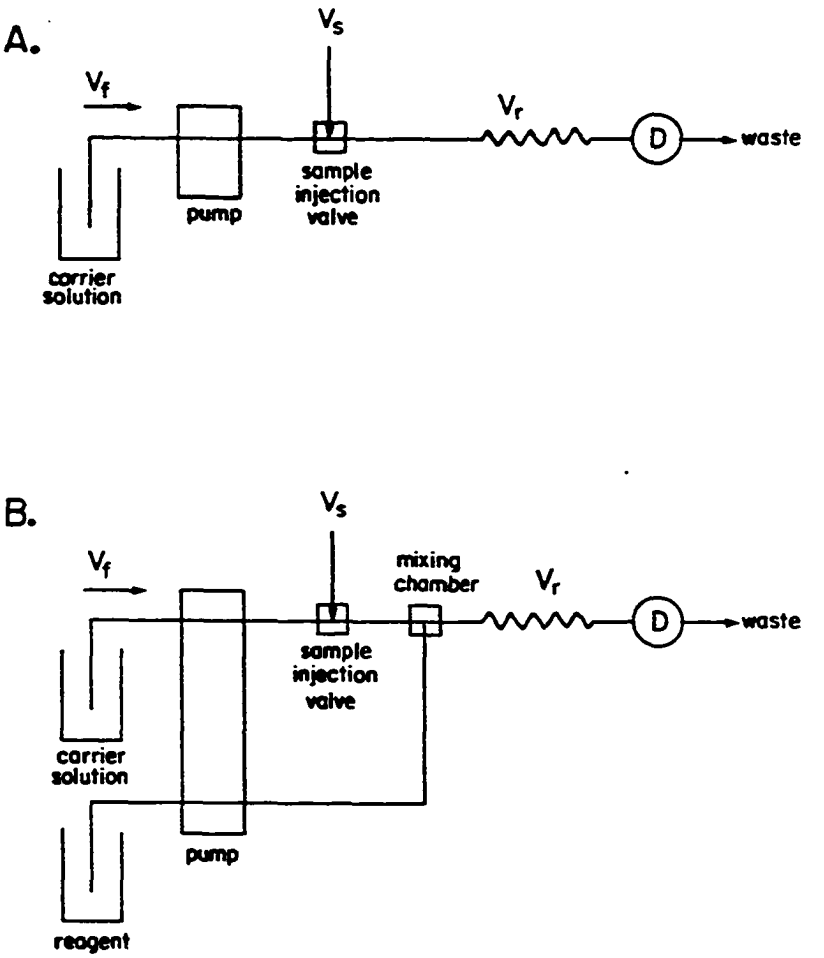

Figure 30. The schematic representation of a flow-injection system

A. Direct detection of the analyte
B. Detection after reacting the analyte with a reagent stream

V_f = flowrate, ml/min

V_s = the sample volume

V_r = the dead volume of the tubing

D = detector

The most widely used electrochemical method of detection is direct current (DC) amperometry which involves the measurement of electrode current in response to a fixed electrode potential. Amperometry is a hydrodynamic technique, i.e., it is normally carried out in flowing or stirred solutions. It is necessary to have knowledge of the response of the analyte in order to determine the operating potential of electrode that would yield an optimum response. Analytical application of amperometry usually is preceded by hydrodynamic voltammetry. A hydrodynamic voltammogram is obtained by slowly scanning the electrode potential in a positive or negative direction. The electrode current is measured as the electroactive species is oxidized or reduced. Individual hydrodynamic voltammograms of several hypothetical species are shown in Figure 31. Since the magnitude of current in the plateau region is independent of potential, slight variation in the applied potential in the plateau region does not result in any change in the observed current. In some cases, however, it is advantageous to select the potential in the rising part of the curve, for example, E_4 for compound C. This is true particularly if the components of a mixture are detected electrochemically after being separated by lquid chromatography. If A and B are not well-resolved by the column, it will be difficult to detect B at E_1 in the presence of, for example, a thousandfold excess of A. If the potential is increased to E_3, the sensitivity to B will decrease severalfold but the sensitivity to A will decrease dramatically. The choice of operating potential,

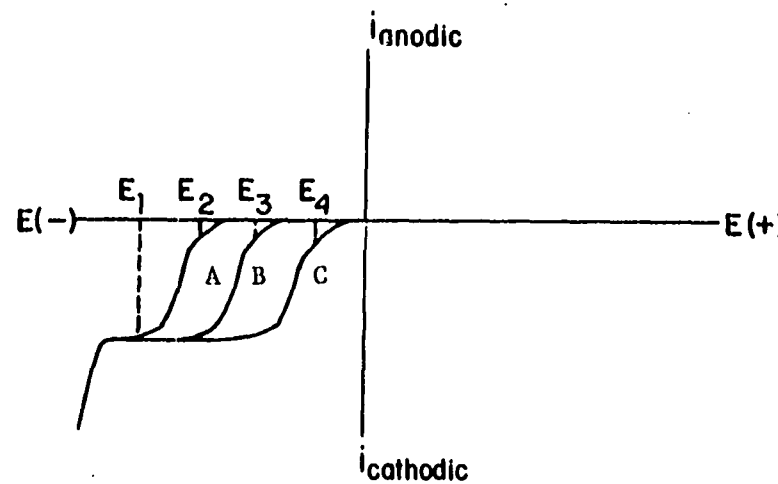

Figure 31. The choice of detection potential in hydrodynamic voltammetry - a schematic representation

thus, offers a useful experimental variable for achieving the desired sensitivity and response characteristics. Referring again to Figure 31, the operating potential selected for the determination of compound A must be E_1. However, at this potential, all the three compounds will be detected. Therefore, a prior separation is necessary. This illustrates the difficulty with the simple amperometric detection and the need for resorting to the use of liquid chromatography coupled with the amperometric detection. The separation of S^{2-}, SO_3^{2-} and $S_2O_3^{2-}$ employed in this research using HPLC prior to electrochemical detection at the DME is discussed in Chapter V.

Referring to equation 12, the electrode current is shown to decay with $t^{-1/2}$. In the absence of convection, the current continues to decay, but in a convective system it ultimately approaches the steady-state value as shown in Figure 32.

The limiting response of an amperometric flow-through detector is described empirically (92) by the general equation

$$i_\ell = nFAK_1V_f^\alpha C \tag{43}$$

where

i_ℓ = the limiting current (amps)

n = the number of electons in the reaction equivalents/mole)

F = Faraday's constant (96,500 coul/equivalent)

A = surface area of the electrode (cm^2)

V_f = fluid flow rate (ml/min)

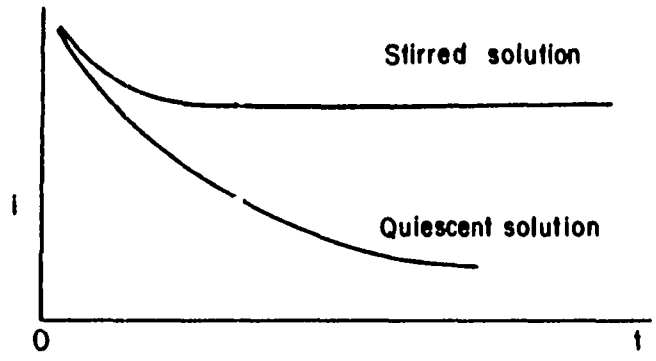

Figure 32. The current-time relationship at a stationary electrode with and without stirring

α = a constant characteristic of the electrode geometry and fluid dynamics

C = analyte concentration (mole/ml)

K_ℓ = the limiting mass-transfer coefficient ($Cm^{1-3\alpha} \cdot s^{\alpha-1}$)

Under laminar flow conditions, the value of α is ca. -0.50 for a planar electrode and ca. -0.33 for a cylindrical electrode (92).

Experimental

A Gilson Minipulse peristaltic pump (Rainin Instruments Company, Inc., Woburn, MA) was used to maintain the flowrate of the aqueous carrier stream. An inverted T-tube was used as the pulse dampener (53). Sample injection was achieved using a Lachet FIA 1000 Automatic Sample Injector (Lachet Chemicals, Inc., Mequon, WI) which had a sample volume of 50 µL. The design of the flow-through cell is shown in Figure 33. The carrier stream is directed onto the surface of mercury drop using an LC adaptor assembly that snap-fits onto the lower end of the glass capillary of the DME as shown in Figure 33. The Princeton Applied Research Model 174A potentiostat and X-Y recorder were mentioned earlier. Excess waste solution and mercury in the detector cell was drawn off by an aspirator to a collection bottle.

Results and Discussion

Selection of drop time

The studies done on the dependence of peak current (i_p) as a function of drop time (τ) showed that the longer the τ, the greater the i_p

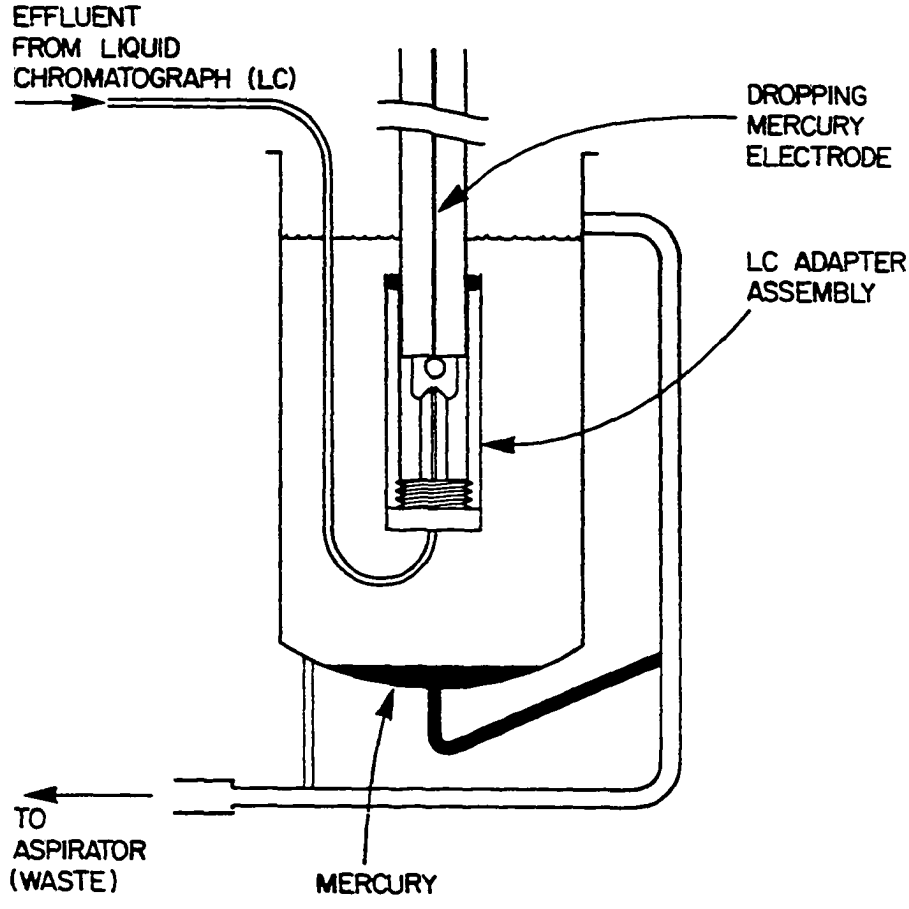

Figure 33. The polarographic flow-through detector

(53). This leads to the choice of a longer drop time for achieving the best sensitivity. However, considering the design of the polarographic flow-through detector shown in Figure 33, it is seen that the electrode current be sampled as frequently as possible, in order to reflect the concentration of the analyte corresponding to the peak, as the analyte plug flows past the surface of the DME. In other words, a higher sampling frequency of the electrode current is desired which cannot be achieved at longer τ. The minimum number of data points, according to Perone and Jones (93) required to faithfully trace a peak signal is 10. Therefore, it is desirable to select shorter τ. Thus, the FIA data were obtained by setting the drop time at 1 s.

Flowrate study

The dependence of i_p on flowrate (V_f) was studied by injecting the S^{2-} solution into the fluid stream over a range of flowrates. The i_p was measured as a function of V_f. The limiting current for the continuous flow of a S^{2-} solution has a steady-state value (i_{ss}). In this case, $V_s >> V_r$ and the analyte concentration is maintained at C^b at all times. Thus, $i_p = i_{ss}$. The results of the studies of flowrate dependence on i_p and i_{ss} are given in Table 15. The flowrate dependence of electrode current at the DME, according to equation 43, is a combination of dispersion and fluid dynamics at the electrode surface. Let us consider the dispersion first.

When a sample solution of concentration C^b is injected into a

Table 15. i_p and i_{ss} as a function of V_f

V_f, ml/min	i_p, μA	i_{ss}, μA	i_{ss}/i_p
0.41	150	210	1.40
0.53	218	242	1.11
0.64	255	273	1.07
0.75	300	308	1.03
0.86	-[a]	340	NA
0.97	-	380	NA

[a] - = very noisy.

fluid stream, the dispersion of the sample plug during its transport from the sample loop to the detector causes the peak concentration of analyte arriving at the detector (C_p) to be lower than C^b. This is demonstrated by the data shown in Table 15 which signifies the effect of dispersion on the concentration of analyte. The ratio (C^b/C_p) is empirically defined as the dispersion (k_d).

$$C^b/C_p = k_d \tag{44}$$

The relationship of i_p and i_{ss} with flowrate is described by equations 45 and 46.

$$i_p = nFAK_1V_f^{\alpha}C_p \tag{45}$$

$$i_{ss} = nDAK_1V_f^{\alpha}C^b \tag{46}$$

The ratio i_{ss}/i_p for an analyte at the same flowrate is, therefore, a

measure of k_d. For the limiting case, as $i_p \rightarrow i_{ss}$, $k_d \rightarrow 1$; meaning that in the absence of dispersion (k_d=1), i_p reflects the analytical concentration C^b of analyte. The ratios i_{ss}/i_p for a 0.1 mM S^{2-} solution, at various flowrates, are shown in the right-hand column of Table 15. It is evident that the dispersion decreases at higher flowrates. This is expected because at higher V_f, the residence time ($t = V_s/V_f$, the time elapsed between sample injection and the peak maximum) of analyte during which dispersion occurs, is shortened. The analyte plug passes through the detector quickly, not letting the analyte ions have enough time to diffuse away.

The dispersion has been classified (93) as limited (k_d = 1 to 3), medium (k_d = 3 to 10) and large (k_d > 10). The system under consideration, therefore, is a case of a low dispersion.

Evaluation of α

The value of α can be determined by taking the logarithm of both sides of equation 45 and plotting ln i_p vs. ln V_f.

$$\ln i_p = \ln nFAKC_p + \alpha \ln V_f \qquad (47)$$

For a given concentration, the slope of such a plot represents α. The values of ln i_p and ln V_f are given in Table 16 and the variation of ln i_p with ln V_f is plotted in Figure 34. A similar set of data for i_{ss} and V_f is also given in Table 16 and is plotted also in Figure 34. From the graph shown in Figure 34, it is observed that the value of α represented by the slope of the curve is not the same for the

Table 16. The dependence of anodic peak current (i_p) and the steady-state current (i_{ss}) of Na_2S on flowrate (V_f)

V_f, ml/min	ln V_f	ln i_p	ln i_{ss}
0.41	-0.89	5.01	5.35
0.53	-0.64	5.38	5.49
0.64	-0.45	5.54	5.61
0.75	-0.29	5.70	5.73
0.86	-0.15	-	5.83
0.97	-0.03	-	5.94

range of V_f values studied. Between 0.4 and 0.5 ml/min, for example, the value of α is about 2, whereas between 0.5 and 0.7 ml/min it is 1, for curve A. The electrode reaction, initially, increases at an increasing rate as the V_f is increased from 0.4 to 0.5 ml/min, because of the increased flux of analyte at the surface of electrode. After 0.5 ml/min, however, further increase in V_f does not result in the same rate of increase in current because after maximizing the flux of analyte at the electrode surface, the dispersion effects become important thereby increasing α. The average value of α, as obtained by the regression line is 1.13.

The value of α calculated from curve B is less than that of curve A. This can also be explained on the basis of the dispersion effect. At higher flux of analyte, the concentration gradient also increases, thus, promoting the dispersion.

In literature, the value of α has been reported (92) to be 1/3

Figure 34. Evaluation of α for a Na_2S solution using flow injection and electrochemical detection (FI/EC)

A. ln i_p vs. ln V_f

B. ln i_{ss} vs. ln V_f

0.1 M Na_2S

0.1 M NaOH
SDCP
DME, 1 s

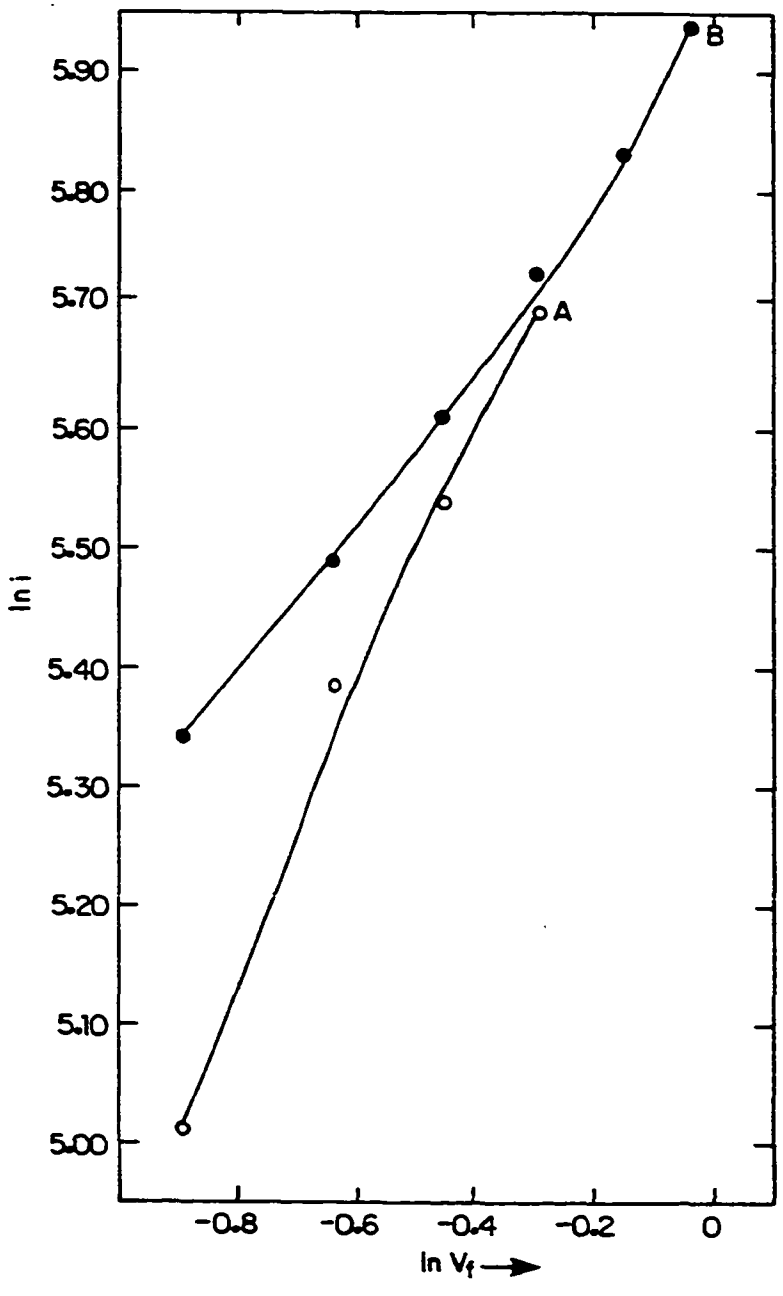
5.90
5.80
5.70
5.60
5.50
5.40
5.30
5.20
5.10
5.00
ln i
-0.8
-0.6
-0.4
-0.2
0
ln V_f →
A
B

for a tubular electrode and 1/2 for the rotating disk electrode (RDE). The value obtained in this work is certainly high. As stated earlier, α is a function of electrode geometry and fluid dynamics. The fluid movements relative to the electrode surface for various electrode geometries are shown in Figure 35. A higher value of α for RDE is obvious because of convection. For the configuration of the polarographic flow-through detector, c in Figure 35, it is observed that the fluid stream containing the analyte is released with pressure at the surface of electrode thus facilitating the electrode reaction. The portion of part c in Figure 35 marked by a dotted circle is expanded in part d to show the flow pattern at DME.

Substituting $\alpha = 1$ in equation 43

$$i = nFAK_{\ell}V_{f}C^{b} \tag{48}$$

the current should vary linearly with V_f which is found to be the case. The current is plotted as a function of V_f in Figure 36 where almost linear relationship of current with V_f is obvious.

Typical anodic amperamoetric response for injections of S^{2-} solution is shown in Figure 37. The relative standard deviation of the peak currents is 0.0651%. The peak detection response was found linear with concentration as shown in Table 17 and Figures 38 and 39. The correlation coefficient, r, of the regression line is observed to be 0.9978. It is evident that a relatively high sample throughput is achieved, as 11 peaks are obtained in less than 1/2 hr. The method can be adapted

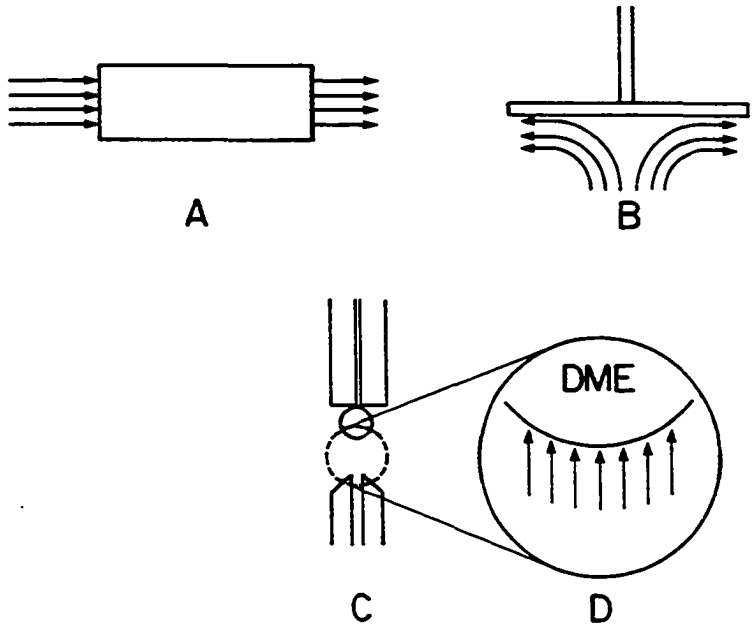

Figure 35. Fluid movements for various electrode geometries

A. A tubular electrode
B. Rotating disk electrode (RDE)
C. DME
D. The portion of C, marked by the dotted circle, to show the fluid movements

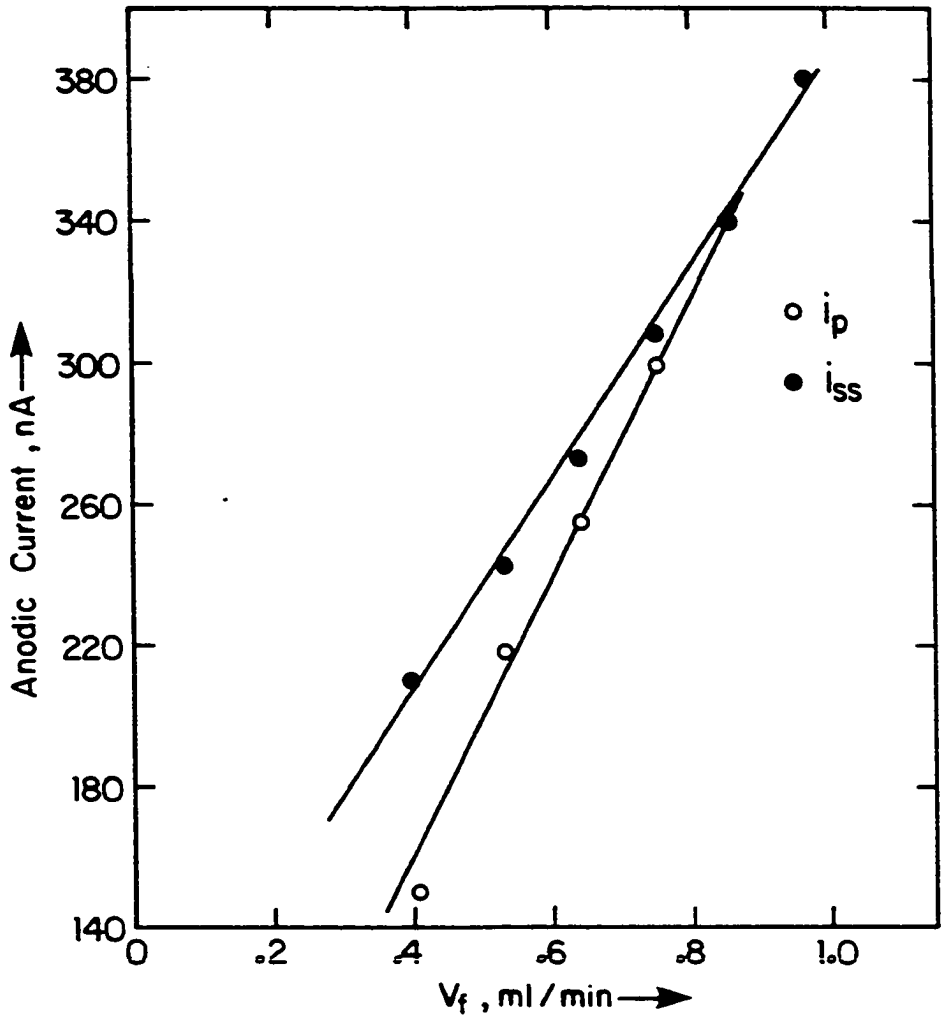

Figure 36. The i_p and i_{ss} for Na_2S as function of V_f

FI/EC
0.1 mM Na_2S
0.7 ml/min
SDCP
DME, 1 s

Table 17. The anodic peak current for various S^{2-} concentrations using FIA

$[S^{2-}]$, mM	$I_{a,nA}$
0	0
.05	200
0.10	430
0.20	860
0.30	1340
0.40	1800
0.50	2280

for automated analysis in a situation where a large number of samples are to be analyzed. The main advantage is that the analysis can be performed without having to remove the dissolved oxygen which poses a big problem in most polarographic work. Oxygen removal in a batch determination, particularly at low sulfide levels, is absolutely necessary. An explanation as to why the deoxygenation is important in a batch cell whereas it can be avoided in a flow injection method is provided as follows: A schematic diagram showing the reduction of dissolved oxygen in aqueous solution is presented by the curve abc in Figure 40. The anodic wave for sulfide in deoxygenated solution is shown by the curve labelled df. The sum of the anodic and the cathodic currents will be the curve labelled abgh, representing the polarographic response of sulfide in the presence of dissolved oxygen. If the amperometric method of detection is employed by selecting the

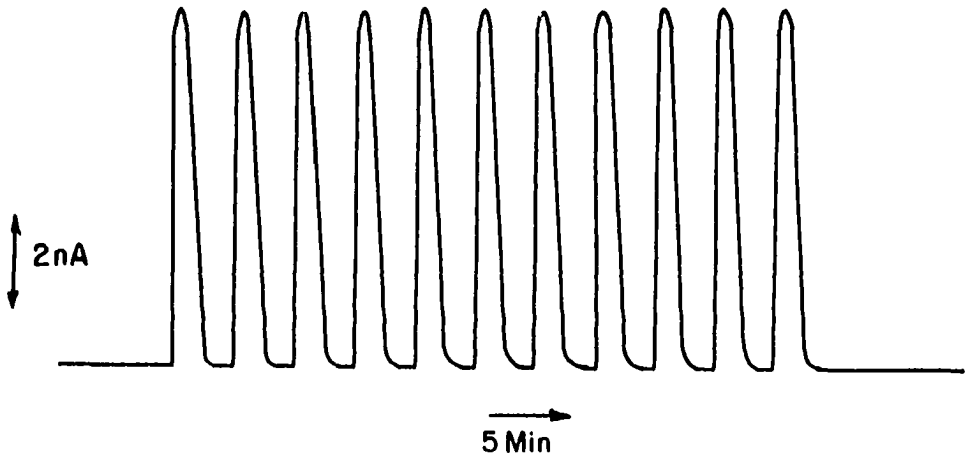

Figure 37. Flow injection detection of sulfide

NPP
V_s = 50 µl
E = 50 mV
2 mM Na_2S, 0.01 M NaOH
Electrode at 0.3 V(SCE)
0.7 ml/min

Load: 100 sec
Inject: 100 sec
σ = 0.004 nA

Figure 38. The detector response for increasing S^{2-} concentration

FI/EC
SDCP
DME, 1 s
-0.3 V
0.7 ml/min

A. 0.5 mM, 200 nA/in
B. 1.0 mM, 200 nA/in
C. 2.0 mM, 200 nA/in
D. 3.0 mM, 200 nA/in
E. 4.0 mM, 500 nA/in
F. 5.0 mM, 500 nA/in

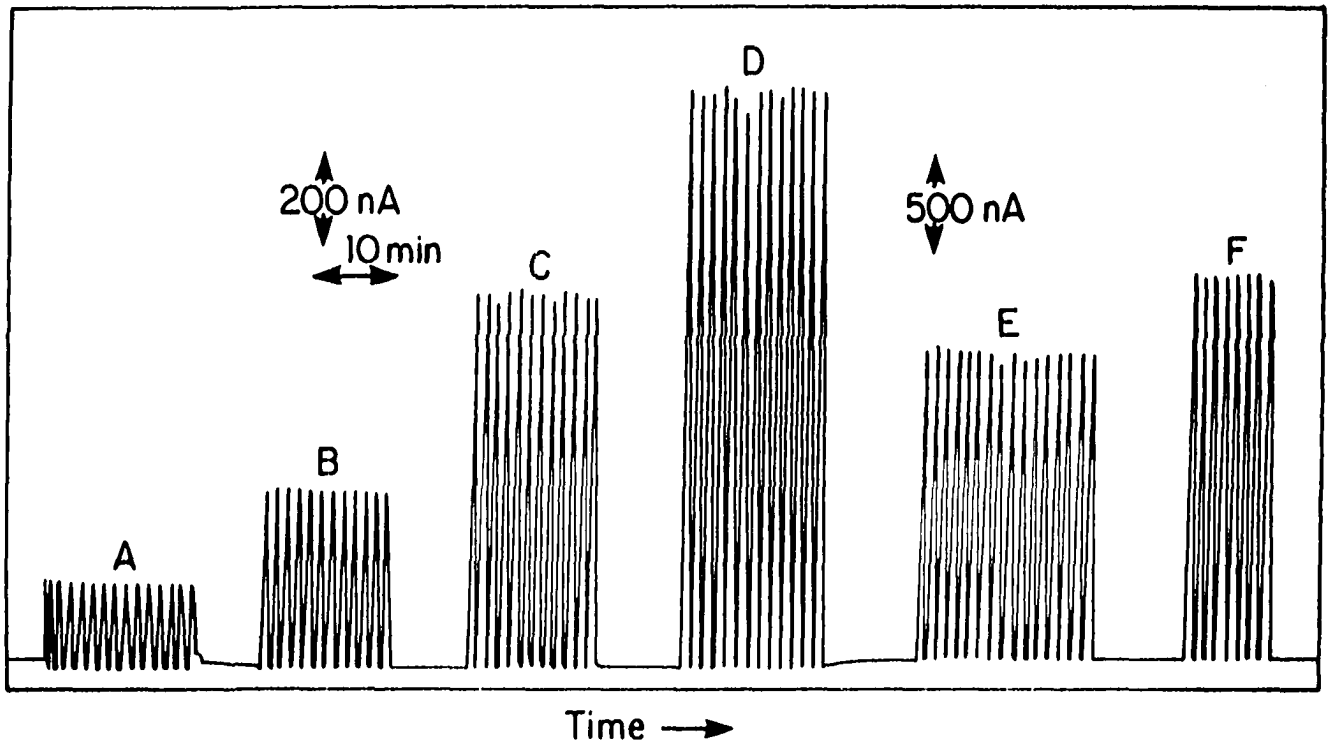
200 nA
10 min
500 nA
A
B
C
D
E
F
Time

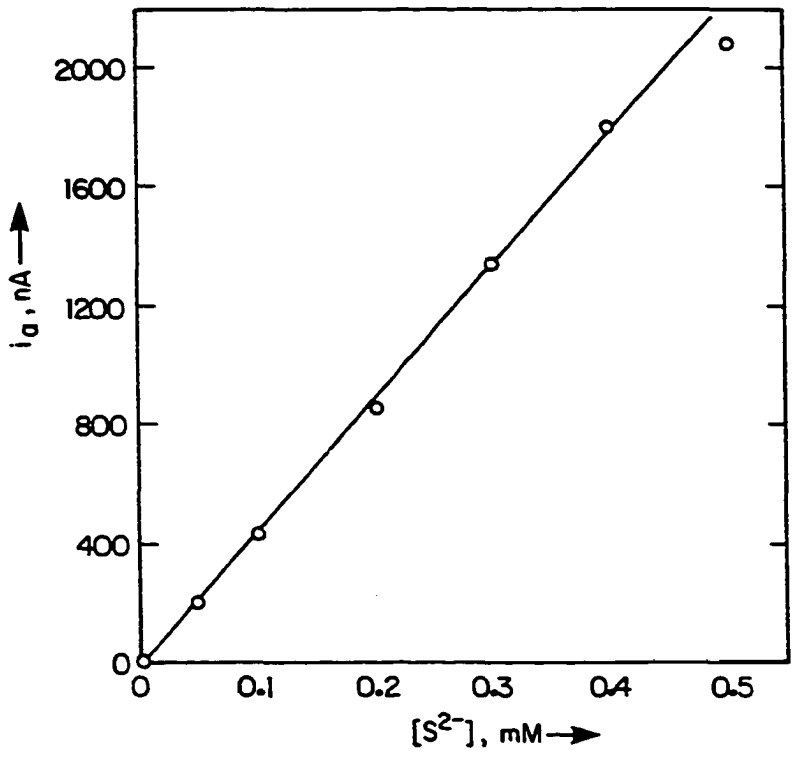

Figure 39. The sulfide calibration curve

FI/EC
SDCP
DME, 1 s
-0.3 V
0.7 ml/min

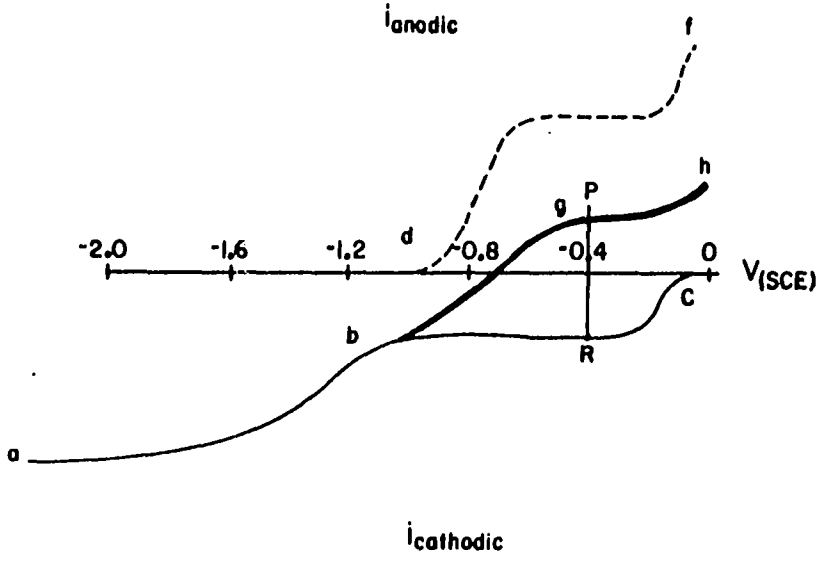

Figure 40. The effect of dissolved O_2 on the i-E curve of S^{2-}
abc: The dissolved O_2 only
df: S^{2-} in the absence of O_2
abgh: S^{2-} in the presence of dissolved O_2
0.1 M NaOH as the supporting electrolyte

electrode potential at -0.4 V, a baseline corresponding to the cathodic current marked R in Figure 40 will be obtained. As soon as the sulfide is injected into the stream, an anodic peak corresponding to the point P will be obtained, thus permitting the detection of sulfide in the presence of dissolved oxygen. In a batch cell, the reproducibility and hence the reliability is lost as a result of a small signal/noise ratio because of the presence of a large background cathodic current of oxygen.

The flow-injection detection peaks for solutions containing 0.4 mM S_2^{2-} and S_5^{2-} are shown in Figure 41. For S_2^{2-}, the relative standard deviation of the mean is 0.265% and for S_5^{2-}, the value is 0.99%. Inspite of a slight drift in the baseline after 30 minutes of operation, reproducibility of the peak heights is observed to be within the relative standard deviation of 3.4%. The calibration data of Na_2S_2 are given in Table 18 and Figure 42.

Table 18. The calibration curve data for Fi/EC of S_2^{2-}

No.	$[S_2^{2-}]$, mM	i_a
1	0	0
2	0.05	200
3	0.10	360
4	0.20	700
5	0.30	1060
6	0.40	1440
7	0.50	1760

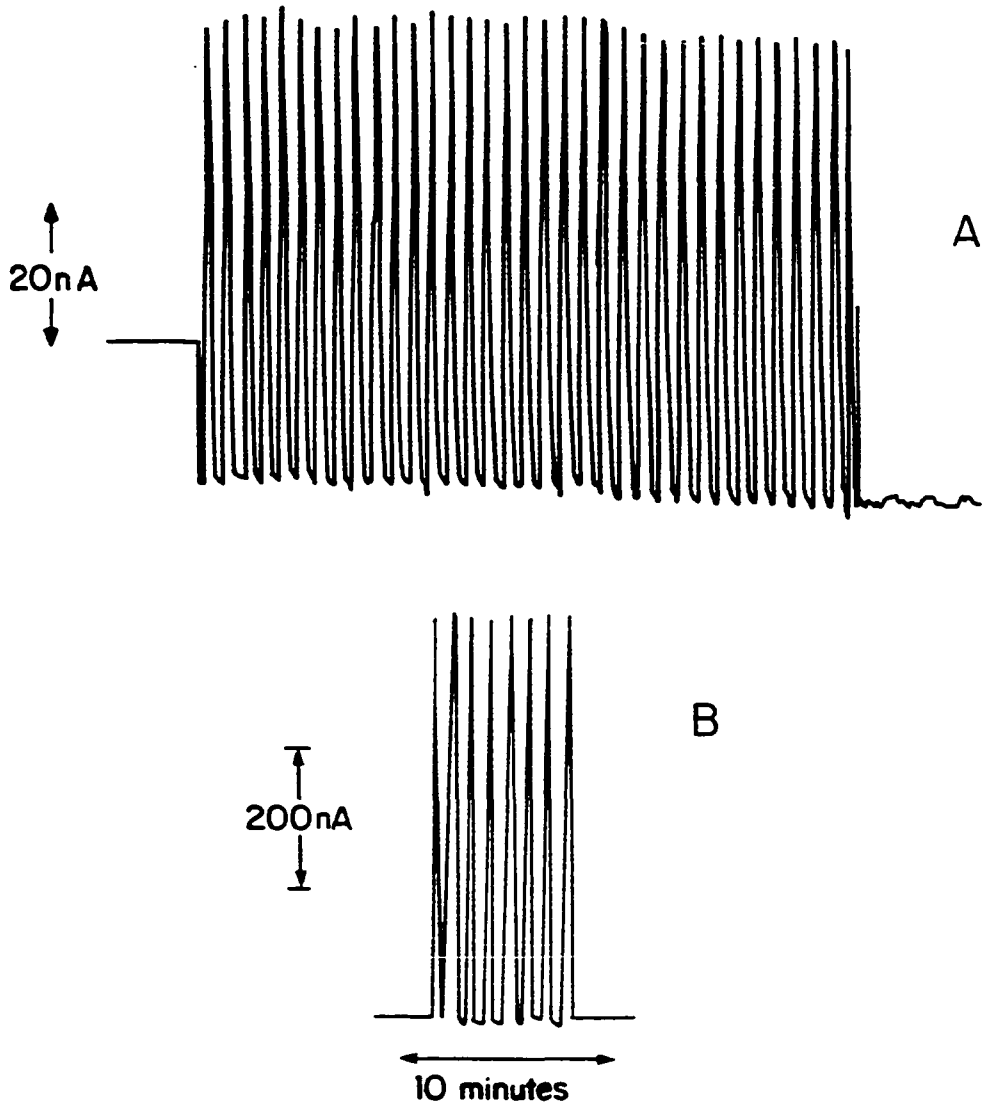

Figure 41. Flow-injection detection of S_x^{2-}
A. S_5^{2-}
B. S_2^{2-}
FI/EC
SDCP
DME, 1 s
-0.3 V
0.7 ml/min

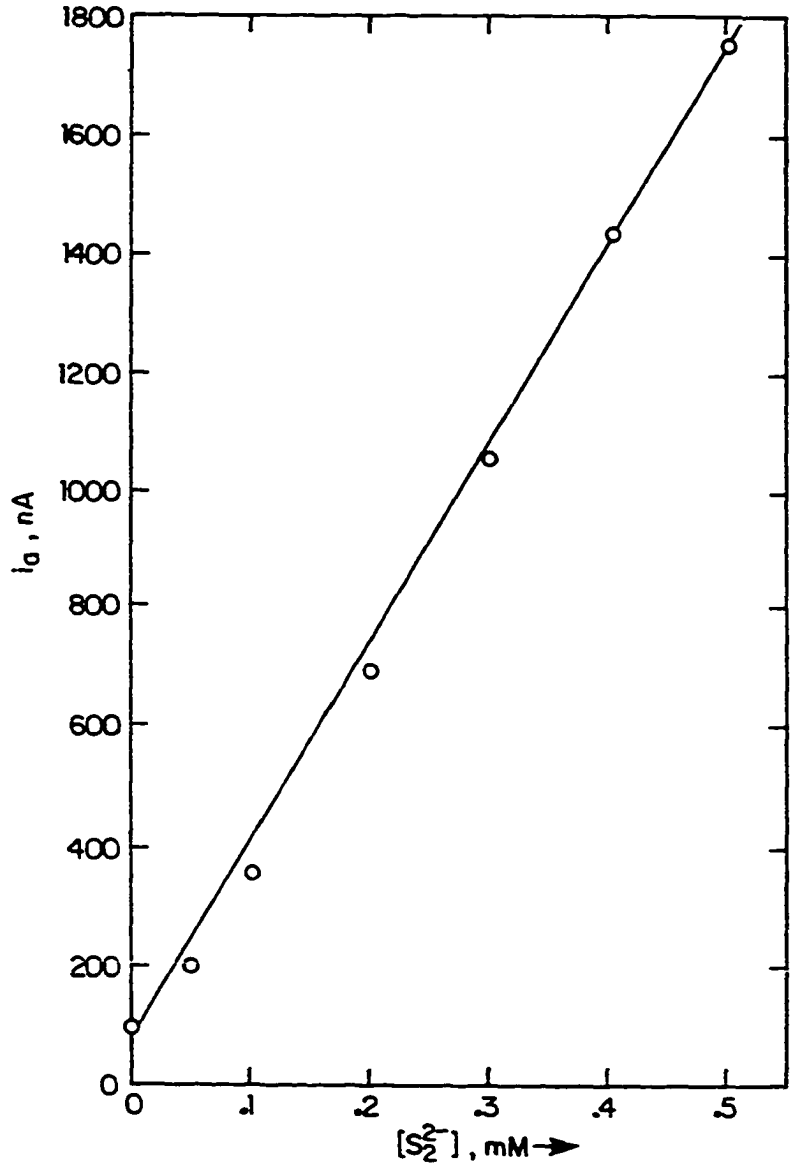

Figure 42. The calibration curve of Na_2S_2 using FI/EC

Na_2S_2
0.1 M NaOH
SDCP
DME, 1 s
-0.3 V
0.7 ml/min

Summary

Flow injection analysis of sulfide and polysulfide solutions was performed by injecting small volume of sample solution into a continuously flowing stream of 0.1 M NaOH solution, and the detection is achieved by using a polarographic flow-through detector. The DME was held at plateau potential of the i-E curve to obtain the amperometric detection of sulfide and polysulfide ions. The peak current and the steady-state currents were obtained over a range of flowrate of hydroxide stream. The value of α was found to be 1.13 for the peak current and 0.75 for the steady-state current. Relatively high value of α is ascribed to the particular electrode geometry and the fluid dynamics. The flow injection detection of sulfide and polysulfide is identified as a low dispersion system.

The peak detection response was found reproducible and linear with concentration. A high sample throughput was achieved.[1] One of the main advantages of using this method is that oxygen, which interferes with most polarographic analyses in batch analyses, does not have to be removed.

FIA is in widespread use because of high sample throughput, accuracy, reproducibility, reliability (in this case, without having to remove the dissolved oxygen), shorter analysis time, easily adaptable to automation using relatively simple and inexpensive equipment.

---

[1] High sample throughput accompanied by high reproducibility makes it an ideal technique for automation.

CHAPTER V. LIQUID CHROMATOGRAPHY

Principles

Liquid chromatography (LC) and electrochemical (EC) detection in flowing solutions are mutually compatible technologies and, when combined (i.e., LCEC), yield important advantages for trace determinations, particularly in complex mixtures (27,92-95). Among the many advantages offered by LCEC, selectivity, sensitivity and economy are the most important. The concept of LCEC can very simply be described as follows: The separation of the species of interest is achieved in a liquid chromatography column and the column effluent passes continually through an electrochemical detection cell where electroactive analyte species can be detected. The electrode current for electroactive analyte is converted to voltage, by an analog converter, which is plotted as a function of time on a stripchart recorder.

Ion chromatography

Ion chromatography is the type of ion-exchange chromatography where the analyte species are separated using a low-capacity separator column. Low capacity columns are packed with pellicular ion-exchange resin constructed by coating a thin film of styrene-divinylbenzene resin on spherical glass beads. The resins are functionalized to provide low ion-exchange capacity.

A small volume of sample is injected into the separator column. The ions of interest are separated by elution with a strong acid,

strong base, or a salt solution. Either cation or anions can be separated by using the appropriate column.

In an anion-chromatographic separation, the eluent is often a solution of $NaHCO_3$ and the separation is based on the following equilibria:

$$\text{Sorption: } Na^+X^- + Na^+Y^- + 2\ \text{Anex} - HCO_3^- \rightleftarrows \text{Anex} - x^- + \text{Anex} - y^- + 2NaHCO_3 \quad (49)$$

$$\text{Elution: } \text{Anex} - x^- + \text{Anex} - y^- + 2NaHCO_3 \rightleftarrows 2\text{Anex} - HCO_3^- + Na^+X^- + Na^+Y^- \quad (50)$$

The separation of ions depends on their relative affinity for the exchange sites. The effluent from the separator column containing the separated anions, in a background of HCO_3^- can be allowed to enter the suppressor column (the "suppressed form" of IC), where the eluent ions are converted to the nonconducting H_2CO_3 according to the reactions:

$$\text{Eluent: } Catex^- - H^+ + Na^+HCO_3^- \rightleftarrows Catex - Na^+ + H_2CO_3 \quad (51)$$

$$\text{Anions: } Catex - H^+ + Na^+X^- \rightleftarrows Catex - Na^+ + H^+X^- \quad (52)$$

The analyte anion (X^-) is converted to the acid HX. If the acidity of HX is greater than H_2CO_3, a conductivity detector registers an increase in conductivity when the eluted anion passes through the detector cell. Alternatively, the effluent from the separator column can direct-

ly go to the detector without suppression of the eluent ions.

The separation of S^{2-}, SO_3^{2-} and $S_2O_3^{2-}$ was achieved by a slightly modified Dionex Ion Chromatograph. The eluent was an aqueous solution of 0.02 M KNO_3 and 0.05 M NaOH. The effluent from the column was mixed with a stream of phosphate buffer solution in a post-column mixer to neutralize NaOH, which interferes with the S^{2-} peak. The analyte species were detected polarographically at a DME operated in the amperometric mode of detection.

Experimental

Analytical Grade Chemicals were used without further purification. The procedure for preparing the sulfide and polysulfide solutions was given earlier.

Polarograms were recorded using a PAR Model 174A potentiostat, the conventional DME and the PAR Model RE 0074 X-Y recorder. All potentials were measured relative to the SCE. A Pt wire electrode was used as the auxiliary electrode.

A schematic diagram of the liquid chromatographic system is shown in Figure 43. A Laboratory Data Control Minipulse Model 396 was used initially with the Dionex Prototype Anion Separator Column HPAS-6. Later, the Laboratory Data Control pump was replaced by the Dionex 2020i Advanced Chromatography Module and the Dionex Analytical Pump. This provided a much more stable and uninterrupted eluent flow. The Dionex HPAS-6 prototype ion exchange column, initially used to effect

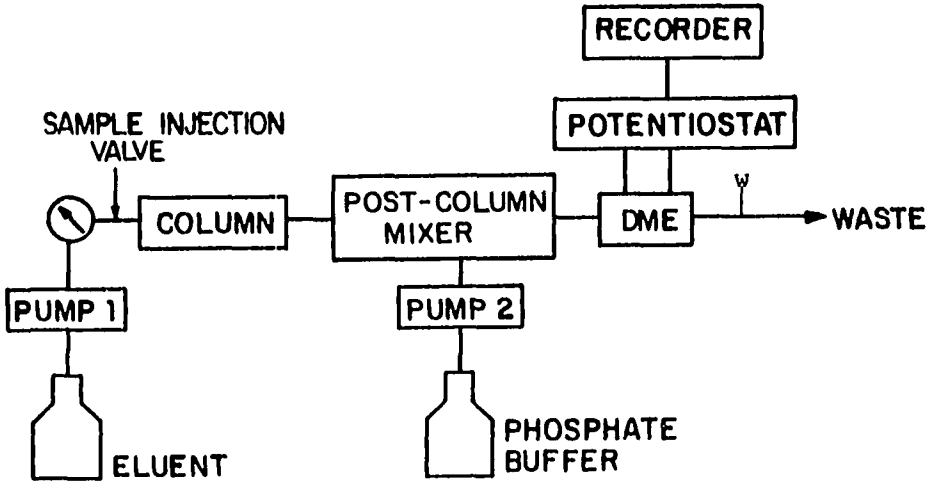

Figure 43. Schematic diagram of LCEC

the separation of sulfide, sulfite and thiosulfate, was substituted later by the Dionex HPAS-3 column, which enhanced the separation efficiency considerably. The sample injection was done initially using a Valco Instruments Universal Inlet System. This system was replaced later by the Dionex Injection System of the Model 2020i. A post-column mixer was constructed by partially filling a 2.5-in piece of Altex tubing, 0.8-mm i.e., with 0.5-mm glass beads (B. Braun Melsungen AG, Germany) and an Altex three-way Teflon connector. A Gilson Minipulse-2 peristaltic pump was used for post-column mixing. The flow-through detection system utilized a PAR Model 174A DME assembly, complete with the drop knocker, a PAR Model H165 flow cell, and a flow adapter constructed in the machine shop of the Department of Chemistry. The design of the detector was derived from the commercially available PAR Model 310 Polarographic Analyzer (Princeton Applied Research).

Results and Discussion

Polarographic responses for aqueous solutions containing various anionic sulfur species are summarized in Figure 44 and the observed half-wave potentials ($E_{\frac{1}{2}}$) are listed in Table 19. Theoretically, a separation of $\leq$150 mV in the half-wave potentials is required to allow complete voltammetric resolution of the polarographic waves in solutions of the mixtures. The i-E curves of a solution containing a mixture of sulfide, sulfite and thiosulfate in aqueous KNO_3 are shown in Figure 45. The close proximity of the half-wave potentials of sulfite and thiosulfate makes it impossible to resolve these two waves.

Figure 44. Sampled DC polarograms of individual sulfur species in 0.1 M KNO_3

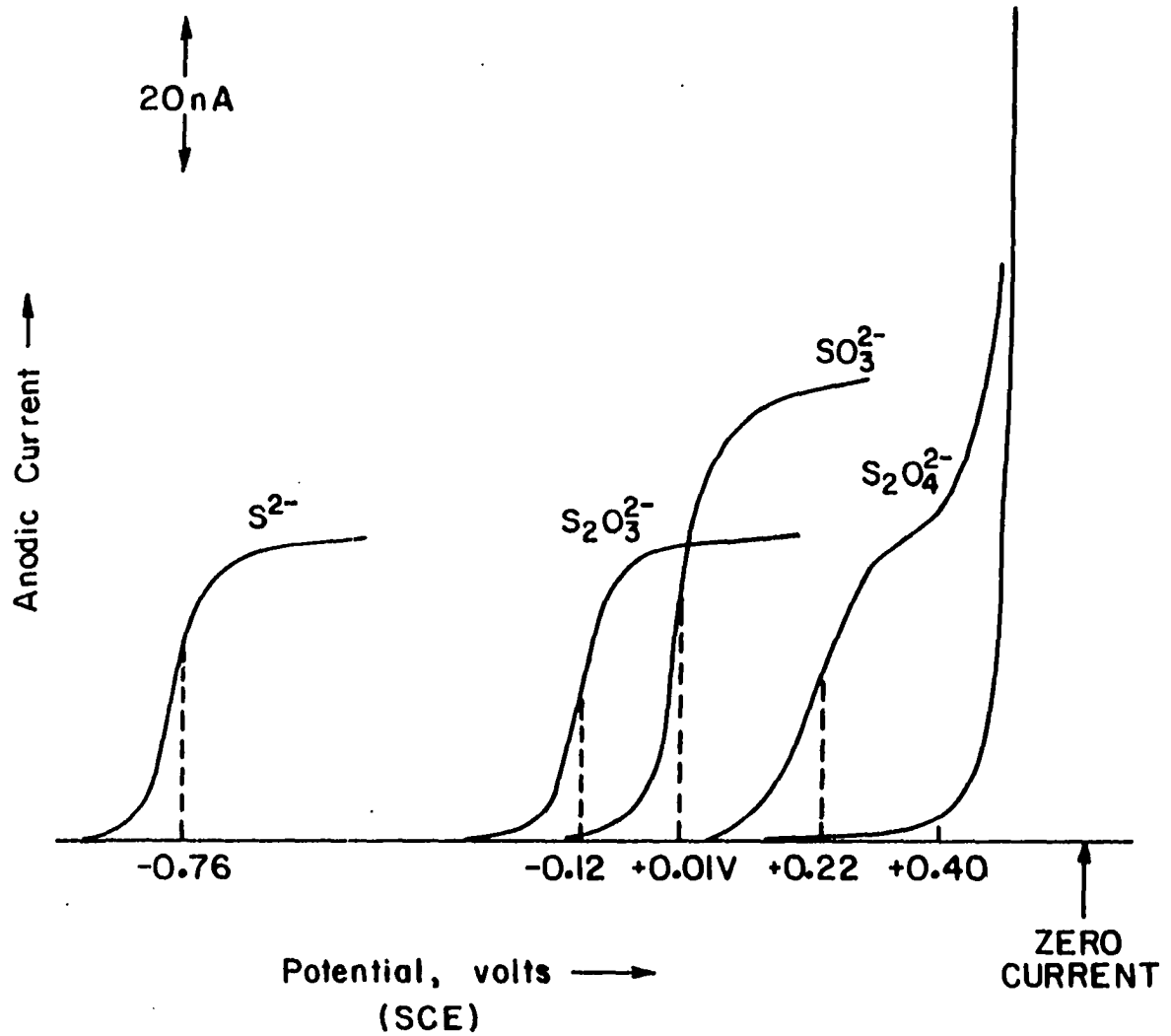
20nA
Anodic Current
S^{2-}
$S_2O_3^{2-}$
SO_3^{2-}
$S_2O_4^{2-}$
-0.76
-0.12
+0.01V
+0.22
+0.40
ZERO CURRENT
Potential, volts
(SCE)

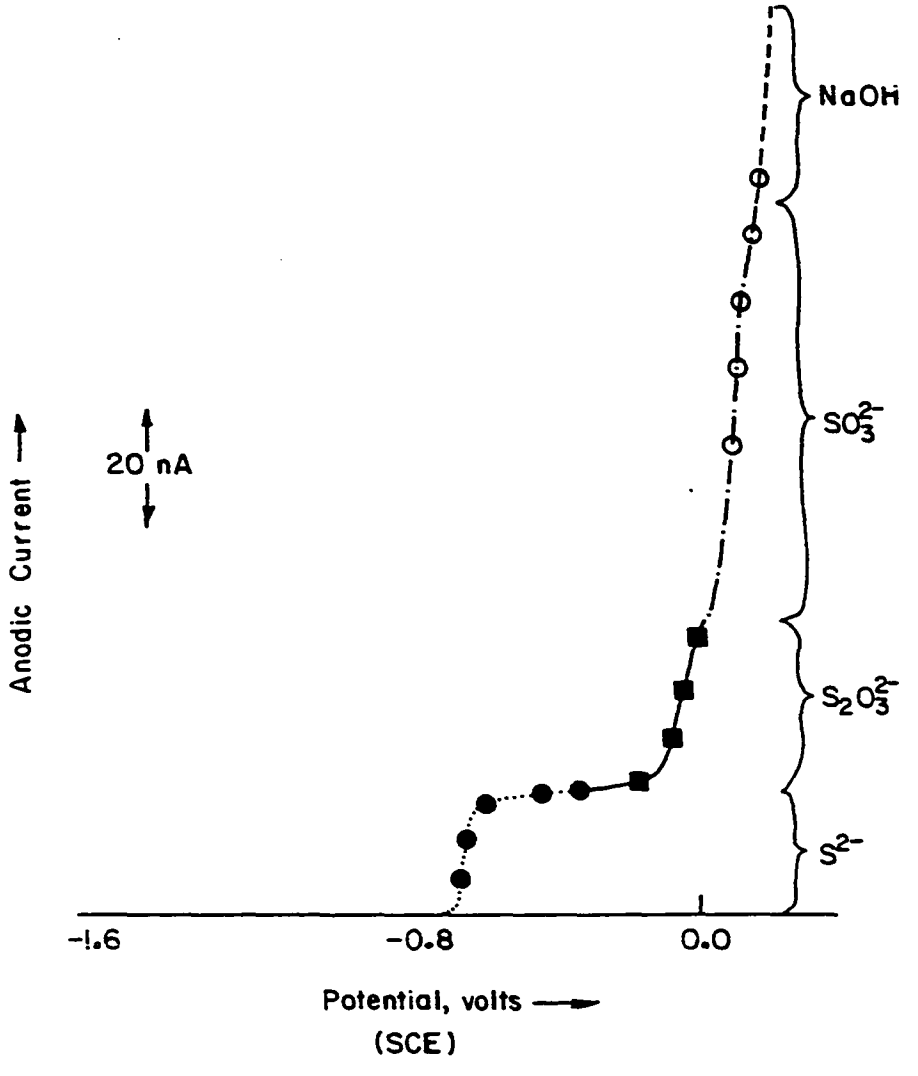

Figure 45. Simultaneous determination of sulfide, sulfite and thiosulfate by sampled DC polarography using 0.1 M NaOH as supporting electrolyte

Table 19. The half-wave potentials of sulfur compounds in 0.1 M KNO_3

Anion	$E_{1/2}$, V
S^{2-}	-0.76
$S_2O_3^{2-}$	-0.12
SO_3^{2-}	+0.01
$S_2O_4^{2-}$	+0.22
S_x^{2-}	-0.76

It is, therefore, necessary to separate these compounds before they can be detected by the polarographic method.

Optimization

The schematic diagram of liquid chromatography employing the polarographic detector was shown in Figure 43. The eluent was a 0.05 M NaOH solution containing 0.02 M KNO_3. The $pK_{a,1}$ for H_2S is 7.04 and the ratio $[H_2S]/[HS^-]$ in a neutral solution is ca. 1.0. In order to keep the ratio $[H_2S]/[HS]^- \leq 0.001$ it is necessary to keep the pH $\geq$ 10. Hence, the alkaline eluents containing 0.1 M NaOH were used. An electrode potential of ca. +0.10 V was found to provide optimum sensitivity for the detection of sulfur compounds S^{2-}, SO_3^{2-} and $S_2O_3^{2-}$ whereas a detection potential of -0.12 V was found optimum for the S_x^{2-} peak. The high pH of the eluent resulted in a large anodic current at +0.10 V because of the reaction

$$Hg + 2OH^- \rightarrow Hg(OH)_2 + 2e;\ E_{\frac{1}{2}} = +0.08\ V \qquad (23)$$

making it impossible to keep the baseline within the operating range of the recorder. The OH^- from the sample, therefore, needed to be neutralized after the chromatographic separation before being detected at the DME. This was accomplished by directing the column-effluent into a post-column mixer where the OH^- was neutralized by a phosphate buffer at pH 7 (0.02 M NaH_2PO_4/0.02 M Na_2HPO_4). The combined solutions of column effluent and buffer had a pH of approximately 7.

A typical chromatographic separation of S^{2-}, SO_3^{2-} and $S_2O_3^{2-}$ is shown in Figure 46. It is important to note that the sulfide peak is preceded by the OH^- peak, as expected. The observation of a peak for OH^- indicated that not all OH^- present in the injected sample was neutralized in the post-column mixer.

The retention time of the $S_2O_3^{2-}$ peak is ca. 20 min in Figure 46 and the peak is asymmetric. In order to decrease the retention time and improve the peak shape of $S_2O_3^{2-}$, a commercially available, Dionex HPIC-AS3 column was used. The amperometric response for a solution containing S^{2-}, SO_3^{2-} and $S_2O_3^{2-}$ using the Dionex Advance Chromatography Module is shown in Figure 47. The separation that previously took 20 minutes with the HPIC-AS6 column (Figure 46) is now completed in 6 minutes. This is possible because of the use of lower capacity ion-exchange resin in the HPIC-AS3 column and the use of substantially higher flowrates.

The response of the three sulfur species, using the Dionex HPIC-AS6

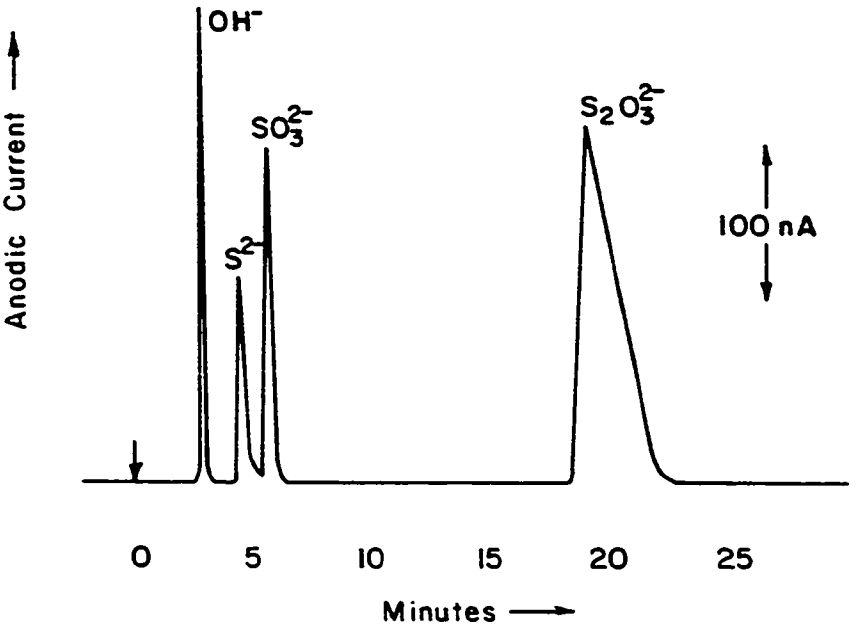

Figure 46. Determination of sulfide, sulfite and thiosulfate in NaOH using LCEC

DME at +0.08 V (SCE)
1.1 ml/min
0.01 M NaOH
0.05 M KNO_3

0.02 M phosphate buffer, pH 7.6 at post-column mixer

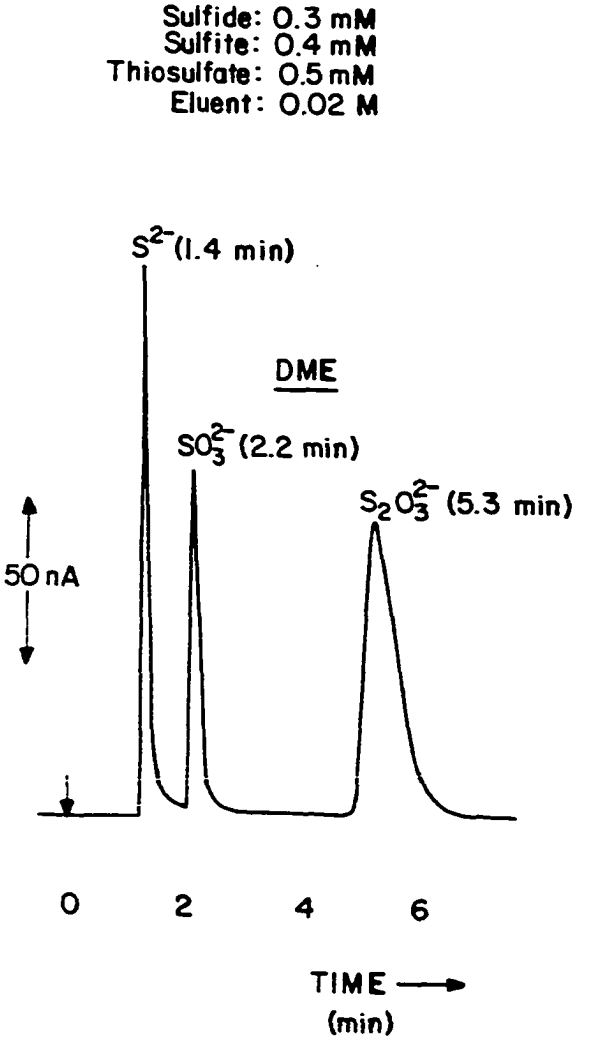

Figure 47. The response of electrochemical detector using the Dionex chromatograph

column, was observed as a function of electrode potential, the eluent flowrate and the concentration of NO_3^- in the eluent. Successive chromatograms of a solution containing S^{2-}, SO_3^{2-} and $S_2O_3^{2-}$ were obtained by varying the electrode potential from -0.6 V to 0.10 V. The anodic current of each of the components in the solution was obrained by measuring the peak height of the corresponding species. The data shown in Table 20 are plotted in Figure 48. The optimum potential range for the DME is found to be 0.0 V to +0.10 V, and any value chosen in this range will provide adequate response for the detection of S^{2-}, SO_3^{2-} and $S_2O_3^{2-}$ at the DME.

Table 20. The dependence of anodic current of S^{2-}, SO_3^{2-} and $S_2O_3^{2-}$ on detection potential

Applied potential, V	i_a, nA		
	S^{2-}	SO_3^{2-}	$S_2O_3^{2-}$
+0.10	12.0	17.0	6.2
0.00	10.0	12.0	5.4
-0.10	13.0	13.2	7.0
-0.20	14.0	0.4	8.0
-0.30	17.0	-[a]	4.1[b]
-0.40	19.0	-	4.0
-0.50	18.2	-	-
-0.60	17.0	-	-

[a]No peak.

[b]Very broad peak.

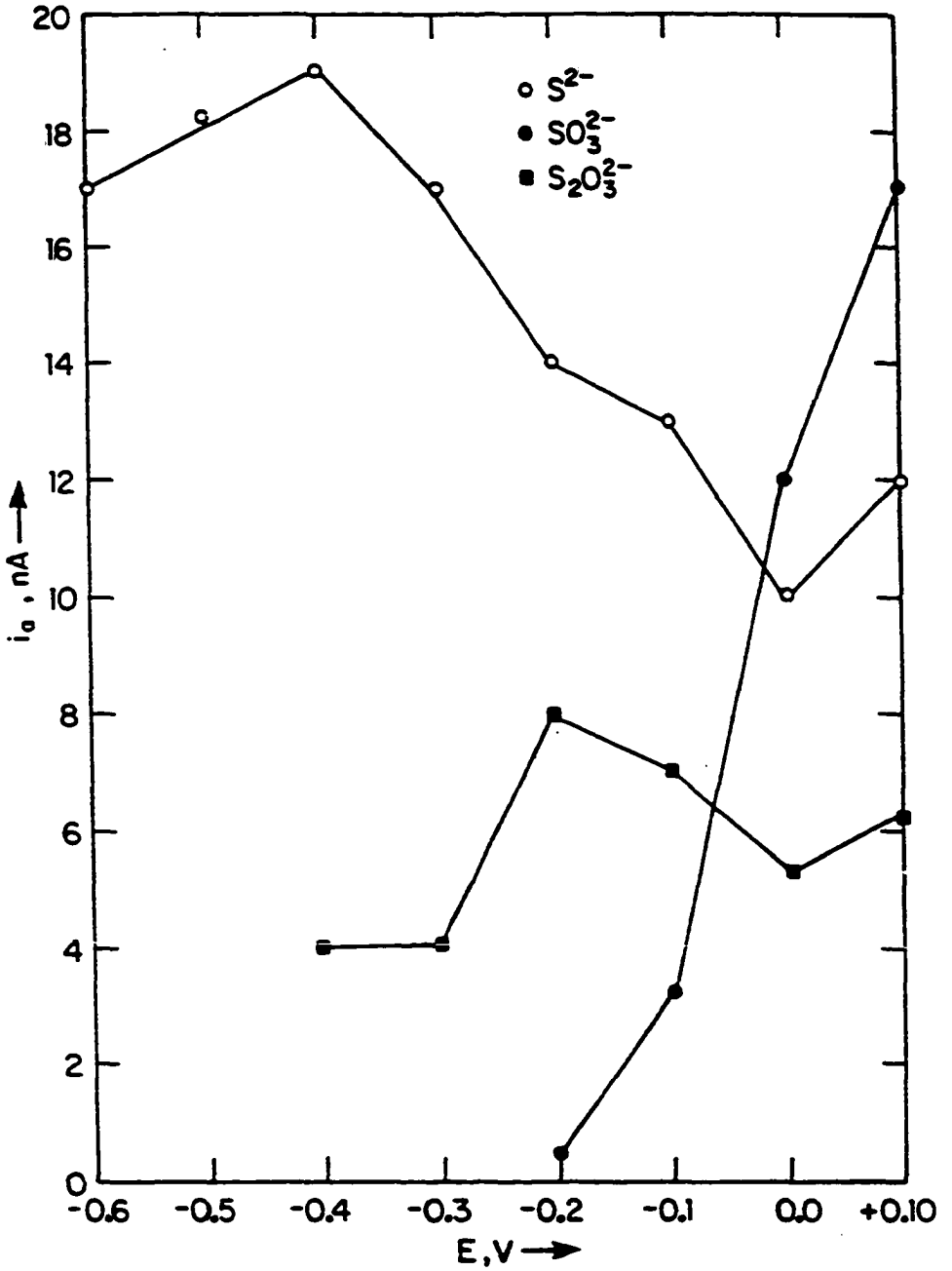

Figure 48. Anodic current of S^{2-}, SO_3^{2-} and $S_2O_3^{2-}$ as a function of detection potential

The effect of flowrate on the anodic peaks of S^{2-}, SO_3^{2-} and $S_2O_3^{2-}$ was observed by injecting a solution, containing those compounds, into the liquid chromatograph operated at a range of flowrates. The anodic current and the retention time for each of these compounds were measured and plotted as a function of flowrate. The data shown are shown in Table 21 and Figure 49.

Since the limiting response of an amperometric detector is given by the equation

$$i_\ell = nFAK_\ell V_f^\alpha C^b \tag{43}$$

where all symbols carry the usual meanings stated on pages 89-91, the value of α is obtained by the equation

$$\ln i = \text{constant} + \alpha \ln V_f \tag{47}$$

Table 21. The variation of anodic currents and retention times of S^{2-}, SO_3^{2-} and $S_2O_3^{2-}$ with eluent flowrate

V_f ml/min	t_R, min			i_a, nA		
	S^{2-}	SO_3^{2-}	$S_2O_3^{2-}$	S^{2-}	SO_3^{2-}	$S_2O_3^{2-}$
0.6	5.0	6.3	25.0	7.2	4.8	1.8
0.8	3.8	4.9	19.0	8.0	5.4	2.2
1.0	3.0	3.9	15.5	9.0	6.0	2.6
1.2	2.7	3.3	13.0	9.8	6.8	2.8
1.4	2.3	2.9	11.5	10.2	7.0	3.0
1.6	2.0	2.7	10.4	10.0	6.8	3.0
1.8	2.0	2.4	10.0	6.6	4.4	2.0

The values of ln i and ln V_f obtained from Table 21 are given in Table 22 and plotted in Figure 50. The values of α obtained from the straight-line portion of Figure 50 are stated also in the lower portion of Table 22. The α values shown agree with the literature value (92) and appear to represent the experimental observations closely in the sense that whereas the relative increase in the anodic current of S^{2-} by increasing V_f is not as large as it is for SO_3^{2-} and $S_2O_3^{2-}$.

Table 22. ln i and ln V_f for S^{2-}, SO_3^{2-} and $S_2O_3^{2-}$

ln V_f	ln i		
	S^{2-}	SO_3^{2-}	$S_2O_3^{2-}$
-0.51	1.97	1.57	0.58
-0.22	2.08	1.69	0.79
0.0	2.20	1.79	0.96
0.18	2.28	1.92	1.03
0.34	2.32	1.95	1.10
0.47	2.30	1.92	1.10
0.59	1.89	1.48	0.69
slope	0.29	0.35	0.64

In addition to observing the effect of flowrate on the amperometric response of the three sulfur species, the retention time (t_R) of S^{2-}, SO_3^{2-} and $S_2O_3^{2-}$ was studied as a function of NO_3^- concentration in the eluent. The results of this study are given in Table 23 and plotted in Figure 51.

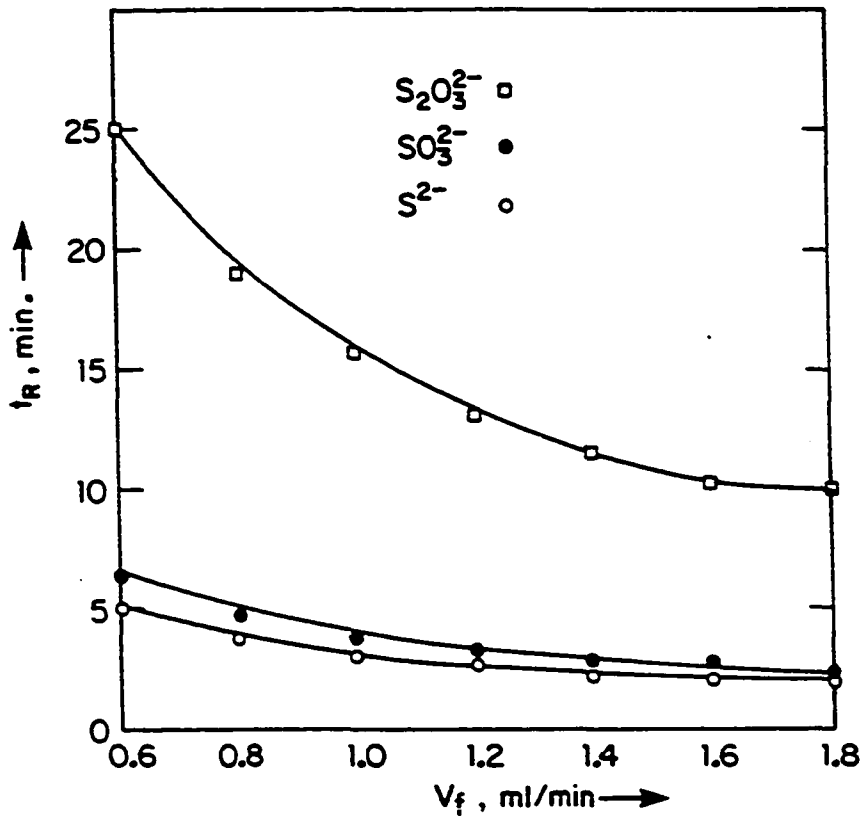

Figure 49. Retention time of S^{2-}, SO_3^{2-} and $S_2O_3^{2-}$ as a function of eluent flowrate

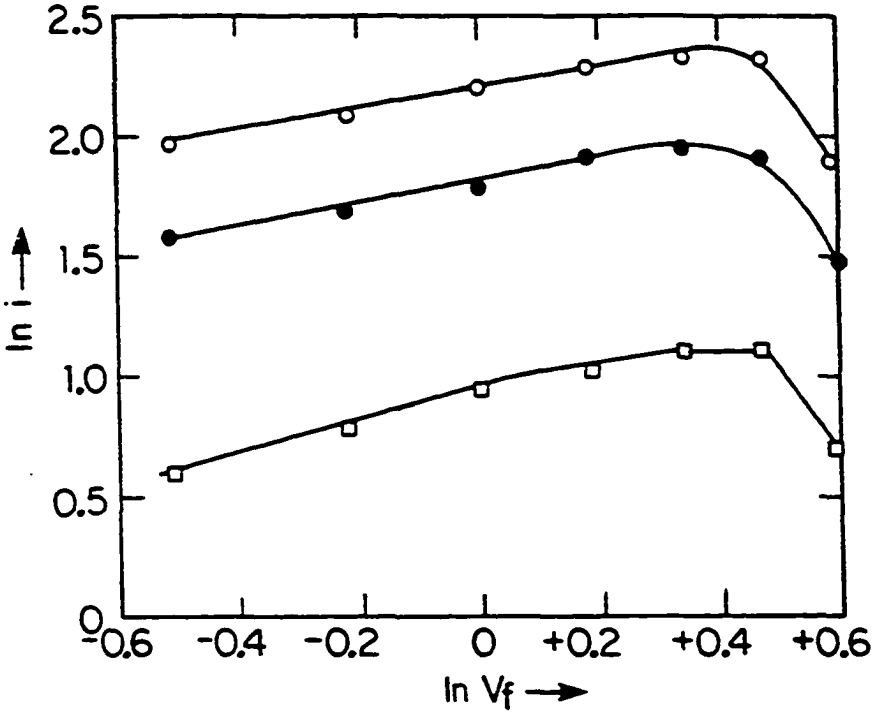

Figure 50. Evaluation of α for S^{2-}, SO_3^{2-}, $S_2O_3^{2-}$ using LCEC

Table 23. Effect of $M_{NO_3^-}$ on retention time of S^{2-}, SO_3^{2-}, $S_2O_3^{2-}$, S_2^{2-} and S_5^{2-}

$M_{NO_3^-}$	S^{2-}	SO_3^{2-}	$S_2O_3^{2-}$	S_2^{2-}	S_5^{2-}
0.02	3.5	11.0	-	9.0	9.0
0.04	2.5	3.9	17.0	9.0	9.0
0.06	2.2	2.8	11.0	9.0	9.0
0.08	1.8	1.8	5.0	9.0	9.0
0.10	1.5	1.7	3.5	9.0	9.0

It is observed from Figure 51 that the retention times for S^{2-}, SO_3^{2-} and $S_2O_3^{2-}$ decrease with increasing the concentration of NO_3^- and that the variation is not linear. The retention time of S_2^{2-} and S_5^{2-} is the same and is independent of the NO_3^- concentration, suggesting that the retention mechanism for S_x^{2-} does not involve ion exchange. The cathodic peak at 9 min grows only by the addition of S_x^{2-} whereas the anodic peak at 11 min increases only by the addition of $S_2O_3^{2-}$, thus, verifying the correctness of the assignment of peaks. It was later questioned whether the peak obtained at 9 min by injecting S_x^{2-} is cathodic. A series of injections of a 5 mM S_5^{2-} solution were made. The chromatographic response obtained by varying the potential of the DME from -1.8 V to +0.2 V is shown in Figure 52. The peaks at 9 min are in the anodic direction but lie in the cathodic current region, as is evident by referring to the zero current line shown at the top of Figure 52. As the detection potential is moved from -1.8 to 0.0 V, the anodic peak of $S_2O_3^{2-}$ is also seen at 11 min as expected because

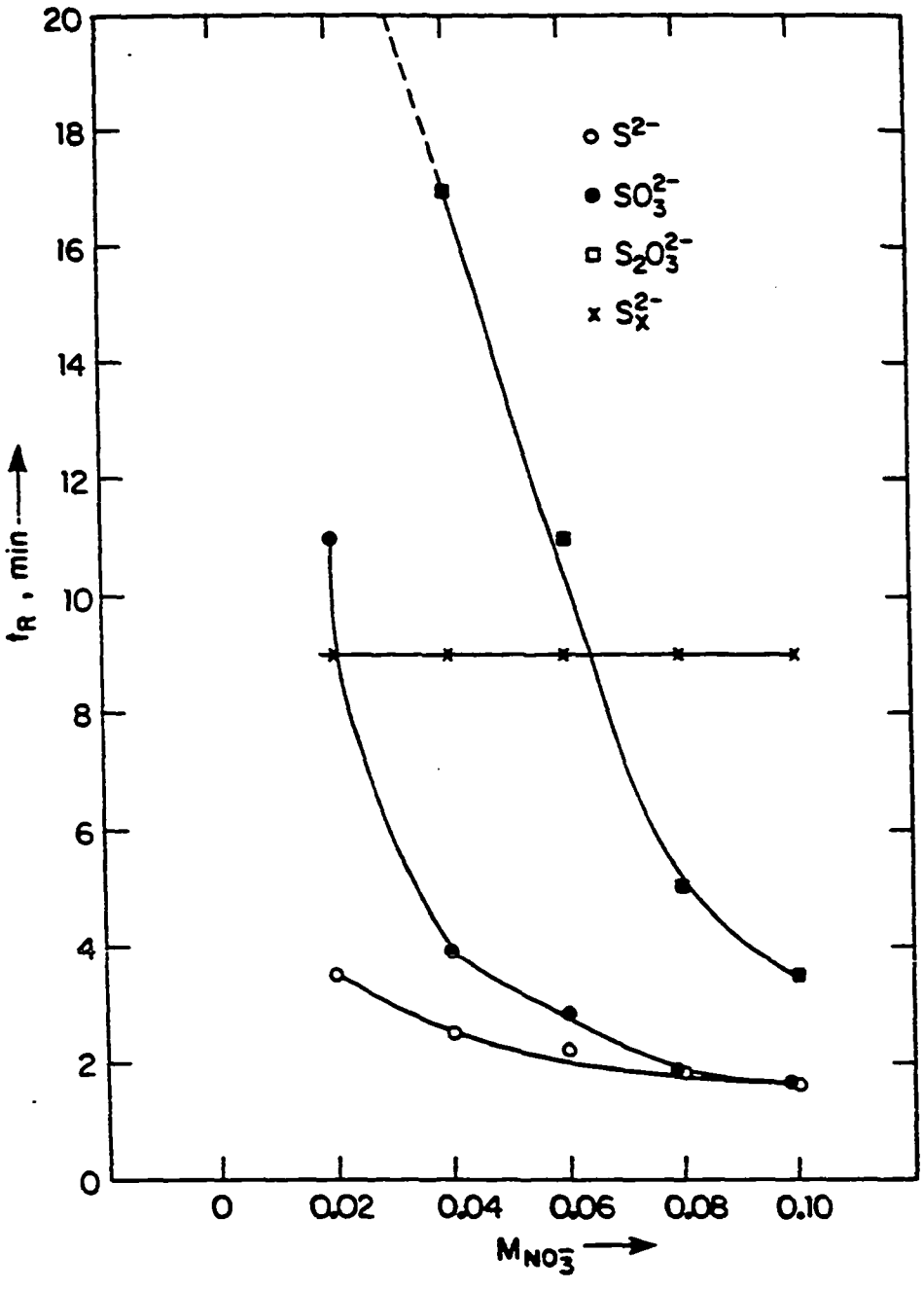

Figure 51. The retention time of S^{2-}, SO_3^{2-}, $S_2O_3^{2-}$ and S_x^{2-} as a function of $M_{NO_3^-}$

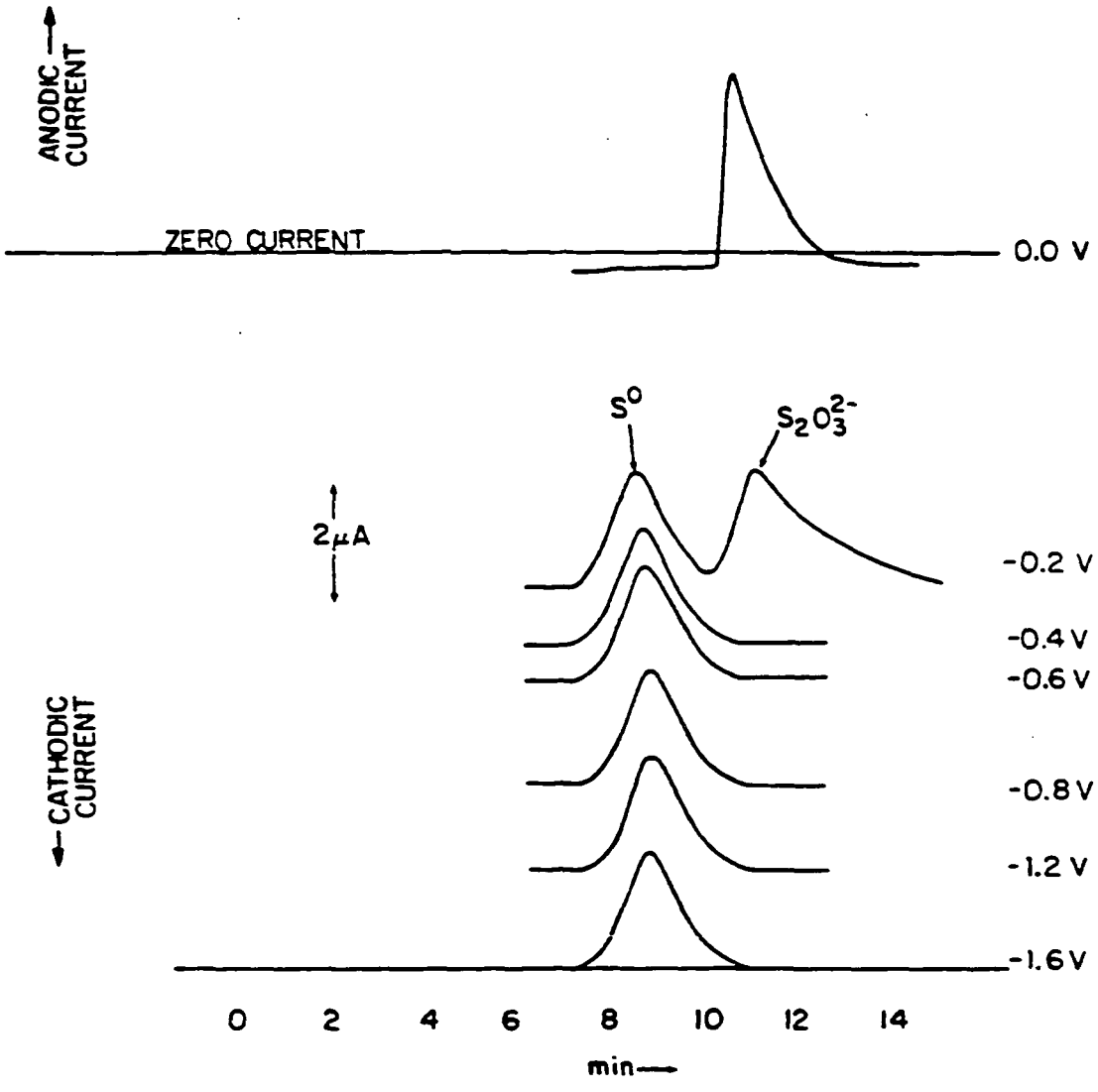

Figure 52. The chromatographic response of S_5^{2-} using polarographic detection at various applied potentials

$S_2O_3^{2-}$ gives an anodic response at potentials positive of -0.4 V (Figure 48). At potentials positive of -0.2 V, the 9-minute peak disappears. The fact that the 9-min peak is typically obtained in the negative end of the range of applied potentials, precludes the possibility that the peak is anodic, even though it is pointed in the direction of the anodic current. It is tentatively assigned to the S^o dissociated from S_x^{2-} when the ion is strongly adsorbed.

$$S_x^{2-} \rightarrow S^{2-} + (x - 1)S^o \qquad (53)$$

The suggestion is supported by the fact that no other peak for S_x^{2-} is obtained in the anodic region which would be characteristic of S_x^{2-}. A S^{2-} peak and the 9-min "cathodic" peak are invariably obtained when S_x^{2-} is injected into the chromatograph. Furthermore, these two peaks vary with the S_x^{2-} concentration. No cathodic response typical of S_x^{2-} is observed in the chromatographic effluent.

It is speculated that the eluted S^o species is adsorbed and changes the doubles layer capacity resulting in the change of current recorded as a peak at 9 min.

Application to coal samples

The method was applied for determining sulfide, sulfite and thiosulfate in the alkaline process-stream samples derived from the desulfuration of coal by molten caustic. The caustic desulfurization of coal is presently being carried out by Fossil Energy Group of the Ames Laboratory at Iowa State Univesity. In this process, a 50-g sample of coal is

mixed with 500 g of a 80:20 (wt %) mixture of solid NaOH and KOH and heated to 375°C for one hour in a crucible. The treated coal is separated from the molten caustic solution by a stainless steel wire basket. The spent caustic in the crucible is leached with 1-2 L of water to produce a solution termed as a process stream 1 (PS-1). The treated coal carries with it about two times its own weight of NaOH which is washed with 1-2 L of water to produce a solution termed process stream 2 (PS-2). The final volume of both PS-1 and PS-2 is 2 L; therefore, the OH^- concentration in PS-1 and PS-2 is ca. 4.5 M and 1.3 M, respectively. In view of such a large OH^- concentration, it was necessary to determine the effect of an excess of OH^- on the separation of sulfide, sulfite and thiosulfate. The effect of an excess of OH^- on the resolution of S^{2-}, SO_3^{2-} and $S_2O_3^{2-}$ was studied and the problem of the interference of a large OH^- peak with the S^{2-} peak was solved by making use of a flow-programmed separation as described below.

The use of a flow-programmed separation A typical chromatogram for a solution containing sulfide, sulfite and thiosulfate in 5 mM OH^- is compared with a similar solution containing 0.5 M NaOH in Figure 53. The sulfide peak is not resolved from the large OH^- peak, making it impossible to determine S^{2-} in the presence of a large concentration of OH^-. The desired separation was, eventually, achieved by using flow-programmed elution, with a decreased NO_3^- concentration, and after diluting the sample. In the flow-programmed separation, the sample was injected at a slower flowrate (0.9 mL/min) and, after the sulfide peak was obtained, the flowrate was increased to three times

its original value in order to produce the later eluting peaks. The chromatogram for such a separation is shown in Figure 54. The retention times of S^{2-}, SO_3^{2-} and $S_2O_5^{2-}$ are compared with those from Figure 46 as shown in Table 24.

Table 24. The improvement achieved in the retention data of S^{2-}, SO_3^{2-} and $S_2O_3^{2-}$ as a result of using the flow-programmed separation

Constituent	Retention time, min	
	Flow-programmed separation	No flow programming
S^{2-}	3	5
SO_3^{2-}	5	6.5
$S_2O_3^{2-}$	9	20

It can be seen that significant improvement is achieved by using the flow-programmed separation, especially the retention time of the $S_2O_3^{2-}$ peak has been decreased dramatically.

Calculation of analytical results The concentration of S^{2-}, SO_3^{2-} and $S_2O_3^{2-}$ in the unknown sample were determined by the method of standard additions. An injection of the unknown solution was made into the liquid chromatograph and the values of the anodic peak currents for S^{2-}, SO_3^{2-} and $S_2O_3^{2-}$ obtained. A series of injections were then made from the unknown solution into which successively increasing amounts of concentrated standard solutions of S^{2-}, SO_3^{2-} and $S_2O_3^{2-}$ were added, and the values of the anodic peak currents obtained from the respective chromatograms. Sample data from process stream No. 1 (PS-1)

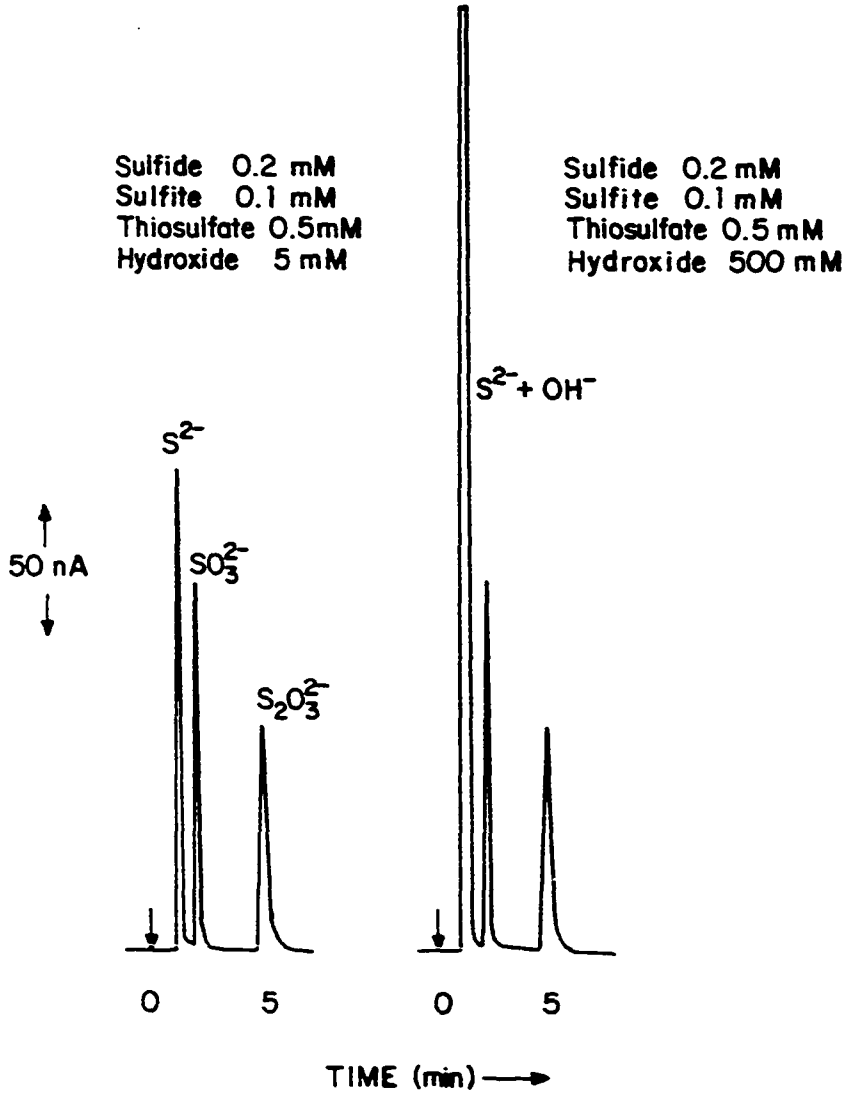

Figure 53. The interference of the hydroxide peak with the sulfide peak

Figure 54. Chromatogram of a solution containing sulfide, sulfite and thiosulfate using LCEC with flow-programmed separation

0.02 M KNO_3

0.005 M NaOH

0.02 M phosphate buffer at post-column mixer

Initial flowrate 1 ml/min

Final flowrate 3 ml/min

S^{2-} 0.9 mM

SO_3^{2-} 0.3 mM

$S_2O_3^{2-}$ 0.5 mM

OH^- 100 mM

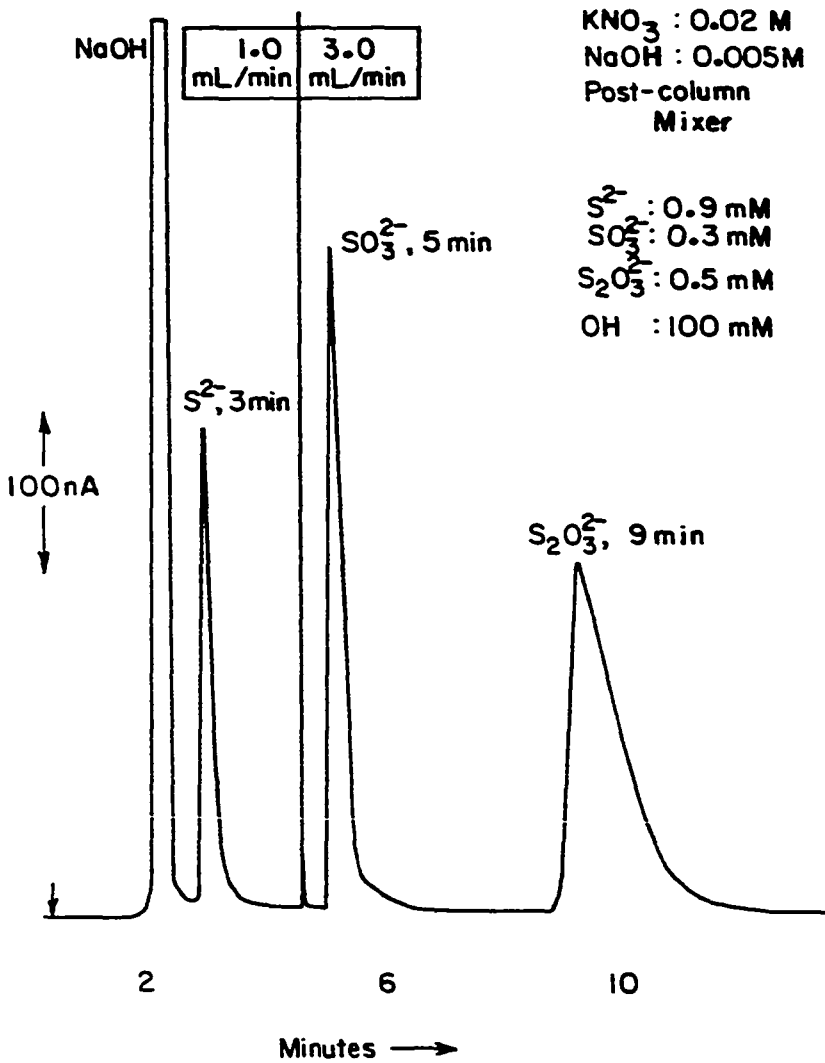
NaOH
1.0 mL/min
3.0 mL/min
KNO_3 : 0.02 M
NaOH : 0.005M
Post-column Mixer
S^{2-} : 0.9 mM
SO_3^{2-} : 0.3 mM
$S_2O_3^{2-}$: 0.5 mM
OH : 100 mM
SO_3^{2-}, 5 min
S^{2-}, 3min
100nA
$S_2O_3^{2-}$, 9 min
2
6
10
Minutes

from Illinois No. 6 sample #8 are given in Tables 25 and 26 and plotted in Figure 55. The calculations and results of the analysis are shown in Table 26.

Table 25. Anodic currents of S^{2-}, SO_3^{2-} and $S_2O_3^{2-}$ as a function of the standard additions of S^{2-}, SO_3^{2-} and $S_2O_3^{2-}$

Solution no.	Concentration of the standards added, mM			Anodic current (i_a), nA		
	S^{2-}	SO_3^{2-}	$S_2O_3^{2-}$	S^{2-}	SO_3^{2-}	$S_2O_3^{2-}$
1	0	0	0	170	200	30
2	0.4	0.4	0.5	450	320	90
3	0.6	0.6	0.7	500	430	110
4	0.8	0.8	1.0	680	540	140
5	1.2	1.2	1.2	940	680	150

Table 26. Calculations of the quantity of sulfur present in the unknown sample using the data from Figure 56

	S^{2-}	SO_3^{2-}	$S_2O_3^{2-}$
mM	0.27	0.55	0.30
Dilution factor	5	5	5
Concentration in unknown, mM	1.35	2.75	1.50
Grams of sulfur/L	0.0432	0.088	0.096
Grams of sulfur/2L	0.0864	0.176	0.192

Figure 55. The standard additions of S^{2-}, SO_3^{2-} and $S_2O_3^{2-}$ in the unknown solution

LCEC
KNO_3 0.02 M
NaOH 0.005 M
SDCP
DME, 1 s

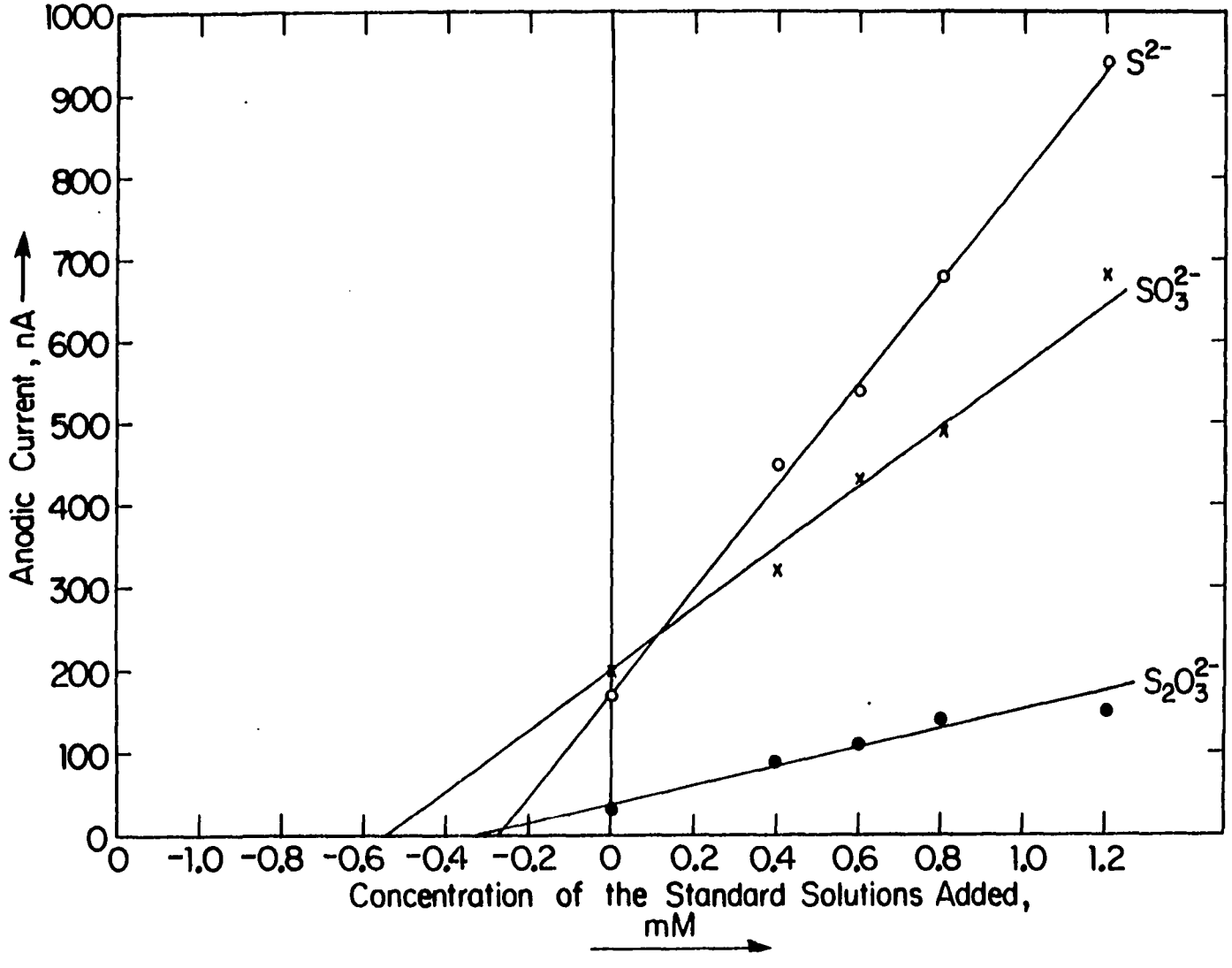
1000
900
800
700
600
500
400
300
200
100
0
Anodic Current, nA
S^{2-}
SO_3^{2-}
$S_2O_3^{2-}$
0 -1.0 -0.8 -0.6 -0.4 -0.2 0 0.2 0.4 0.6 0.8 1.0 1.2
Concentration of the Standard Solutions Added, mM

A series of process-stream samples from Illinois No. 6 coal was analyzed to determine sulfide, sulfite and thiosulfate. The results of the analysis calculated by using the method described above are summarized in Table 27.

Table 27. Grams of sulfur present in the process-stream samples derived from 50 g of Illinois No. 6 coal

Run no.	Process stream (PS)	Sulfide	Sulfite	Thiosulfate
7	1	0.13	0.45	0.04
	2	-	0.10	0.12
8	1	0.09	0.18	0.19
	2	0.04	0.05	0.09
9	1	0.44	0.28	0.26
	2	0.15	0.21	0.19
10[a]	1	0.29	0.12	<0.1
11[a]	1	0.74	0.12	<0.1
12[a]	1	0.64	0.07	<0.1

[a]Under nitrogen atmosphere.

Comparison of detectors

An electrochemical detector marketed by Dionex Corporation (94) is available which is based on the oxidation of Ag electrode for the detection of sulfide as shown by

$$Ag \rightarrow Ag^{+} + e^{-} \qquad (54)$$

$$Ag^{+} + S^{2-} \rightarrow AgS \qquad (55)$$

It was decided to compare the amperometric response obtained by the polarographic detector with that of the Dionex detector.

The anodic amperometric response of a solution containing S^{2-},

SO_3^{2-} and $S_2O_3^{2-}$ using the DME is compared with that using the Dionex Ag detector in Figure 56. It is noted that the resolution of sulfide and sulfite, using the Ag detector is poor because the product of the detector reaction (Ag_2S) stays at the surface of the electrode, blocking the access of unreacted analyte. This results in much greater peak tailing. The surface of the DME, in contrast to the Ag electrode, is continually renewed and surface fouling is relatively inconsequential.

The chromatogram of a solution containing sulfide, sulfite and thiosulfate, using the Dionex conductance detector, is shown in Figure 57. A good sensitivity to sulfide is observed but the sensitivity to thiosulfate and especially to sulfite is low. In addition, the peak resolution of sulfide and sulfite is lost because of the considerable tailing of the sulfide peak.

It is, therefore, concluded that the DME provides better resolution as well as sensitivity for the sulfur species being studied, because of continuous renewal of the electrode surface as opposed to any solid electrode where the products of electrode reaction stay at the surface of electrode and foul the electrode surface to the extent that sensitivity, resolution and reproducibility are lost.

Summary

The plot of the anodic currents of S^{2-}, SO_3^{2-} and $S_2O_3^{2-}$ at various detection potentials appears well-behaved. The variation in anodic current of S^{2-}, SO_3^{2-} and $S_2O_3^{2-}$ as a function of V_f permitted the calcu-

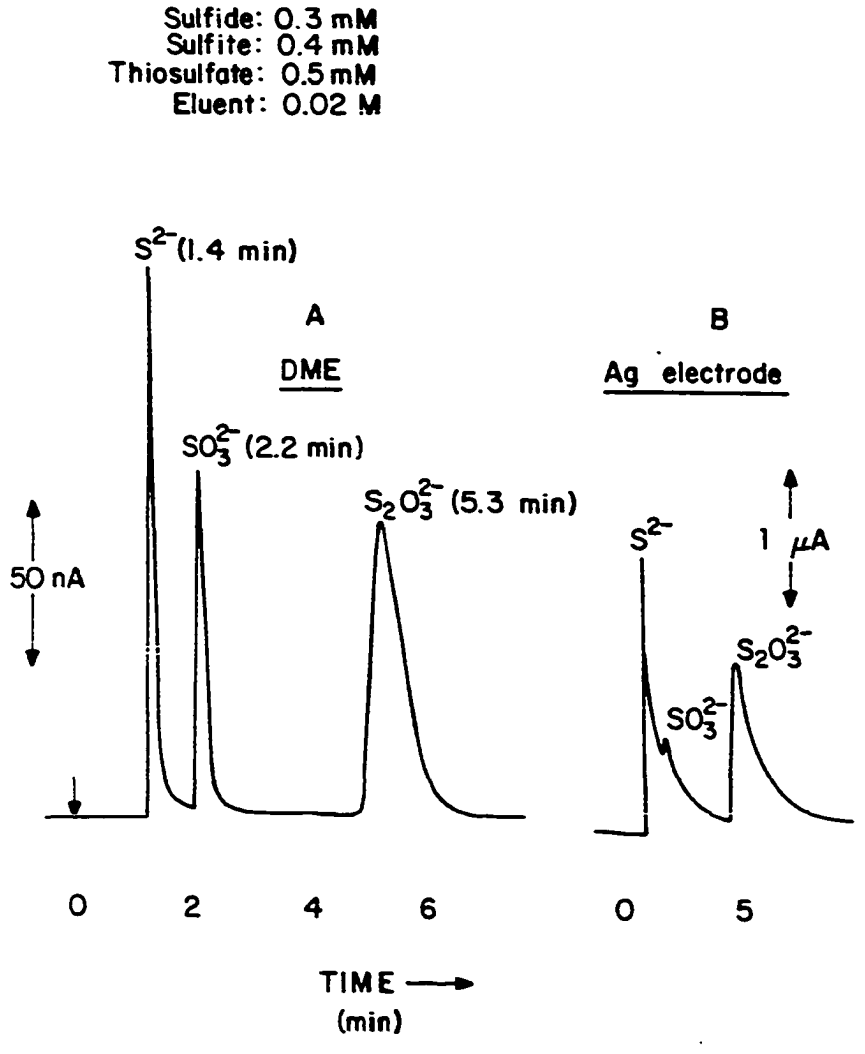

Figure 56. The response of electrochemical detectors

A. The DME
B. The Dionex Ag detector

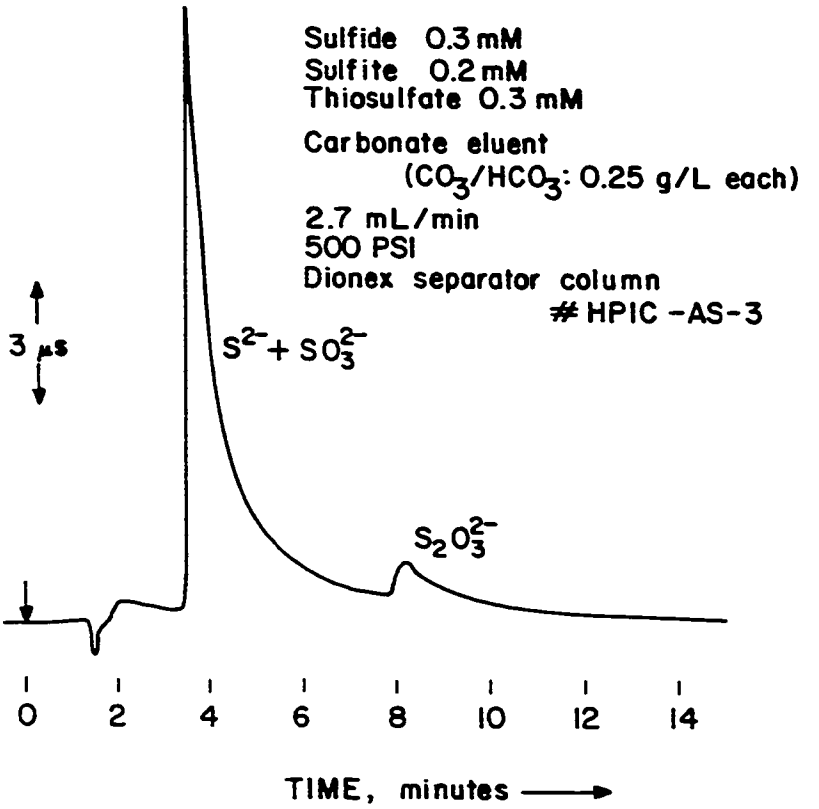

Figure 57. The response of the Dionex conductance detector

lation of α, which varies from 0.3 for S^{2-} to 0.6 for $S_2O_3^{2-}$. The values reported in the literature (92) for the laminar flow of solution varies from 0.3 to 0.5.

It is demonstrated that although S_x^{2-} undergoes a cathodic reaction at the DME in a batch cell, no cathodic response for a S_x^{2-} species is obtained with the chromatographic system, probably, because of the dissociation of S_x^{2-} into S^{2-} and S^o. The conclusion is in agreement with that presented on page 149: "S_5^{2-} breaks up into S^{2-} and S^o in the chromatographic column. S^{2-} is detected anodically and S^o is detected cathodically." This explains why there is no single anodic peak characteristic of S_x^{2-}. The peak in the cathodic region of the potential is, strictly, not a cathodic peak because it is pointed in the anodic direction. The fact that it is observed only in the cathodic range and disappears in the positive range of potentials, is an evidence that it is not an anodic peak. It is, therefore, speculated that the peak is obtained because of the change in the double-layer capacity as the S^o species dissociated from S_x^{2-} adsorbs at the surface of the electrode. The current, therefore, is produced as a result of a charging rather than a faradaic process.

CHAPTER VI. SUMMARY

The objectives of this work included the study of the voltammetric behavior of sulfide and polysulfide under sampled DC and pulse polarographic conditions in alkaline solutions to develop a method for quantitative determination of sulfide and polysulfide and other inorganic sulfur anions. Furthermore, a polarographic method was desired for the unambiguous determination of the number of sulfur atoms, x, present in a polysulfide ion, and to allow the polarographic method to be applied for the rapid determination of inorganic sulfur compounds expected to be present in aqueous samples derived from the chemical desulfurization of coal.

It was demonstrated that sulfide and polysulfide ions have characteristically different current-voltage (i-E) curves. Sulfide was quantitatively determined at a dropping mercury electrode (DME) on the basis of the anodic oxidation of mercury producing a well-defined wave. The limiting current for the anodic response was found to be reproducible and to vary linearly with the concentration. The anodic limiting current obtained by the pulse polarographic mode is much higher than that in the sampled DC mode, as expected. The anodic wave is distorted at high S^{2-} concentration because of the deposition of insoluble HgS at the surface of electrode.

The i-E curve of polysulfide, in contrast to that for sulfide, is characterized by an anodic and cathodic wave. As the potential is scanned in a positive direction from an initial value of -1.8 V,

the current decreases and goes through a minimum followed by a sharp cathodic peak; the current then becomes anodic until the potential reaches the positive limit of ca. -0.4 V. A well-defined anodic current plateau is obtained.

A cathodic plateau for S_x^{2-} is not obtained which is attributed to the large cathodic irreversibility resulting from the strong electrostatic repulsion between the analyte S_x^{2-} ions and the S^{2-} ions produced by the cathodic reaction. Both S^{2-} and S_x^{2-} are known to be strongly surface-active ionic species and compete for the adsorption sites at the surface of the electrode. Because of the similarity of the anionic charge, not as many analyte S_x^{2-} ions are able to contact the electrode surface resulting in a continuously decreasing current until the current reaches a minimum value that corresponds to the maximum anionic repulsion. A cathodic current plateau is obtained when a solution of tetraalkylammonium hydroxide is used instead of alkali hydroxide. The bulky R_4N^+ ions are adsorbed preferentially and decrease the repulsion of the adsorbed S^{2-} and S_x^{2-} ions. The cathodic peak, most likely, is observed because of the reaction of the insoluble HgS film surrounding the surface of the electrode. The peak is superimposed on a cathodic polarographic maximum which can be suppressed, to some degree, by the surfactant Triton X-100. As the potential is scanned further in the positive direction, anodic oxidation of Hg occurs, the resulting Hg++ ions react with S_x^{2-} ions to form HgS and elemental sulfur. An anodic wave is obtained in this

region of potential. Both the limiting anodic and cathodic currents were found to vary linearly with the concentration of S_x^{2-} in solution. The cathodic peak ascribed by Werner and Konopik (25) to the anionic effect, i.e., at a potential where the electrode charge changes sign, was not found to correspond to the electrocapillary maximum.

The relative values of the diffusion coefficients of various S_x^{2-} species, for x = 1 to 5, were determined by analyzing the i-E curves of S^{2-} and S_x^{2-}. The values calculated by taking the ratio of the limiting anodic currents of S^{2-} and S_x^{2-} ($i_{\ell,a,S^{2-}}/i_{\ell,a,S_x^{2-}}$) were found in excellent agreement with the values calculated by taking the ratio of the limiting anodic current of S^{2-} and the limiting cathodic current of S_x^{2-} ($i_{\ell,a,S^{2-}}/i_{\ell,c,S_x^{2-}}$). It was also observed that the slope of the calibration curve decreases as the value of x in S_x^{2-} increases because of the increasing formula weight and hence the increasing diffusion coefficient of the S_x^{2-} species.

Regarding the possibility of re-equilibration of S_x^{2-} to other S_x^{2-} species having lower x, by the addition of a S^{2-} solution, it was demonstrated that such thermodynamically allowed disproportionation reactions do not proceed at a measurable rate. This explained the observation that the anodic current for a solution containing S^{2-} and S_5^{2-} is the sum of the anodic currents of the individual S^{2-} and S_5^{2-} species.

The value of x in S_x^{2-} was determined to be 5 by recording the cathodic current as a function of x by varying the number of sulfur

atoms in S_x^{2-} for the same S_x^{2-} concentration. The value was verified by measuring the absorbance of these S_x^{2-} solutions as a function of x, since the S_x^{2-} solutions absorb energy in the visible region of electromagnetic spectrum. Further evidence was obtained by precipitating S_x^{2-} as ZnS_x and measuring the weight of precipitated sulfur as a function of x. The polarographic spectrophotometric and the gravimetric methods yielded a value of 5 for x and is in excellent agreement with Pringle's conclusion (5). The improvement of this work over Pringle's is that whereas Pringle studied the S_x^{2-} solutions containing stoichiometric quantity of S^o for S^{2-}:S^o ratios of 1:4, this work was performed by studying the solutions containing up to 1:10 mole ratio.

Since the quantitative characterization of a solution of S^{2-} and S_x^{2-} requires the knowledge of x, the number of S atoms in S_x^{2-}, $C_S^b 2-$, the bulk concentration of S^{2-} and $C_{S_x}^b 2-$, the bulk concentration of S_x^{2-} and because the polarographic method provides only the values of the limiting anodic and cathodic currents which are not enough for the quantitative description of an unknown solution containing S^{2-} and S_x^{2-}, it was concluded that the polarographic method must be supplemented with other appropriate analytical method to provide a way to determine S^{2-} in the presence of S_x^{2-}.

The cyclic voltammograms of S^{2-} and S_x^{2-} were obtained to verify the features of the i-E curves of S^{2-} and S_x^{2-} using DC polarography. The separation of the anodic and cathodic peaks provided further evidence of the irreversibility of the cathodic process for S^{2-} and S_x^{2-}.

Using a flow-injection apparatus, the anodic amperometric peaks for S^{2-} and S_x^{2-} were studied. In amperometry, the current is measured by holding the potential of electrode at a value in the limiting plateau region. Because Amperometry is normally carried out in the presence of convection, whether for a large electroanalytical cell or in a stream, it serves as a well-suited method for flow-injection analysis (FIA). The anodic peaks of S^{2-} and S_x^{2-}, obtained by FIA, were highly reproducible and the sample throughput, i.e., samples per hour, was found considerably higher than for conventional polarographic analysis. The main advantage of FIA is that the analysis can be performed in the presence of the dissolved oxygen which must be removed prior to conventional polarographic measurements. The method of flow injection detection of S^{2-} and S_x^{2-} seems suitable for the automation of the analyses in quality control work, where the quick suitability of a large number of results is desired.

It was found that the anionic sulfur species such as sulfide, sulfite, thiosulfate, tetrathionite, polysulfide, etc., are all electroactive. However, their half-wave potentials are too similar to permit the polarographic resolution in mixtures. It is, therefore, necessary to separate these compounds before they can be detected. Liquid chromatography with electrochemical detection (LCEC) was employed to achieve this task. In LCEC, the separation of the species of interest is achieved in a chromatographic column followed by detection in a flow-through electrochemical cell of very small

volume. The separation of sulfide, sulfite and thiosulfate was achieved using anion chromatography. Previously, the separated ions have been detected by a conductance detector in a commercial ion chromatograph. One of the objectives of this research was to demonstrate that the electrochemical detectors constitute a general class of universal detectors used for liquid chromatography. The flow-through electrochemical detector using a DME was used after making necessary modifications in the ion-chromatograph, for example, by-passing the suppressor column and the conductance detector in order to meet the needs of chromatographic separation as well as of the electrochemical detection. The amperometric peaks obtained are fully resolved and the chromatographic separation is completed in less than 8 minutes. A large excess of hydroxide interferes with the sulfide peak. The resolution was restored by making use of a flow-programmed technique. The sample was injected at a slower flowrate in the beginning of the chromatographic run and, after the sulfide peak is obtained, the flowrate is momentarily increased to three times its original value in order to obtain the later eluting peaks in a minimum amount of time. The determination of S_x^{2-} was done on the basis of the cathodic current by obtaining the i-E curve.

The method was tested to determine sulfide, sulfite, thiosulfate and polysulfide in the process stream samples derived from the caustic desulfurization of coal samples. The desulfurization, presently, is being studied at the Ames Laboratory.

Only qualitative information is obtained about S_x^{2-} because of the nonavailability of the value x in the samples. Finally, it is hoped that this work paves the way for the determination of individual sulfur-containing compounds in a wide variety of samples.

CHAPTER VII. SUGGESTIONS FOR FUTURE RESEARCH

The method of liquid chromatography with electrochemical detection (LCEC) has been applied for the determination of several anionic, organic sulfur species. As far as the determination of sulfur compounds is concerned, the method is of general applicability to numerous sulfur compounds, both organic and inorganic. Although the DME has been used in this research, flow-through detectors using solid electrodes are equally compatible with liquid chromatography. Pulsed amperometric detection can be employed to solve the problems related to the adsorption of the reaction products at the electrode surface.

Although the polarographic behavior of S_x^{2-} ions is mostly understood, the exact nature of the cathodic peak and the multiplicity of the anodic waves for polysulfide is in need of more investigation to provide the definitive explanation. The maximum number of sulfur atoms, x, present in S_x^{2-} has been determined to be 5; however, there is some evidence in literature for the existence of higher S_x^{2-} species. The behavior of S_x^{2-} ion on the chromatographic column has, so far, been mysterious. The cathodic current peak mentioned in Chapter III affords a convenient method for providing quick, qualitative information, however, the peaks are found to be of little quantitative value.

The availability of post-column mixing provides an additional experimental parameter that can be exploited for the optimization of the analytical procedures. The chromatographic separation prior to electrochemical detection at the DME was done by using ion-exchange

chromatography which constitute just one of the many techniques used in the liquid chromatographic work. Reverse-phase separations, for example, appear to be well suited for the selection and optimization of the eluents used for separation of the organic sulfur-containing compound process stream samples derived from caustic desulfurization of coal.

BIBLIOGRAPHY

1. Chakrabarti, J. N. "Analytical Methods for Coal and Coal Products"; Karr, C., Jr., Ed.; Academic Press: New York, 1978; Vol. 1, Chapter 9.

2. Treadwell, F. P.; Hall, W. T. "Analytical Chemistry", 9th ed.; John Wiley & Sons: New York, 1942; Vol. 88, pp. 617.

3. Tamale, M.; Ryland, L. Ind. Eng. Chem. Analytical Edition, 1936, 8, 16.

4. Story, J. N. J. Chem. Sci., 1983, 21, 272.

5. Pringle, D. L. Ph.D. Dissertation, Iowa State University, Ames, Iowa, 1967.

6. Ravenda. J. Collect. Czech. Chem. Commun. 1934, 6, 433.

7. Kolthoff, I. M.; Miller, C. S. J. Am. Chem. Soc. 1941, 63, 1405-1411.

8. Trifinov, A. Izv. Khim. Inst. Bulg. Akad. Nauk 1956, 4, 21.

9. Zhadanov, S.; Kiselev, B. In "Polarography", Hills, G. J., Ed.; Macmillan: London, 1966; Vol. 1, pp. 473.

10. Julien, L.; Bernard, M. L. Rev. Chim. Min., 1968, 5, 521.

11. Canterford, D. R.; Buchanan, A. S. J. Electroanal. Chem. 1973, 45, 193.

12. Canterford, D. R. Anal. Chem. 1973, 45, 2414-2417.

13. Canterford, D. R.; Buchanan, A. S. J. Electroanal. Chem. Interfacial Electrochem. 1973, 44, 291-298.

14. Canterford, D. R. J. Electroanal. Chem. Interfacial Electrochem. 1974, 52, 144-147.

15. Canterford, D. R. Anal. Chem. 1975, 47, 88-92.

16. Yousseffi, M.; Birke, R. L. Anal. Chem. 1977, 49, 1380.

17. Miwa, T.; Fujii, Y.; Mizuike, A. Anal. Chim. Acta 1972, 60, 475.

18. Burge, H.; Jeroscewski, P. Z. Anal. Chem. 1965, 207, 110.

19. Noel, D. L. Tappi, 1978, 61, 73.

20. Boettger, H. Justus Liebigs Annalen der Chemie, 1884, 224, 335-348.

21. Bloxam, W. P. J. Chem. Soc. London 1900, 77, 753-755.

22. Rule, A.; Thomas, J. S. J. Chem. Soc. London 1914, 105, 177-189.

23. Pearson, T. G.; Robinson, P. L. J. Chem. Soc. 1930, 1473-1497.

24. Werner, E.; Konopik, N. Montash 1952, 83, 599-613.

25. Werner, E.; Konopik, N. Montash 1952, 83, 1187-1197.

26. Werner, E.; Konopik, N. Montash 1952, 83, 1369-1384.

27. Schwarzenbach, G.; Fischer, A. Helv. Chim. Acta 1960, 43, 1365.

28. Arnston, R. H.; Dickson, F. W.; Tunnel, G. Science, 1958, 128, 716.

29. Giggenbach, W. Inorg. Chem. 1972, 11, 1201.

30. Nagy, G.; Feher, Z.; Pungor, E. Anal. Chim. Acta 1970, 52, 47.

31. Ruzicka, J.; Hansen, E. H. Anal. Chim. Acta 1975, 78, 145.

32. Stewart, K. K.; Beecher, G. R.; Hare, P. E. Anal. Biochem. 1976, 70, 167.

33. Skeggs, L. T. Am. J. Clin. Pathol. 1957, 13, 451.

34. Kissinger, P. T. Anal. Chem. 1977, 49, 447A.

35. Blaedel, W. J.; Todd, J. W. Anal. Chem. 1958, 30, 182.

36. Robertus, R. L.; Cappell, R. J.; Bond, G. W. Anal. Chem. 1958, 30, 1825.

37. Blaedel, W. J.; Todd, J. W. Anal. Chem. 1961, 33, 205.

38. Buchanan, E. B., Jr.; Bacon, J. R. Anal. Chem. 1967, 39, 615.

39. Veradi, M; Feher, Z.; Pungor, E. J. Chromatography 1974, 90, 259.

40. Drake, B. Acta Chem. Scand. 1950, 4, 554-55.

41. Kemula, W. Roczniki Chem. 1952, 25, 281-287.

42. Mann, C. K. Anal. Chem. 1952, 29, 1385.

43. Blaedel, W. J.; Todd, J. W. Anal. Chem. 1958, 30, 1821.

44. Blaedel, W. J.; Strohl, J. H. Anal. Chem. 1961, 33, 1631.

45. Janata, J.; Mark, I. B., Jr. Anal. Chem. 1967, 39, 1896.

46. Koen, J. G.; Huber, J. F. K.; Poppe, H.; denBoef, G. J. Chromatog. Sci. 1970, 8, 192.

47. Takemori, Y.; Honda, M. Rev. Polarogr. 1970, 16, 96.

48. Wasa, T.; Musha, S. Bull. Chem. Soc. Japan 1975, 48, 2176-81.

49. Johnson, D. C.; Larochelle, J. H. Talanta, 1973, 20, 959.

50. Taylor, R. L.; Johnson, D. C. Anal. Chem. 1974, 46, 262.

51. Davenport, R. J.; Johnson, D. C. Anal. Chem. 1974, 46, 1971.

52. Andrews, R. W.; Johnson, D. C. Anal. Chem. 1975, 48, 1075.

53. Larochelle, J. H.; Johnson, D. C. Anal. Chem. 1978, 50, 240.

54. Lown, J.; Koile, R.; Johnson, D. C. Anal. Chim. Acta 1980, 116, 33-39.

55. Maitoza, P.; Johnson, D. C. Anal. Chim. Acta 1980, 118, 233.

56. Hsi, T. Ph.D. Dissertation, Iowa State University, Ames, Iowa.

57. Hughes, S.; Johnson, D. C. Anal. Chem. 1981, 132, 11.

58. Hughes, S.; Johnson, D. C. Agric. Food Chem. 1980, 30, 713.

59. Polta, J.; Johnson, D. C. J. Liquid Chromatogr. 1983, 6, 1727-1743.

60. Ryan, T. H., ed. "Electrochemical Detectors, Fundamental Aspects and Analytical Applications", Plenum Press: New York, 1984.

61. Kissinger, P. "Liquid Chromatography/Electrochemistry: Principles and Applications", BAS Press: West Lafayette, IN, 1983.

62. Frezenius, Z. Anal. Chem. 1982, 311, 197-200.

63. Cox, J. A.; Przyajazny, A. Anal. Lett. 1977, 10, 869.

64. Lawrence, J. F.; Iverson, F.; Hanekamp, H. B.; Box, P.; Frei, R. W. J. Chromatogr. 1981, 212, 245.

65. Hanekamp, H. B.; Box, P.; Frei, R. W. J. Chromatogr. 1979, 186, 489.

66. Stillman, R.; Ma, T. S. Microchim. Acta 1973, (Wien), 194.

67. Stillman, R.; Ma, T. S. Microchim. Acta 1974, (Wien), 641.

68. Saetre, R.; Rabenstein, D. L. Anal. Biochem. 1978, 90, 684.

69. Eggli, R.; Asper, R. Anal. Chim. Acta 1978, 101, 253.

70. Saetre, R.; Rabenstein, D. L. Anal. Chem. 1978, 50, 276.

71. Bergstrom, R. F.; Kay, D. R.; Wagner, J. G. Life Sci. 1980, 27, 189.

72. Saetre, R.; Rabenstein, D. L. J. Agric. Food Chem. 1978, 26, 982.

73. Rabenstein, D. L.; Saetre, R. Anal. Chem. 1977, 49, 1036.

74. Bard, Allen J.; Lund, Henning, Eds. "Encyclopedia of Electrochemistry of the Elements", Marcel Dekker Inc.: New York; 1978; Vol. XII.

75. Pollard, F. H.; McOmie, J. F. W.; Jones, D. J. J. Chem. Soc. 1955, 4337.

76. Bighi, C.; Trabanelli, G.; Pancaldi, G. Boll. Sci. Fac. Chim. Ind. Bologna, 1955, 13, 100; 1958, 16, 92.

77. Scoffone, E.; Carini, E. Ric. Sci. 1955, 25, 2109.

78. Wolkoff, A. W.; Larose, R. H. Anal. Chem. 1975, 47, 1003.

79. Wolkoff, A. W.; Larose, R. H. J. Chromatogr. Sci. 1976, 14, 353.

80. Chapman, J. N.; Beard, H. R. Anal. Chem. 1973, 45, 2268.

81. Goguel, R. Anal. Chem. 1969, 41, 1034.

82. Bard, A. J.; Faulkner, L. R. "Electrochemical Methods", Wiley: New York, 1980.

83. Meites, Louis, "Polarographic Techniques", Second Edition, Interscience Publishers: New York, 1965.

84. Vogel, A. I. "Vogel's Textbook of Quantitative Inorganic Analysis", Longman: New York, 1978; pp. 925.

85. Nickless, G., Ed. "Inorganic Sulfur Chemistry", Elsevier: New York, 1968; pp. 215.

86. Zhadanov, S. I.; Kiselev, B. A. Collect. Czech. Commun. 1966, 31, 788-805.

87. Wagman, D. D. "Selected Values of Chemical Thermodynamic Properties", NBS Technical Note 270-8, U.S. Government Printing Office: Washington, D.C., 1981.

88. Stephenson, Michael D. M.S. Thesis, Library, Iowa State University, Ames, Iowa, 1982, pp. 176.

89. Hall, M. E. Anal. Chem. 1953, 25, 556-561.

90. Karchmer, J. H.; Walker, M. T. Anal. Chem. 1954, 26, 271-280.

91. Bard, A. J. "Encyclopedia of Electrochemistry of Elements", Marcel Dekker: New York, 1975; Vol. IV, pp. 279.

92. Mackoul, David and Johnson, D. C. Anal. Chem. 1984, 56(3), 436-439.

93. Perone, S. P.; Jones, D. V. "Digital Computers in Scientific Instrumentation: Applications to Chemistry", McGraw-Hill, Inc.: New York, 1973; p. 246.

94. Ruzicka, J.; Hansen, E. H. "Flow and Analysis", John Wiley & Sons: New York, 1981; pp. 16.

95. Dionex Corporation, Sunnyvale, California.

ACKNOWLEDGMENTS

I would like to thank Dr. Dennis C. Johnson for his guidance, support, patience and encouragement throughout this research. His attitude towards his fellow human beings, in general, and towards his students, in particular, deserves special commendations and gratitude.

The financial support of the Department of Chemistry at Iowa State University is greatly acknowledged. The support of Ames Laboratory in the last year of my graduate work deserves special recognition. I would like to thank Dr. Richard Markuszewski for his guidance, suggestions, critical evaluations and his personal interest in the project.

The list cannot be completed without recognizing the services rendered by extremely cooperative staff of the chemistry machine shop, the glass shop and especially the nice people in chemistry stores.

My special thanks to the UTAH study group (Uddin, Tong, Anderson and Hsi) for all the good times we shared together. The personal contribution of David Anderson can neither be stated nor acknowledged in a few lines.

Very special thanks go to my parents and all of my family members in Pakistan who provided the foundations of this accomplishment and of all of my achievements.

Finally, I would like to thank my sincere and beloved wife, Salma, and my children, Samina, Sadaf, Zafar and Sarah, who stood with me "in rain and shine" indeed! Salma invested an amazingly untiring volume of patience and hard work to support me and strived to the best of her

abilities to provide me with everything that was needed to accomplish this task.